FINITE ELEMENT MODELING OF KNEE AND SHOULDER LIGAMENTS

by

Benjamin James Ellis

A dissertation submitted to the faculty of
The University of Utah
in partial fulfillment of the requirements for the degree of

Doctor of Philosophy

Department of Bioengineering

The University of Utah

May 2012

The University of Utah Graduate School

STATEMENT OF DISSERTATION APPROVAL

The dissertation of **Benjamin James Ellis**

has been approved by the following supervisory committee members:

Jeffrey A. Weiss	, Chair	**11/10/11** Date Approved
Richard D. Rabbitt	, Member	**11/10/11** Date Approved
Andrew E. Anderson	, Member	**11/10/11** Date Approved
James E. Guilkey	, Member	**11/10/11** Date Approved
Christopher L. Peters	, Member	**11/10/11** Date Approved

and by **Patrick A. Tresco** , Chair of the Department of **Bioengineering**

and by Charles A. Wight, Dean of The Graduate School.

ABSTRACT

The medial collateral ligament (MCL) is the primary restraint to knee valgus rotation and a secondary restraint to anterior tibial translation. The anterior cruciate ligament (ACL) is a primary restraint to anterior tibial translation, but its contribution to valgus restraint was debated. To address this, a combined experimental and computational study was conducted to determine the effect of ACL injury on MCL insertion site and contact forces during valgus loading and anterior tibial loading. Six finite element (FE) models were constructed and used to simulate boundary and loading conditions from corresponding cadaveric experiments. It was shown that in the ACL-deficient knee, the MCL is indeed subjected to higher insertion site and contact forces in response to an anterior load. However, MCL forces due to a valgus torque were not significantly increased in the ACL-deficient knee. It follows that the MCL resists anterior tibial translation when the ACL is intact, but the ACL is not a restraint to valgus rotation when a healthy MCL is present.

Physical diagnostic exams are the most crucial step for diagnosis of the location of injury to the shoulder capsule, but the exams are relatively imprecise and the joint positions used for these exams are not standardized between physicians. Due to the complexity of the strains in the capsule during joint motion, a method to correlate joint positions and the capsule strains produced by these positions was needed. To address this discrepancy, a methodology for three-dimensional, subject-specific FE modeling of the inferior glenohumeral ligament (IGHL) as a continuous structure was developed. This

FE model was then used to develop a method for evaluating the region of the glenohumeral capsule being tested by clinical exams for shoulder instability. Finally, for the clinical exam known as the simple translation test it was shown that regions of localized strain created by the exam indicate that the joint positions can be used to test the glenoid side of the IGHL, but are not useful for assessing the humeral side of the IGHL.

To my family:

Thank you for supporting me in this endeavor

TABLE OF CONTENTS

LIST OF FIGURES

ACKNOWLEDGMENTS

Financial support for this work was provided by the National Institutes of Health Grants #RO1-AR47369 and #RO1-AR050218, and is gratefully acknowledged.

CHAPTER 1

INTRODUCTION

Motivation

Medial Collateral Ligament Mechanics in the Anterior Cruciate Ligament Deficient Knee

There were over 19 million patient visits made to physician offices due to a knee injury in 2003 [1]. A knee injury was the most common reason for patients to visit an orthopedic surgeon in 2003 [1]. Knee injuries are also particularly prominent in Utah, where during the winter months there will be one injury for every 1000 skier days [2]. Forty percent of these knee injuries will involve the medial collateral ligament (MCL), and the anterior cruciate ligament (ACL) will be the most common ligament injured in conjunction with the MCL [3, 4].

The relationship between the mechanics of the ACL and MCL in the knee remains unclear. It is known that the MCL is a primary restraint to valgus rotation [5-16] and a secondary restraint to anterior tibial translation [5, 8, 17] [13] [18] [4, 19-21]. The ACL is a primary restraint to anterior tibial translation [5, 6, 8, 13, 20-23] and it has also been thought by many to be a secondary restraint to valgus rotation [5, 6, 8, 13, 21-23], but others have shown that valgus laxity is relatively unaffected by ACL deficiency [12, 17, 19].

Conclusions in the literature as to the exact contributions of the MCL and ACL to valgus stability vary within and between studies of ligament healing in animal models and joint kinematics in cadaver models. Many studies have shown that MCL healing is substantially poorer in the case of a combined MCL/ACL injury than it is for an isolated MCL injury [7, 8, 11, 15-17], and one study hypothesized that this was caused by increased strains and forces as a result of ACL deficiency [8], although those strains and forces have not been measured. In contrast to these other animal healing studies, one study of healing in the rabbit showed that valgus rotation does not increase over time in response to healing of the ACL graft after an O'Donoghue triad injury (rupture of the medial collateral ligament, anterior cruciate ligament and damage to the medial meniscus). However, anterior translation did increase significantly over the same healing period [17]. Further, two previous cadaver studies concluded that valgus laxity is relatively unaffected by ACL deficiency [12, 19]. In conclusion, before this dissertation research, the actual insertion site and contact forces in the MCL in response to a valgus torque or an anterior tibial load in the intact and ACL-deficient knee, which arguably are the most relevant data for interpretation of ligament contribution to joint function, were unknown.

Inferior Glenohumeral Ligament Modeling and Clinical Exams

Glenohumeral joint dislocations are very common [24, 25], and most dislocations occur due to forces applied in the anterior direction [26]. The inferior glenohumeral ligament (IGHL) is thought to be the primary restraint to anterior translation [27-29]. A very common injury resulting from anterior dislocation is detachment of the IGHL from

the anterior glenoid [30, 31]. Physical diagnostic exams are the most crucial step for diagnosis of the location of injury to the capsule, but the exams are relatively imprecise and the glenohumeral joint positions used for these exams are not standardized between physicians [32-35]. Treatments for these injuries depend on the region of the capsule that is injured [36], but misdiagnosis of the injured region has been blamed for over 38% of recurring injuries [37-39].

Although the development of shoulder clinical exams remains an open area of research, clinical exams to evaluate knee ligament injuries are well established and a similar process that was used to establish these exams should be applied to the shoulder. Poor clinical outcomes, inconsistent clinical exams and complex glenohumeral capsule anatomy have motivated researchers to investigate the function of the specific regions of the glenohumeral capsule by evaluating strain distributions [28, 32, 40-42]. A similar approach was used to study the ACL in the knee [43-47], and these studies led to the development of clinical exams to diagnose knee instability and injury to the ACL [48]. Due to the complexity of the strains in the glenohumeral capsule during joint motion [41, 42, 49], a method to correlate glenohumeral joint positions and the capsule strains produced by these positions is needed. As with the ACL, identifying the positions in which the glenohumeral capsule is strained and where those strains occur in the capsule should be the first step to developing shoulder clinical exams.

Before the larger problem of developing better clinical exams could be addressed, it was first necessary to develop a method for accurately determining glenohumeral capsule strains, as well as insertion site and contact forces. This led to a collaboration between Dr. Richard Debski's lab at the University of Pittsburgh and Dr. Jeffrey Weiss' lab at the

University of Utah. Dr. Debski is an expert in the area of glenohumeral joint injury and experimental techniques, and Dr. Weiss provided his extensive experience with subject-specific modeling of ligaments. Through this collaboration and as part of this dissertation research (Chapter 4) a methodology for three-dimensional, subject-specific, finite element (FE) modeling of the IGHL as a continuous structure was developed and a validated model of the IGHL as part of the entire glenohumeral capsule was created [50].

Research Goals

This research aimed to elucidate the structure-function relationships of commonly injured ligaments in the knee and shoulder and to investigate the mechanics of these ligaments during loading conditions that simulate clinical exams. Specifically, the goal of the knee ligament research was to determine the effects of ACL deficiency on MCL insertion site and contact forces during valgus rotation and anterior tibial loading. For the shoulder, the final objective was to create a method for locating the area of the shoulder capsule that is providing the primary resistance during specific clinical exams. To accomplish this goal a methodology was developed to perform three-dimensional FE modeling of the IGHL as a continuous structure.

Summary of Chapters

The focus of this dissertation is the mechanics of three commonly injured diarthrodial joint ligaments during the clinical exams used to test for injury of those ligaments. Experimental and computational methods were used for this dissertation to answer research questions that could not be addressed otherwise. In Chapter 2 sufficient

background is provided so the reader can understand the structures that are being studied (the ligaments and their associated diarthrodial joints) as well as the methods that are being used for the research.

MCL insertion site and contact forces in the intact and ACL-deficient knee are the focus of Chapter 3. These forces, which arguably are the most relevant data for interpretation of ligament contribution to joint function, were previously unknown. An experimental and computational approach was used to show the relationship between MCL and ACL mechanics in the intact and ACL-deficient knee.

In Chapter 4 the methods utilized in Chapter 3 are extended to study the IGHL, the most injured ligament in the glenohumeral joint. The approach for modeling the IGHL required extensive modifications and additions to the methods used for the MCL. These methods and sensitivity studies for FE modeling of the IGHL are detailed in Chapter 4.

Based on the methods developed for Chapter 4 and a subsequent paper [50], a procedure to assess the region of the glenohumeral capsule being tested during a clinical exam is described in Chapter 5. Clinical exams to test for MCL and ACL injuries are well established, but clinical exams to evaluate shoulder injuries are still being developed. In Chapter 5, it is shown how FE modeling of the glenohumeral capsule can help assess the region being tested during a clinical exam.

The final chapter discusses the findings of the previous three chapters and the limitation of those studies as well as highlighting how the methods developed in those studies have already been utilized in many other studies.

References

[1] AAOS. *Common Knee Injuries*. http://orthoinfo.aaos.org/.

[2] ISSS, "www.ski-injury.com."

[3] Hull, M.L., 1997, "Analysis of skiing accidents involving combined injuries to the medial collateral and anterior cruciate ligaments," Am J Sports Med, 25(1), pp. 35-40.

[4] Miyasaka, K., et al., 1991, "The incidence of knee ligament injuries in the general population," Am J Knee Surg, 4(1), pp. 3-8.

[5] Grood, E.S., Noyes, F.R., Butler, D.L., and Suntay, W.J., 1981, "Ligamentous and capsular restraints preventing straight medial and lateral laxity in intact human cadaver knees," J Bone Joint Surg Am, 63(8), pp. 1257-69.

[6] Markolf, K.L., Mensch, J.S., and Amstutz, H.C., 1976, "Stiffness and laxity of the knee--the contributions of the supporting structures. A quantitative in vitro study," J Bone Joint Surg Am, 58(5), pp. 583-94.

[7] Anderson, D.R., Weiss, J.A., Takai, S., Ohland, K.J., and Woo, S.L., 1992, "Healing of the medial collateral ligament following a triad injury: a biomechanical and histological study of the knee in rabbits," J Orthop Res, 10(4), pp. 485-95.

[8] Abramowitch, S.D., Yagi, M., Tsuda, E., and Woo, S.L., 2003, "The healing medial collateral ligament following a combined anterior cruciate and medial collateral ligament injury--a biomechanical study in a goat model," J Orthop Res, 21(6), pp. 1124-30.

[9] Inoue, M., McGurk-Burleson, E., Hollis, J.M., and Woo, S.L., 1987, "Treatment of the medial collateral ligament injury. I: The importance of anterior cruciate ligament on the varus-valgus knee laxity," Am J Sports Med, 15(1), pp. 15-21.

[10] Ma, C.B., Papageogiou, C.D., Debski, R.E., and Woo, S.L., 2000, "Interaction between the ACL graft and MCL in a combined ACL+MCL knee injury using a goat model," Acta Orthop Scand, 71(4), pp. 387-93.

[11] Loitz-Ramage, B.J., Frank, C.B., and Shrive, N.G., 1997, "Injury size affects long-term strength of the rabbit medial collateral ligament," Clin Orthop, (337), pp. 272-80.

[12] Norwood, L.A. and Cross, M.J., 1979, "Anterior cruciate ligament: functional anatomy of its bundles in rotatory instabilities," Am J Sports Med, 7(1), pp. 23-6.

[13] Ichiba, A., Nakajima, M., Fujita, A., and Abe, M., 2003, "The effect of medial collateral ligament insufficiency on the reconstructed anterior cruciate ligament: a study in the rabbit," Acta Orthop Scand, 74(2), pp. 196-200.

[14] Mazzocca, A.D., Nissen, C.W., Geary, M., and Adams, D.J., 2003, "Valgus medial collateral ligament rupture causes concomitant loading and damage of the anterior cruciate ligament," J Knee Surg, 16(3), pp. 148-51.

[15] Woo, S.L., Jia, F., Zou, L., and Gabriel, M.T., 2004, "Functional tissue engineering for ligament healing: potential of antisense gene therapy," Ann Biomed Eng, 32(3), pp. 342-51.

[16] Woo, S.L., Young, E.P., Ohland, K.J., Marcin, J.P., Horibe, S., and Lin, H.C., 1990, "The effects of transection of the anterior cruciate ligament on healing of the medial collateral ligament. A biomechanical study of the knee in dogs," J Bone Joint Surg Am, 72(3), pp. 382-92.

[17] Engle, C.P., Noguchi, M., Ohland, K.J., Shelley, F.J., and Woo, S.L., 1994, "Healing of the rabbit medial collateral ligament following an O'Donoghue triad injury: effects of anterior cruciate ligament reconstruction," J Orthop Res, 12(3), pp. 357-64.

[18] Butler, D.L., Noyes, F.R., and Grood, E.S., 1980, "Ligamentous restraints to anterior-posterior drawer in the human knee. A biomechanical study," J Bone Joint Surg Am, 62(2), pp. 259-70.

[19] Gardiner, J.C. and Weiss, J.A., 2003, "Subject-specific finite element analysis of the human medial collateral ligament during valgus knee loading," J Orthop Res, 21(6), pp. 1098-106.

[20] Lujan, T.J., Dalton, M.S., Thompson, B.M., Ellis, B.J., Rosenberg, T.D., and Weiss, J.A., 2005, "MCL strains and joint kinematics in the ACL-deficient and posteromedial meniscus injured knee," American Journal of Sports Medicine, In Review.

[21] Moglo, K.E. and Shirazi-Adl, A., 2003, "Biomechanics of passive knee joint in drawer: load transmission in intact and ACL-deficient joints," Knee, 10(3), pp. 265-76.

[22] Kanamori, A., Sakane, M., Zeminski, J., Rudy, T.W., and Woo, S.L., 2000, "In-situ force in the medial and lateral structures of intact and ACL-deficient knees," J Orthop Sci, 5(6), pp. 567-71.

[23] Robins, A.J., Newman, A.P., and Burks, R.T., 1993, "Postoperative return of motion in anterior cruciate ligament and medial collateral ligament injuries. The

effect of medial collateral ligament rupture location," Am J Sports Med, 21(1), pp. 20-5.

[24] Hovelius, L., 1982, "Incidence of shoulder dislocation in Sweden," Clin Orthop, (166), pp. 127-31.

[25] Nelson, B.J. and Arciero, R.A., 2000, "Arthroscopic management of glenohumeral instability," Am J Sports Med, 28(4), pp. 602-14.

[26] Cave, E., Burke, J., Boyd, R., *Trauma Management* 1974, Chicago, IL: Year Book Medical Publishers. 437.

[27] Malicky, D.M., Soslowsky, L.J., Blasier, R.B., and Shyr, Y., 1996, "Anterior glenohumeral stabilization factors: progressive effects in a biomechanical model," Journal of Orthopaedic Research: Official Publication of the Orthopaedic Research Society, 14(2), pp. 282-8.

[28] Turkel, S.J., Panio, M.W., Marshall, J.L., and Girgis, F.G., 1981, "Stabilizing mechanisms preventing anterior dislocation of the glenohumeral joint," J Bone Joint Surg Am, 63(8), pp. 1208-17.

[29] Ovesen, J. and Nielsen, S., 1985, "Stability of the shoulder joint. Cadaver study of stabilizing structures," Acta Orthopaedica Scandinavica, 56(2), pp. 149-51.

[30] Bankart, A.S.B., 1923, "Recurrent or habitual dislocation of the shoulder joint," Br Med J, 2, pp. 1132-3.

[31] Bankart, A.S.B., 1938, "The pathology and treatment of recurrent dislocation of the shoulder joint," Br J Surg, 26, pp. 23-9.

[32] Brenneke, S.L., Reid, J., Ching, R.P., and Wheeler, D.L., 2000, "Glenohumeral kinematics and capsulo-ligamentous strain resulting from laxity exams," Clin Biomech (Bristol, Avon), 15(10), pp. 735-42.

[33] Mallon, W.J. and Speer, K.P., 1995, "Multidirectional instability: current concepts," J Shoulder Elbow Surg, 4(1 Pt 1), pp. 54-64.

[34] Matsen, F.A., 3rd, 1991, "Capsulorrhaphy with a staple for recurrent posterior subluxation of the shoulder," J Bone Joint Surg Am, 73(6), pp. 950.

[35] Pollock, R.G. and Bigliani, L.U., 1993, "Glenohumeral instability: evaluation and treatment," J Am Acad Orthop Surg, 1(1), pp. 24-32.

[36] Gerber, C. and Ganz, R., 1984, "Clinical assessment of instability of the shoulder. With special reference to anterior and posterior drawer tests," J Bone Joint Surg Br, 66(4), pp. 551-6.

[37] Cooper, R.A. and Brems, J.J., 1992, "The inferior capsular-shift procedure for multidirectional instability of the shoulder," J Bone Joint Surg Am, 74(10), pp. 1516-21.

[38] Hawkins, R.H. and Hawkins, R.J., 1985, "Failed anterior reconstruction for shoulder instability," J Bone Joint Surg Br, 67(5), pp. 709-14.

[39] Lusardi, D.A., Wirth, M.A., Wurtz, D., and Rockwood, C.A., Jr., 1993, "Loss of external rotation following anterior capsulorrhaphy of the shoulder," J Bone Joint Surg Am, 75(8), pp. 1185-92.

[40] Bigliani, L.U., Pollock, R. G., Soslowsky, L. J., Flatow, E. V., Pawluk, R. J., Mow, V. C., 1992, "Tensile properties of the inferior glenohumeral ligament," J Orthop Res, 10(2), pp. 187-197.

[41] Malicky, D.M., Soslowsky, L.J., Kuhn, J.E., Bey, M.J., Mouro, C.M., Raz, J.A., and Liu, C.A., 2001, "Total strain fields of the antero-inferior shoulder capsule under subluxation: a stereoradiogrammetric study," J Biomech Eng, 123(5), pp. 425-31.

[42] Moore, S.M., Stehle, J.H., Rainis, E.J., McMahon, P.J., Debski, R.E., 2008, "The current anatomical description of the inferior glenohumeral ligament does not correlate with its functional role in positions of external rotation," Journal of Orthopaedic Research, In Press.

[43] Butler, D.L., 1989, "Kappa Delta Award paper. Anterior cruciate ligament: its normal response and replacement," J Orthop Res, 7(6), pp. 910-21.

[44] Henning, C.E., Lynch, M.A., and Glick, K.R., Jr., 1985, "An in vivo strain gage study of elongation of the anterior cruciate ligament," Am J Sports Med, 13(1), pp. 22-6.

[45] Howe, J.G., Wertheimer, C., Johnson, R.J., Nichols, C.E., Pope, M.H., and Beynnon, B., 1990, "Arthroscopic strain gauge measurement of the normal anterior cruciate ligament," Arthroscopy, 6(3), pp. 198-204.

[46] Renstrom, P., Arms, S.W., Stanwyck, T.S., Johnson, R.J., and Pope, M.H., 1986, "Strain within the anterior cruciate ligament during hamstring and quadriceps activity," Am J Sports Med, 14(1), pp. 83-7.

[47] Woo, S.L., Hollis, J.M., Roux, R.D., Gomez, M.A., Inoue, M., Kleiner, J.B., and Akeson, W.H., 1987, "Effects of knee flexion on the structural properties of the rabbit femur-anterior cruciate ligament-tibia complex (FATC)," J Biomech, 20(6), pp. 557-63.

[48] Katz, J.W. and Fingeroth, R.J., 1986, "The diagnostic accuracy of ruptures of the anterior cruciate ligament comparing the Lachman test, the anterior drawer sign, and the pivot shift test in acute and chronic knee injuries," Am J Sports Med, 14(1), pp. 88-91.

[49] Malicky, D.M., Kuhn, J.E., Frisancho, J.C., Lindholm, S.R., Raz, J.A., and Soslowsky, L.J., 2002, "Neer Award 2001: nonrecoverable strain fields of the anteroinferior glenohumeral capsule under subluxation," J Shoulder Elbow Surg, 11(6), pp. 529-40.

[50] Moore, S.M., Ellis, B., Weiss, J.A., McMahon, P.J., and Debski, R.E., 2010, "The glenohumeral capsule should be evaluated as a sheet of fibrous tissue: a validated finite element model," Annals of Biomedical Engineering, 38(1), pp. 66-76.

CHAPTER 2

BACKGROUND

Ligaments

Ligaments are soft fibrous tissues that connect bone to bone at the joints. They help to guide and limit the motion of the bones so that the joint articulates with no separation or only a limited separation of the bones. Ligaments are passive stabilizers and work in conjunction with other passive stabilizers including the articulating surfaces of the bones and, in most diarthrodial joints (major joints – knee, hip and shoulder), other soft tissues like the meniscus in the knee and the labrum in the shoulder and hip. In diarthrodial joints, ligaments mainly take two forms. In the knee, ligaments are generally banded or look similar to rope or cord. The Medial Collateral Ligament (MCL) is a banded type ligament and the Anterior Cruciate Ligament (ACL) is a cord-like ligament. These knee ligaments essentially resist motion along a single line of action similar to a rope or strap, but also experience shear, transverse and compressive loads. For example, the ACL primarily constrains anterior motion of the tibia with respect to the femur and the MCL primarily resists valgus knee motion, which are essentially uniaxial loads, but will also see shear, transverse and compressive loads due to articulation of the joint and contact with the bones. The ligaments in the shoulder and hip are known as capsular ligaments because they are essentially just thicker and/or denser tissue bands in the larger

continuous capsule. The Inferior Glenohumeral Ligament (IGHL), for example, is a capsular ligament in the shoulder. While it can be argued that capsular ligaments still resist motion primarily in one direction, they are generally thought of as constraining more complex motions than banded or cord-like ligaments through their connection with the rest of the capsule.

Ligament consists primarily of collagen and water [1]. The tissue is a composite material composed of collagen fibers surrounded by a ground substance matrix. Type I collagen makes up 70-80% of the dry weight of ligament, while type III collagen makes up less than 10% of the dry weight. Type I, II, and II collagens are fibrillar protein collagens ("fiber-forming" collagens) and it is the collagen fibers in ligament that provide the high tensile strength. Proteoglycans, glycolipids, and fibroblasts make up the ground substance and allow ligament to store water, but are less than 1% of the tissue by dry weight [2]. Water makes up 60-70% of the wet weight and is largely responsible for the viscoelastic and nearly-incompressible properties of the tissue. Ligaments also consist of small quantities of Elastin (<5% by dry weight) and this protein provides both some of the tensile strength as well as the ability for elastic recovery from tensile loads[3]. Fibroblasts are the most prevalent cell type found in ligament and the tissue is relatively hypocellular. The fibroblasts in ligament tend to be elongated and interconnected in the mid-substance and more rounded near the insertion-sites, where ligament connects to bone [4]. The purpose of these cells is to maintain the collagen fibers.

Collagen

The collagen in ligaments is formed from a structural hierarchy that begins with linear polypeptide chains being formed into alpha-helix chains that intern coil together to make the triple helix shaped tropocollogen molecule[5]. Five tropocollagen molecules are wound together in a left-handed configuration with a quarter-staggered pattern, yielding a cross-striated collagen fibril, which is the most basic, or representative unit within the tissue [6]. These fibrils then associate to become fibers, which then group to form fascicles and finally ligament (Fig. 2.1). The fibers have a longitudinal waveform, which is commonly known as the collagen crimp pattern and is visible under polarized light microscopy.

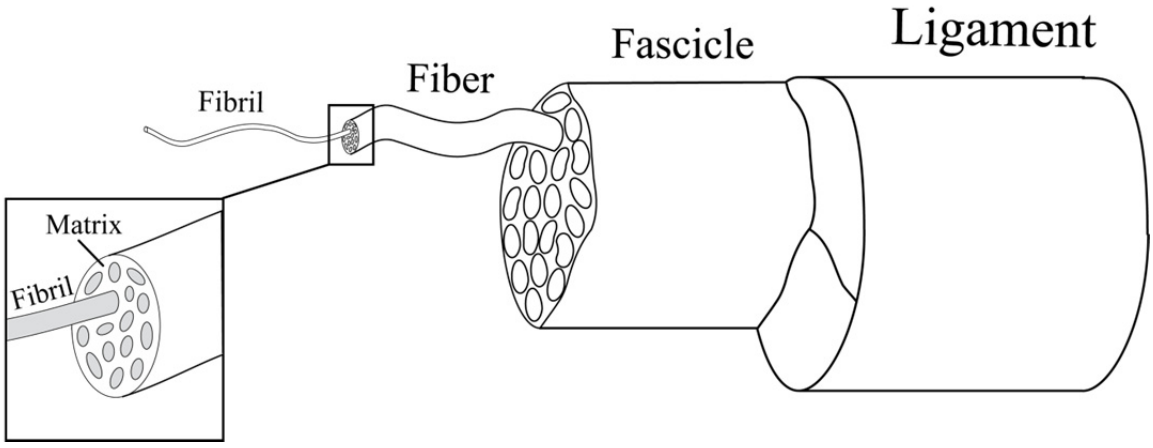

Fig. 2.1. Schematic of the structural hierarchy of tendon and ligament. Adapted from Reese [6].

This crimp pattern is created when the surrounding matrix shrinks during maturation, causing load to be transferred to the fiber by collagen-interfibrillar interactions [7, 8]. It is commonly accepted that collagen crimp causes the nonlinear response of ligaments to quasi-static, uniaxial, tensile loading along the predominant fiber direction. The waveform is only visible below a certain tensile load, and the response of the tissue is essentially linear beyond this load (Fig. 2.2). Below this loading threshold, when the crimp is being straightened, the response of the material is upwardly concave. This is commonly known as the "toe region" of the ligament stress-strain curve that is seen during quasi-static, uniaxial, tensile loading along the predominant fiber direction that is used for material characterization [9]. Beyond the toe region, ligament tissue is a relatively stiff material and this is caused by collagen's molecular coil configuration and its ability to form intramolecular and intermolecular crosslinks [10].

Water and the Ground Substance Matrix

Two thirds of ligaments' weight comes from water, which is stored in the ground substance matrix that surrounds the collagen fibers [11]. This storage is made possible by the proteoglycans in the ground substance matrix even though they constitute less than 1% of the dry weight of ligament [12]. Through their aggregation with hyaluronic acid, hydrophilic molecules are created that associate with water, creating the gel-like extracellular matrix. These charged proteoglycan molecules inhibit the exudation of water [2], although some exudation does occur during cyclic loading [13]. It is this limited ability of water to move through the tissue that largely causes the time- and history-dependent viscoelastic properties of ligament [14, 15] and its nearly-

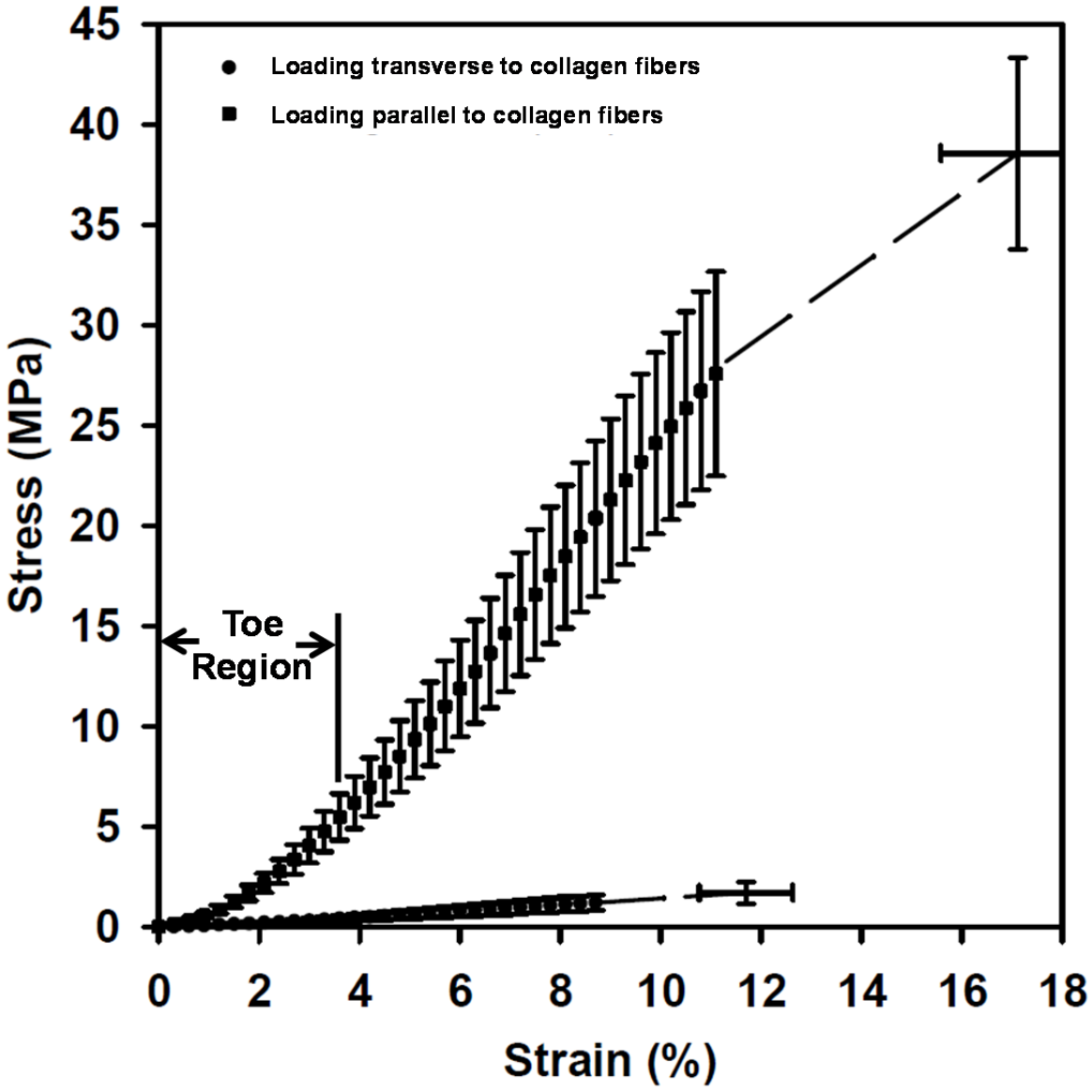

Fig. 2.2. Stress-strain curves from testing ligament parallel to and transverse to the collagen fiber direction. Adapted from Quapp [9].

incompressible response to loading [16, 17]. The response of the ground substance matrix to quasi-static loads, which can be obtained by testing ligament tissue transverse to the collagen fibers, is essentially linear and far more compliant than in the fiber reinforced direction (Fig. 2.2).

In Situ Stress

Although ligaments are considered passive stabilizers, there are stresses in the tissue when the joint is in a neutral position. These in situ stresses are responsible for the stability of the joint when muscle and tendon forces, the active stabilizers, are not present. Due to the difficulty in measuring in situ stresses, in situ strains are usually measured [18, 19]. Ligament in situ strains are inhomogenous, subject-specific, and vary depending on joint position [18, 19]. Previous research has shown that computational models must accurately represent ligament in situ strains to accurately predict ligament strains and stresses due to external loading [18]. Neglecting ligament in situ strains in computational models leads to very poor predictions of the inhomogenous strains in the tissue and an under-prediction of the stresses caused by external loading [18].

Insertion Sites

Ligament connects to bone at insertion sites and there are two types of insertion sites that have been defined: direct and indirect insertions. Direct insertion sites occur over a smaller distance of usually less than 1 mm [4], and consist of a distinct right-angle boundary where deep collagen fibrils extend out of the ground substance matrix and

become fibrocartilage tissue, mineralized fibrocartilage tissue, and then bone [20]. Indirect insertion sites occur over a larger area where predominantly superficial collagen fibers gradually blend into the periosteum at more acute angles. Deep collagen fibers also make attachments at indirect insertion sites, but the connections are fewer than at direct insertion sites, occur at more acute angles and without the fibrocartilagenous transitional zone observed in direct insertions [21]. Some ligaments have the same type of insertion site on both ends, while other ligaments have different types. The ACL in the knee, for example, has direct insertion sites on both ends, while the MCL in the knee attaches to the femur with a direct insertion, but attaches to the tibia with an indirect insertion. So, both types of insertions can occur at the same joint and at opposite ends of the same ligament.

MCL and ACL Structure and Function

Knee Ligaments and Bones

Knee ligaments are one focus of this research due to the high incidence of knee injuries. There are four major ligaments in the knee that connect three bones (Fig. 2.3). The major ligaments in the knee are the MCL, Lateral Collateral Ligament (LCL), ACL, and Posterior Cruciate Ligament (PCL). There are actually four bones in the knee, but only three are connected with tissue that is defined as ligament. The four bones that make up the knee are the femur, tibia, fibula and the patella. The MCL connects the femur and tibia on the medial side of the knee, while the LCL connects the femur and fibula on the lateral side of the knee. The MCL resists primarily valgus loads and the LCL resists varus loads. The cruciate ligaments (ACL and PCL) also connect the femur

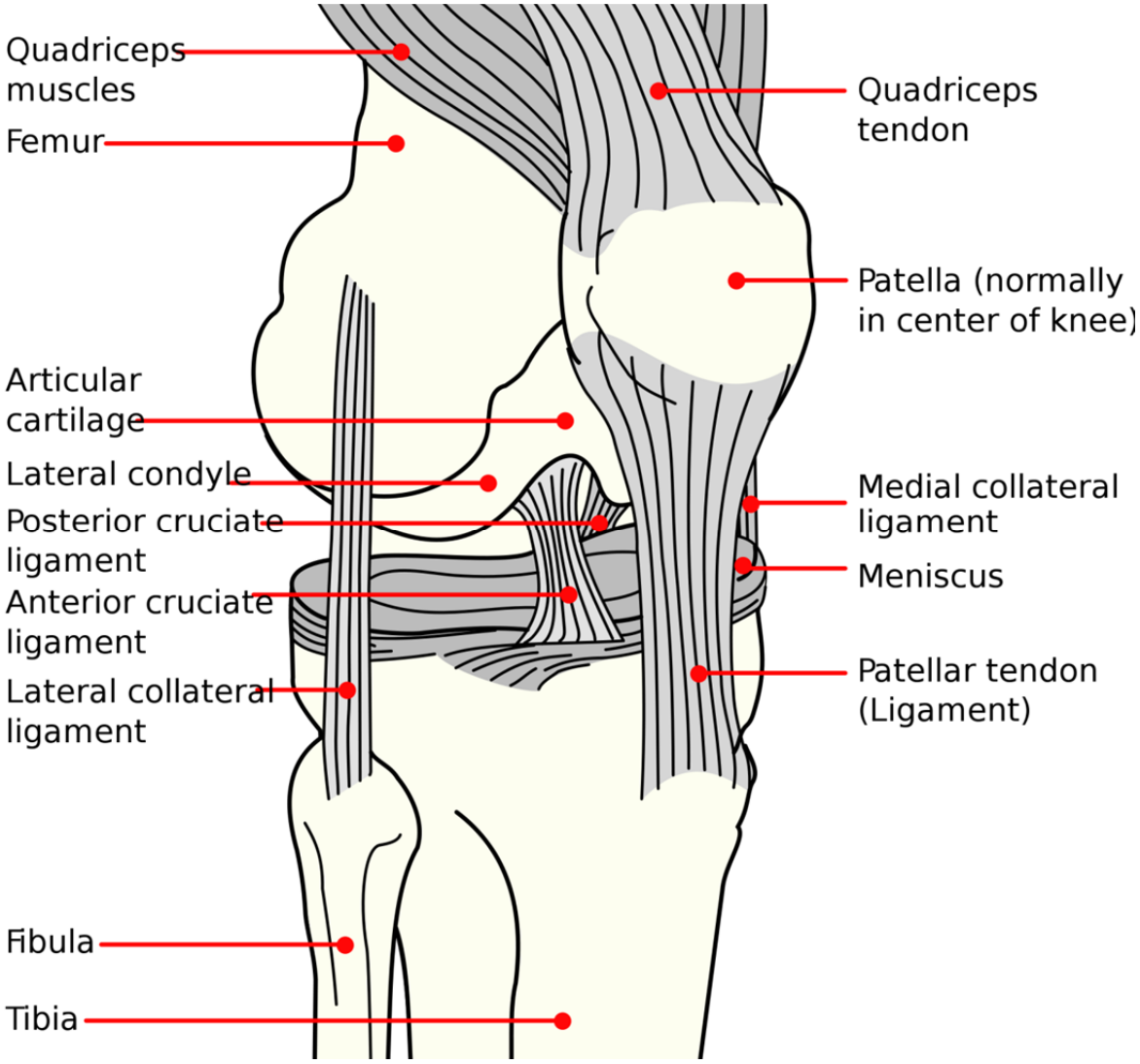

Fig. 2.3. Schematic of right knee anatomy.

to the tibia and are located between the femoral condyles. The ACL and PCL make a crossing pattern within the femoral notch such that the ACL resists anterior motion of the tibia with respect to the femur and the PCL resists posterior motion. The patella is connected to the tibia by the patellar tendon. Knee articulation is also aided by the meniscus, which is a fibrocartilagenous structure that sits on the tibial plateau.

MCL Structure and Function

The MCL is one of the most studied ligaments due to its high incidence of injury and relatively superficial location, and yet the definition of its anatomy has been debated [22, 23]. Historically, the MCL is considered to have two structural units: the superficial MCL and deep MCL [23]. The superficial MCL is the most prominent structure, consisting of long, vertical fibers running between a direct insertion on the medial femoral epicondyle to an indirect insertion on the medial side of the proximal tibia. This is the portion of the MCL that has been used for material characterization and modeled in computational studies [9, 18, 24, 25]. The deep MCL is a thickening of the joint capsule with short fibers that run adjacent to the medial meniscus and includes the meniscofemoral and meniscotibial ligaments [22]. The deep MCL is generally thought to provide connections between the medial meniscus and the tibia and femur. This portion has not been characterized and has not been included in computational models. The final portion of the MCL consists of posterior oblique fibers that run between the superficial MCL and the posterior part of the knee capsule. Historically, this portion has been considered part of the superficial MCL [23], but more recently it has been thought of as a

third structural unit [22]. Regardless of the exact definition, the posterior oblique portion of the MCL has not been characterized or included in computational models.

The MCL is a primary restraint to valgus knee rotation and internal tibial rotation, and a secondary restraint to anterior tibial translation. These functions have been directly attributed to specific parts of the MCL's structure. The superficial MCL is a primary restraint to valgus knee rotation [23, 26-28] and internal tibial rotation [23, 27-29], as well as being a secondary restraint to anterior tibial translation [27, 29]. The deep MCL is a primary restraint to interior tibial rotation [23, 27-29] and a secondary restraint to anterior tibial translation [27, 29]. The posterior oblique fibers that run between the superficial MCL and the posterior part of the knee capsule aid the superficial MCL in restraining the tibial translation and rotation.

ACL Structure and Function

The ACL is the most injured ligament in the knee, and the ACL and MCL are often injured together [30, 31]. The ACL is comprised of two bundles of collagen fibers that directly insert into the ridge on the tibial plateau in an oval shaped footprint and to the inside of the femoral notch, on the lateral condyle, in an "L" shaped footprint. It has been reported that the ACL and MCL share responsibilities in restraining anterior tibial translation and valgus knee rotation. The ACL is the primary restraint to anterior tibial translation and a secondary restraint to valgus knee rotation [26, 27, 32-37].

IGHL Structure and Function

Glenohumeral Capsule Structure

The glenohumeral capsule and specifically the IGHL portion of the glenohumeral capsule is another focus of this research due to its high incidence of injury and poor clinical outcomes following repair. The glenohumeral capsule is a continuous sheet of fibrous tissue [38] that encircles and attaches to the head of the humerus and the glenoid portion of the scapula. Along this continuous tissue are five discrete thickenings that run between the humerus and glenoid, known as the glenohumeral ligaments [39, 40]. Burkart et al. provide wonderful images of the glenohumeral ligaments and their insertion sites from a cadaver dissection [40]. The glenohumeral ligaments include the superior glenohumeral ligament (SGHL), the middle glenohumeral ligament (MGHL), the anterior band of the IGHL, the posterior band of the IGHL, and the long head of the biceps tendon. Further, there is a structure commonly referred to as the axillary pouch of the IGHL that is a thinner structure and not one of the glenohumeral ligaments, but it is studied as part of the IGHL because it is located between the anterior and posterior bands of the IGHL. On the glenoid, the glenohumeral ligaments blend into the glenoid labrum, which is a vascularized ring of fibrous tissue extending distally from the glenoid [41]. On the humerus, the glenohumeral ligaments directly attach to locations around the humeral head, adjacent to the articulating surface. For example, the SGHL and MGHL insert just superior and just medial to the lesser tuberosity, respectively, while the IGHL inserts just below the articular margin of the humeral head. The anatomy of the glenohumeral ligaments have been studied through cadaver dissections [42, 43] and observations made during surgery [44, 45] for decades. These studies, as well as recent

arthroscopic examinations have reported a high variability in size and appearance [46, 47].

Inferior Glenohumeral Ligament Structure

The IGHL is composed of three structures: the anterior band, posterior band and the axillary pouch. In general, the delineation of these structures and the boundaries of the IGHL are defined by the thickenings of the anterior and posterior bands. Although the thicker bands are used to define the boundaries of the structures, the collagen fiber structure within and between these structures is not easily defined and is still debated in the literature [39, 48]. In an effort to better understand the collagen fiber structure of the IGHL, the orientation of the collagen fibers has been examined qualitatively utilizing standard and polarized light microscopy [39, 41, 48, 49]. One study reported that the collagen fibers in the axillary pouch are less organized than either the anterior or posterior bands, and that there is a great deal of intermingling of the fibers [39]. This study also pointed out that in some shoulders, the three regions of the IGHL are best visualized when the capsule is loaded by placing the humeral head in internal or external rotation in varying degrees of abduction. In contrast, another study found an organized pattern of collagen fibers in the axillary pouch [48]. The collagen fibers were predominantly oriented in the direction of the anterior and posterior bands. Both studies reported that the collagen fibers in the bands are more aligned than those in the axillary pouch [39, 48].

Glenohumeral Capsule Function

The glenohumeral capsule provides passive stability in the extreme positions of glenohumeral joint motion and is most effective at stabilizing the joint when the joint is externally rotated [50]. At the midrange of motion, where the shoulder muscles provide active stability, the entire capsule is relatively lax and plays a small role in stability [51, 52]. The contributions of the glenohumeral ligaments to joint stability have primarily been elucidated through selective sectioning experiments [50, 52, 53]. From these studies it has been shown that the SGHL limits external rotation in the lower range of abduction [52]. It has also been shown that during the midrange of abduction, the MGHL and the anterior band of the IGHL provide anterior restraint and at 90° of abduction the anterior band and the axillary pouch of the IGHL are the dominant anterior stabilizers. Finally, the lower portion of the anterior capsule became the dominant restraint as abduction increased with the humerus externally rotated [53].

Clinical Exams to Diagnose Shoulder Instability

During clinical exams to diagnose shoulder instability, clinicians apply forces to the humerus to translate the humeral head with respect to the glenoid. This produces strains in the glenohumeral capsule [54, 55] because it is the primary stabilizer of the glenohumeral joint in the examination position. The magnitudes of the resulting translations are then graded [56]. Assessments are based on the application of a manual maximum force so that a firm end point is reached, restricting further translation [56-58]. The orientation of the glenohumeral joint has been shown to influence both the magnitude of the translations [59] and the clinician's diagnostic reproducibility [60, 61].

Further, intra- and interobserver repeatability of clinical exams is quite poor [60]. Finally, as the external rotation angle is increased patients often feel a sense of apprehension and/or discomfort caused by the exam [62-64]. The patient's indication of apprehension and/or pain is useful for the physician to help diagnose the injury, but this method is purely subjective, depending as much on the patient's pain threshold as on the extent of the injury.

There are currently three clinical exams commonly used to test for shoulder instability. They are the Simple Translation Test, Load and Shift Test, and Anterior Drawer Test. During the Simple Translation Test, the examiner stands behind the patient, positions the shoulder in abduction and external rotation, and stabilizes the shoulder girdle with one hand while the other grasps the proximal humerus. The test is performed by applying a minimally compressive load to center the humerus in the glenoid, followed by pushing the humerus forward to determine the amount of anterior translation relative to the scapula. At the initiation of the Load and Shift Test, the humeral head is "loaded" by pushing the humeral head into the glenoid and then "shifted" in the anterior, posterior, or inferior direction to slide the humeral head out of the glenoid. The compressive load is applied by holding the elbow and applying an axial load along the shaft of the humerus, while the shifting load is applied by the opposite hand at the mid-shaft of the humerus. To assess the amount of translation, clinicians describe the feel of the humeral head relative to the glenoid and use a numeric grading system that is nonstandardized. The Anterior Drawer Test is similar to the Simple Translation Test. However clinician positioning during loading and the joint position are different. These clinical exams are performed with the patient's torso in multiple positions as well as with the patient's arms

in multiple orientations. After determining the amount of translation, clinicians always try to correlate the findings with the patient's symptoms, and compare the results to the contralateral shoulder.

Finite Element Modeling of Ligaments

This dissertation research uses a combined experimental and computational approach to study ligament mechanics during boundary and loading conditions that simulate clinical exams. The computational side of the research utilizes the finite element (FE) method, which is a numerical solution technique for discretizing and analyzing discrete systems [65]. There are essentially four steps to analyzing a discrete system, which remain the same whether the problem is static or dynamic, linear or nonlinear, and regardless of the initial, boundary, and loading conditions. The four steps are the idealization of the system, establishment of equilibrium conditions, assemblage of the discrete element system into a set of simultaneous equations, and solution of these equations to determine the response of the state variables [66]. The FE method is very powerful and has been widely used in the field of biomechanics, but although it is often applied, it is not always used appropriately or accurately. A number of items must be considered to apply the FE method correctly to the modeling of diarthrodial joint ligaments. Ligament models often include complicated three-dimensional geometry, nonlinear and/or inhomogeneous material properties, and complex initial, boundary and loading conditions. Further, to insure predications from the model are accurate enough for their intended use, appropriate verification and validation methods must be utilized.

An overview of each of these topics will be addressed in the remainder of this chapter to facilitate the reader's understanding of the following chapters.

Diathrodial joint structures are quite complicated and representing their geometry accurately is very difficult, but an accurate representation of geometry is absolutely critical if the ensuing model predictions are to be trusted. Chapters 3 through 5 describe the creation and use of subject-specific FE models. The term "subject-specific" in these chapters refers to the use of a specific cadaveric specimen's anatomy, but could also refer to a specific living human's anatomy. Medical image data from computed tomography (CT) and magnetic resonance imaging (MRI) have been used in many studies to acquire the ligament, cartilage, and bone geometry from cadaveric specimens and living humans for the purpose of building subject-specific FE models [18, 67-73]. Both CT and MRI have strengths and weaknesses for acquiring the data necessary to construct subject-specific FE models and a good discussion of these can be found in Weiss et al. [74].

As discussed earlier in this chapter, the stress-strain response of ligaments to quasi-static, uniaxial, tensile loading along the predominant fiber direction is nonlinear with an upwardly concave region. Representing this behavior accurately for the loading and boundary conditions that simulate clinical exams for the knee and shoulder is arguably accomplished best with a hyperelastic constitutive equation, as was used for the FE models in Chapters 3. The models in Chapters 4 and 5 use a hypoelastic constitutive equation to represent the IGHL, which provides a reasonable approximation of the tissues response to the boundary and loading conditions. The limitations of this approach are discussed thoroughly in Chapter 4. An appropriate algorithm for representing in situ strain must also be used when necessary. A thorough discussion of constitutive modeling

of ligaments is beyond the scope of this dissertation, but can be found in Weiss et al. [74]. Also, as discussed earlier, ligaments attach to and make contact with bones during regular motions, including those seen during clinical exams. That means the bone material must also be represented appropriately for the model predictions to be accurate. Since the stiffness of bone is several orders of magnitude higher than the stiffness of ligament, bone has been appropriately represented in many FE models as a rigid body [18, 38, 68-70, 72, 73, 75-77]. In the shoulder, the capsule also makes contact with the femoral cartilage during clinical exams. The appropriate material representation for cartilage in this scenario had not been addressed until this dissertation research (Chapter 4).

Contact is arguably the most difficult boundary condition to represent accurately when modeling diarthrodial joint ligaments. Enforcing the constraint that there is no interpenetration between the ligament and bone structures is especially difficult due to the very large difference in stiffness between the relatively soft ligament tissue and the rigid body representation for bone. This has been accomplished using both a penalty method and an augmented lagrangian routine [78, 79]. The problem is made somewhat easier because the generally smooth bone surfaces and moist environment associated with diarthrodial joints allows the use of frictionless sliding contact in these models.

The other boundary and loading conditions associated with ligament FE models originate from the validation experiments that provide a "gold standard" for which to compare the model predictions. For this reason, it will help the reader to first have a basic understanding of the concepts of verification and validation, which were explained very well in our review article [80]:

> Verification and validation (V&V) are processes by which evidence is generated and credibility is thereby established that a computer model yields results with sufficient accuracy for its intended use [81]. More specifically, verification is the process of determining that a model implementation accurately represents the conceptual description and solution to the model [82]. Validation is a process by which computational predictions are compared to experimental data (the "gold standard") in an effort to assess the modeling error. Put simply, verification deals with "solving the equations right" whereas validation is the process of "solving the right equations" [83].

For this dissertation research, verification was associated with ensuring that the proper element type was used for the discretization and that an adequately fine mesh resolution was used to discretize the structures, as determined by a mesh convergence study. It should also be noted that the FE code, NIKE3D, that was used for all analyses for this dissertation research was previously verified [84].

When designing a study that uses a combined experimental and computational approach with the intention of using measurements from the experiments to validate the predictions from the models, the boundary and loading conditions used for the analyses must match the experiments. If not, it is likely that the model predictions will not compare well to the "gold standard" experimental data. This may seem obvious, but in practice it can be quite difficult to accomplish, and the problems that occur are often on the experimental side of the study. Inaccurate kinematics and/or load cell measurements as well as poor quality experimental fixtures are all common causes of boundary and loading conditions not matching between the experiments and the analyses. It is also important to pick the right gold standard metric to compare between the experiment and analysis. For the research in the next chapter and for the validation study that built upon the research in Chapter 4 [38], tissue strain was used for the comparison metric. This is usually described as a local metric because it looks at the local tissue strain in response to

the more globally applied loading and boundary conditions. This is in contrast to a global metric, like the bone rigid body reaction forces, which is also appropriate for some studies [85].

To summarize this chapter, a background on ligament constituents, structure and function as well as the diarthrodial joints they are part of was discussed so the reader can understand what was being modeled using the FE method. The FE method, itself, was then explained briefly and the factors directly involved with modeling ligaments discussed, so the reader can understand the process being utilized in the following chapters.

References

[1] Amiel, D., Frank, C., Harwood, F., Fronek, J., and Akeson, W., 1984, "Tendons and ligaments: a morphological and biochemical comparison," Journal of Orthopaedic Research : Official Publication of the Orthopaedic Research Society, 1(3), pp. 257-65.

[2] Daniel DM, A.W., O'Connor JJ, ed. *Knee Ligaments: Structure, Function, Injury and Repair.* 1990, New York: Raven Press.

[3] Minns RJ, S.P., Jackson DS, 1973, "The role of the fibrous components and ground substance in the mechanical properties of biological tissues: a preliminary investigation.," J Biomechanics, 6, pp. 153-165.

[4] Woo SL-Y, B.J., ed. *Injury and Repair of the Musculoskeletal Soft Tissues.* ed. A.A.O.O. Surgeons.1990, Illinois: Park Ridge.

[5] Kastelic, J., Galeski, A., and Baer, E., 1978, "The multicomposite structure of tendon," Connect Tissue Res, 6(1), pp. 11-23.

[6] Reese, S.P., Maas, S.A., and Weiss, J.A., 2010, "Micromechanical models of helical superstructures in ligament and tendon fibers predict large Poisson's ratios," Journal of Biomechanics, 43(7), pp. 1394-400.

[7] Dale, W.C., Baer, E., 1974, "Fibre-buckling in composite systems: a model for the ultra-structure of uncalcified collagen tissue.," J Mater Sci, 9, pp. 369-382.

[8] Viidik, A., *Structure and function of normal and healing tendons and ligaments.*, in *In Biomechanics of Diarthrodial Joints*1990, Springer-Verlag: New York. pp. 3-38.

[9] Quapp, K.M. and Weiss, J.A., 1998, "Material characterization of human medial collateral ligament," J Biomech Eng, 120(6), pp. 757-63.

[10] Tanzer, M.L., 1973, "Cross-linking of collagen," Science, 180, pp. 357-370.

[11] Frank, C., Akeson, W.H., Woo, S.L., Amiel, D., and Coutts, R.D., 1984, "Physiology and therapeutic value of passive joint motion," Clinical Orthopaedics and Related Research, (185), pp. 113-25.

[12] Ogston, A.G., ed. *The Biological Functions of the Glycosaminoglycans*. Chemistry and Molecular Biology of the Intercellular Matrix, ed. E.A. Balasz. Vol. 3. 1970, London: Academic Press.

[13] Hannafin, J.A. and Arnoczky, S.P., 1994, "Effect of cyclic and static tensile loading on water content and solute diffusion in canine flexor tendons: an in vitro study," Journal of Orthopaedic Research : Official Publication of the Orthopaedic Research Society, 12(3), pp. 350-6.

[14] Atkinson, T.S., Haut, R.C., and Altiero, N.J., 1997, "A poroelastic model that predicts some phenomenological responses of ligaments and tendons," Journal of Biomechanical Engineering, 119(4), pp. 400-5.

[15] Yin, L. and Elliott, D.M., 2004, "A biphasic and transversely isotropic mechanical model for tendon: application to mouse tail fascicles in uniaxial tension," Journal of Biomechanics, 37(6), pp. 907-16.

[16] Adeeb, S., Ali, A., Shrive, N., Frank, C., and Smith, D., 2004, "Modelling the behaviour of ligaments: a technical note," Comput Methods Biomech Biomed Engin, 7(1), pp. 33-42.

[17] Wellen, J., Helmer, K.G., Grigg, P., and Sotak, C.H., 2004, "Application of porous-media theory to the investigation of water ADC changes in rabbit Achilles tendon caused by tensile loading," Journal of Magnetic Resonance, 170(1), pp. 49-55.

[18] Gardiner, J.C. and Weiss, J.A., 2003, "Subject-specific finite element analysis of the human medial collateral ligament during valgus knee loading," J Orthop Res, 21(6), pp. 1098-106.

[19] Woo, S.L., Weiss, J.A., Gomez, M.A., and Hawkins, D.A., 1990, "Measurement of changes in ligament tension with knee motion and skeletal maturation," Journal of Biomechanical Engineering, 112(1), pp. 46-51.

[20] Cooper, R.R. and Misol, S., 1970, "Tendon and ligament insertion. A light and electron microscopic study," The Journal of Bone and Joint Surgery. American volume, 52(1), pp. 1-20.

[21] Benjamin, M., Evans, E.J., and Copp, L., 1986, "The histology of tendon attachments to bone in man," Journal of Anatomy, 149, pp. 89-100.

[22] De Maeseneer, M., Van Roy, F., Lenchik, L., Barbaix, E., De Ridder, F., and Osteaux, M., 2000, "Three layers of the medial capsular and supporting structures of the knee: MR imaging-anatomic correlation," Radiographics, 20 Spec No, pp. S83-9.

[23] Warren, L.F. and Marshall, J.L., 1979, "The supporting structures and layers on the medial side of the knee: an anatomical analysis," J Bone Joint Surg Am, 61(1), pp. 56-62.

[24] Gardiner, J.C. and Weiss, J.A., 2001, "Simple shear testing of parallel-fibered planar soft tissues," J Biomech Eng, 123(2), pp. 170-5.

[25] Gardiner, J.C., Weiss, J.A., and Rosenberg, T.D., 2001, "Strain in the human medial collateral ligament during valgus loading of the knee," Clin Orthop, (391), pp. 266-74.

[26] Grood, E.S., Noyes, F.R., Butler, D.L., and Suntay, W.J., 1981, "Ligamentous and capsular restraints preventing straight medial and lateral laxity in intact human cadaver knees," J Bone Joint Surg Am, 63(8), pp. 1257-69.

[27] Markolf, K.L., Mensch, J.S., and Amstutz, H.C., 1976, "Stiffness and laxity of the knee--the contributions of the supporting structures. A quantitative in vitro study," J Bone Joint Surg Am, 58(5), pp. 583-94.

[28] Seering, W.P., Piziali, R.L., Nagel, D.A., and Schurman, D.J., 1980, "The function of the primary ligaments of the knee in varus-valgus and axial rotation," J Biomech, 13(9), pp. 785-94.

[29] Shoemaker, S.C. and Markolf, K.L., 1985, "Effects of joint load on the stiffness and laxity of ligament-deficient knees. An in vitro study of the anterior cruciate and medial collateral ligaments," J Bone Joint Surg Am, 67(1), pp. 136-46.

[30] Hull, M.L., 1997, "Analysis of skiing accidents involving combined injuries to the medial collateral and anterior cruciate ligaments," Am J Sports Med, 25(1), pp. 35-40.

[31] Miyasaka, K., et al., 1991, "The incidence of knee ligament injuries in the general population," Am J Knee Surg, 4(1), pp. 3-8.

[32] Abramowitch, S.D., Yagi, M., Tsuda, E., and Woo, S.L., 2003, "The healing medial collateral ligament following a combined anterior cruciate and medial collateral ligament injury--a biomechanical study in a goat model," J Orthop Res, 21(6), pp. 1124-30.

[33] Ichiba, A., Nakajima, M., Fujita, A., and Abe, M., 2003, "The effect of medial collateral ligament insufficiency on the reconstructed anterior cruciate ligament: a study in the rabbit," Acta Orthop Scand, 74(2), pp. 196-200.

[34] Kanamori, A., Sakane, M., Zeminski, J., Rudy, T.W., and Woo, S.L., 2000, "In-situ force in the medial and lateral structures of intact and ACL-deficient knees," J Orthop Sci, 5(6), pp. 567-71.

[35] Lujan, T.J., Dalton, M.S., Thompson, B.M., Ellis, B.J., Rosenberg, T.D., and Weiss, J.A., 2005, "MCL strains and joint kinematics in the ACL-deficient and posteromedial meniscus injured knee," American Journal of Sports Medicine, In Review.

[36] Moglo, K.E. and Shirazi-Adl, A., 2003, "Biomechanics of passive knee joint in drawer: load transmission in intact and ACL-deficient joints," Knee, 10(3), pp. 265-76.

[37] Robins, A.J., Newman, A.P., and Burks, R.T., 1993, "Postoperative return of motion in anterior cruciate ligament and medial collateral ligament injuries. The effect of medial collateral ligament rupture location," Am J Sports Med, 21(1), pp. 20-5.

[38] Moore, S.M., Ellis, B., Weiss, J.A., McMahon, P.J., and Debski, R.E., 2010, "The glenohumeral capsule should be evaluated as a sheet of fibrous tissue: a validated finite element model," Annals of Biomedical Engineering, 38(1), pp. 66-76.

[39] O'Brien, S.J., Neves, M.C., Arnoczky, S.P., Rozbruck, S.R., Dicarlo, E.F., Warren, R.F., Schwartz, R.E., and Wickiewicz, T.L., 1990, "The anatomy and histology of the inferior glenohumeral ligament complex of the shoulder," Am J Sports Med, 18(5), pp. 449-56.

[40] Burkart, A.C. and Debski, R.E., 2002, "Anatomy and function of the glenohumeral ligaments in anterior shoulder instability," Clinical Orthopaedics and Related Research, (400), pp. 32-9.

[41] Cooper, D.E., Arnoczky, S.P., O'Brien, S.J., Warren, R.F., DiCarlo, E., and Allen, A.A., 1992, "Anatomy, histology, and vascularity of the glenoid labrum. An

anatomical study," The Journal of Bone and Joint Surgery. American volume, 74(1), pp. 46-52.

[42] Ferrari, D.A., 1990, "Capsular ligaments of the shoulder. Anatomical and functional study of the anterior superior capsule," The American Journal of Sports Medicine, 18(1), pp. 20-4.

[43] Sarrafian, S.K., 1983, "Gross and functional anatomy of the shoulder," Clinical Orthopaedics and Related Research, (173), pp. 11-9.

[44] Neer, C.S., 2nd and Foster, C.R., 1980, "Inferior capsular shift for involuntary inferior and multidirectional instability of the shoulder. A preliminary report," The Journal of Bone and Joint Surgery. American volume, 62(6), pp. 897-908.

[45] Rowe, C.R., Patel, D., and Southmayd, W.W., 1978, "The Bankart procedure: a long-term end-result study," The Journal of Bone and Joint Surgery. American volume, 60(1), pp. 1-16.

[46] Warner, J.J.P., Caborn, D.N., Berger, R., Fu, F.H., and Seel, M., 1993, "Dynamic capsuloligamentous anatomy of the glenohumeral joint," J Should Elbow Surg, 2, pp. 115-33.

[47] Warner, J.J.P., Deng, X.H., Warren, R.F., and Torzilli, P.A., 1992, "Static capsuloligamentous restraints to superior-inferior translation of the glenohumeral joint," Am J Sports Med, 20(6), pp. 675-85.

[48] Gohlke, F., Essigkrug, B., Schmitz, F., 1994, "The patterns of the collagen fiber bundles of the capsule of the glenohumeral joint," J Shoulder Elbow Surg, 3(3), pp. 111-28.

[49] Clark, J.M. and Harryman, D.T., 2nd, 1992, "Tendons, ligaments, and capsule of the rotator cuff. Gross and microscopic anatomy," The Journal of Bone and Joint Surgery. American volume, 74(5), pp. 713-25.

[50] Malicky, D.M., Soslowsky, L.J., Blasier, R.B., and Shyr, Y., 1996, "Anterior glenohumeral stabilization factors: progressive effects in a biomechanical model," Journal of Orthopaedic Research: Official Publication of the Orthopaedic Research Society, 14(2), pp. 282-8.

[51] Debski, R.E., Wong, E.K., Woo, S.L.-Y., Sakane, M., Fu, F.H., and Warner, J.J., 1999, "In situ force distribution in the glenohumeral joint capsule during anterior-posterior loading," J Orthop Res, 17(5), pp. 769-76.

[52] Turkel, S.J., Panio, M.W., Marshall, J.L., and Girgis, F.G., 1981, "Stabilizing mechanisms preventing anterior dislocation of the glenohumeral joint," J Bone Joint Surg Am, 63(8), pp. 1208-17.

[53] Ovesen, J. and Nielsen, S., 1985, "Stability of the shoulder joint. Cadaver study of stabilizing structures," Acta Orthopaedica Scandinavica, 56(2), pp. 149-51.

[54] Malicky, D.M., Kuhn, J.E., Frisancho, J.C., Lindholm, S.R., Raz, J.A., and Soslowsky, L.J., 2002, "Neer Award 2001: nonrecoverable strain fields of the anteroinferior glenohumeral capsule under subluxation," J Shoulder Elbow Surg, 11(6), pp. 529-40.

[55] Moore, S.M., Stehle, J.H., Rainis, E.J., McMahon, P.J., Debski, R.E., 2008, "The Current Anatomical Description of the Inferior Glenohumeral Ligament Does Not Correlate with its Functional Role in Positions of External Rotation," Journal of Orthopaedic Research, In Press.

[56] Rockwood, C.A., F.A. Matsen, 3rd, M.A. Wirth, and D.T.Harryman, 2nd,, 1998, "*The Shoulder*," 2nd ed. 1998, Philadelphia, PA: W. B. Saunders Co.

[57] Harryman, D.T., 2nd, Sidles, J.A., Matsen, F.A., 3rd, 1992, "Laxity of the normal glenohumeral joint: a quantitative in vivo assessment," J Should Elbow Surg, 1, pp. 66-76.

[58] Lippitt, S. and Matsen, F., 1993, "Mechanisms of glenohumeral joint stability," Clin Orthop Relat Res, (291), pp. 20-8.

[59] Moore, S.M., Musahl, V., McMahon, P.J., and Debski, R.E., 2004, "Multidirectional kinematics of the glenohumeral joint during simulated simple translation tests: impact on clinical diagnoses," J Orthop Res, 22(4), pp. 889-94.

[60] Levy, A.S., Lintner, S., Kenter, K., and Speer, K.P., 1999, "Intra- and interobserver reproducibility of the shoulder laxity examination," Am J Sports Med, 27(4), pp. 460-3.

[61] Tzannes, A., Paxinos, A., Callanan, M., and Murrell, G.A., 2004, "An assessment of the interexaminer reliability of tests for shoulder instability," J Shoulder Elbow Surg, 13(1), pp. 18-23.

[62] Gerber, C. and Ganz, R., 1984, "Clinical assessment of instability of the shoulder. With special reference to anterior and posterior drawer tests," J Bone Joint Surg Br, 66(4), pp. 551-6.

[63] Lo, I.K., Nonweiler, B., Woolfrey, M., Litchfield, R., and Kirkley, A., 2004, "An evaluation of the apprehension, relocation, and surprise tests for anterior shoulder instability," Am J Sports Med, 32(2), pp. 301-7.

[64] Silliman, J.F. and Hawkins, R.J., 1993, "Classification and physical diagnosis of instability of the shoulder," Clin Orthop Relat Res, (291), pp. 7-19.

[65] Zienkiewicz, O.C., Taylor, R.L., *The Finite Element Method, Volume 1: Basic Formulation and Linear Problems.*1989: London: McGraw-Hill.

[66] Bathe, K.-J., *Finite Element Procedures*1996: New Jersey: Prentice-Hall.

[67] Anderson, A.E., Ellis, B.J., Maas, S.A., Peters, C.L., and Weiss, J.A., 2008, "Validation of finite element predictions of cartilage contact pressure in the human hip joint," Journal of Biomechanical Engineering, 130(5), pp. 051008.

[68] Ellis, B.J., Debski, R.E., Moore, S.M., McMahon, P.J., and Weiss, J.A., 2007, "Methodology and sensitivity studies for finite element modeling of the inferior glenohumeral ligament complex," J Biomech, 40(3), pp. 603-12.

[69] Ellis, B.J., Lujan, T.J., Dalton, M.S., and Weiss, J.A., 2006, "Medial collateral ligament insertion site and contact forces in the ACL-deficient knee," Journal of Orthopaedic Research, 24(4), pp. 800-10.

[70] Ellis, B.J., Lujan, T.J., Dalton, M.S., and Weiss, J.A., 2006, "MCL insertion site and contact forces in the ACL-deficient knee," Journal of Orthopaedic Research, To Appear, December.

[71] Henak, C.R., Ellis, B.J., Harris, M.D., Anderson, A.E., Peters, C.L., and Weiss, J.A., 2011, "Role of the acetabular labrum in load support across the hip joint," Journal of Biomechanics, 44(12), pp. 2201-6.

[72] Li, G., Gil, J., Kanamori, A., and Woo, S.L., 1999, "A validated three-dimensional computational model of a human knee joint," Journal of Biomechanical Engineering, 121(6), pp. 657-62.

[73] Phatak, N.S., Sun, Q., Kim, S.E., Parker, D.L., Sanders, R.K., Veress, A.I., Ellis, B.J., and Weiss, J.A., 2007, "Noninvasive determination of ligament strain with deformable image registration," Annals of Biomedical Engineering, 35(7), pp. 1175-87.

[74] Weiss, J.A., Gardiner, J.C., Ellis, B.J., Lujan, T.J., and Phatak, N.S., 2005, "Three-dimensional finite element modeling of ligaments: technical aspects," Med Eng Phys, 27(10), pp. 845-61.

[75] Debski, R.E., Weiss, J.A., Newman, W.J., Moore, S.M., and McMahon, P.J., 2005, "Stress and strain in the anterior band of the inferior glenohumeral ligament during a simulated clinical examination," J Shoulder Elbow Surg, 14(1 Suppl), pp. S24-31.

[76] Drury, N.J., Ellis, B. J., Weiss, J. A., McMahon, P.J., Debski, R. E. , 2009, "The impact of glenoid labrum thickness and modulus on labrum and glenohumeral capsule pathology," Submitted.

[77] Drury, N.J., Ellis, B.J., Weiss, J.A., McMahon, P.J., and Debski, R.E., 2011, "Finding consistent strain distributions in the glenohumeral capsule between two subjects: implications for development of physical examinations," Journal of Biomechanics, 44(4), pp. 607-13.

[78] Laursen, T.A. and Maker, B.N., 1995, "Augmented Lagrangian quasi-newton solver for constrained nonlinear finite element applications," International Journal for Numerical Methods in Engineering, 38(21), pp. 3571-3590.

[79] Weiss, J.A., Schauer, D.A., Gardiner, J.C. *Modeling contact in biological joints using penalty and augmented Lagrangian methods*. in *ASME Winter Annual Meeting*. 1996.

[80] Anderson, A.E., Ellis, B.J., and Weiss, J.A., 2007, "Verification, validation and sensitivity studies in computational biomechanics," Computer Methods in Biomechanics and Biomedical Engineering, 10(3), pp. 171-84.

[81] ASME, *Guide for verification and validation in computational solid mechanics*, 2006, American Society of Mechanical Engineers.

[82] AIAA, *AIAA Guide for the verification and validation of computational fluid dynamics simulations*, 1998, American Institute of Aeronautics and Astronautics: Reston, VA.

[83] Boehm, B.W., *Software Engineering Economics* 1981, Englewood Cliffs, New Jersey: Prentice Hall.

[84] Maker, B.N., 1995, "NIKE3D: A nonlinear, implicit, three-dimensional finite element code for solid and structural mechanics," Lawrence Livermore Lab Tech Rept, UCRL-MA-105268.

[85] Elkins, J.M., Stroud, N.J., Rudert, M.J., Tochigi, Y., Pedersen, D.R., Ellis, B.J., Callaghan, J.J., Weiss, J.A., and Brown, T.D., 2011, "The capsule's contribution to total hip construct stability - A finite element analysis," Journal of Orthopaedic Research: Official Publication of the Orthopaedic Research Society.

CHAPTER 3

MCL INSERTION SITE AND CONTACT FORCES IN THE ACL-DEFICIENT KNEE [1]

Abstract

The objectives of this research were to determine the effects of ACL deficiency on MCL insertion site and contact forces during anterior tibial loading and valgus loading using a combined experimental-finite element (FE) approach. Our hypothesis was that ACL deficiency would increase MCL insertion site forces at its attachment to the tibia and femur and increase contact forces between the MCL and these bones. Six male knees were subjected to varus-valgus and anterior-posterior loading at flexion angles of 0° and 30°. Three-dimensional joint kinematics and MCL strains were recorded during kinematic testing. Following testing, the MCL of each knee was removed to establish a stress-free reference configuration. An FE model of the femur-MCL-tibia complex was constructed for each knee to simulate valgus rotation and anterior translation at 0 and 30°, using subject-specific bone and ligament geometry and joint kinematics. A transversely isotropic hyperelastic material model with average material coefficients taken from a previous study was used to represent the MCL. Subject-specific MCL in situ strain

[1] Reprinted from *Journal of Orthopaedic Research*, Vol. 24, No. 4. Ellis, B.J., Lujan, T.J., Dalton, M.S., Weiss, J.A., *"MCL Insertion Site and Contact Forces in the ACL-Deficient Knee,"* pp: 800-810, 2006, with permission from Elsevier

distributions were used in each model. Insertion site and contact forces were determined from the FE analyses. FE predictions were validated by comparing MCL fiber strains to experimental measurements. The subject-specific FE predictions of MCL fiber stretch correlated well with the experimentally measured values (R2 = 0.953). ACL deficiency caused a significant increase in MCL insertion site and contact forces in response to anterior tibial loading. In contrast, ACL deficiency did not significantly increase MCL insertion site and contact forces in response to valgus loading, demonstrating that the ACL is not a restraint to valgus rotation in knees that have an intact MCL. When evaluating valgus laxity in the ACL-deficient knee, increased valgus laxity indicates a compromised MCL.

Introduction

The effect of anterior cruciate ligament (ACL) deficiency on the mechanical function of other knee ligaments remains unclear, although it is known that even knees with reconstructed ACLs often exhibit abnormal knee kinematics (27). The ACL is a primary restraint to anterior tibial translation and a secondary restraint to valgus rotation (1, 2, 5, 13, 14, 16, 19, 23, 26, 34, 35), while the medial collateral ligament (MCL) is a primary restraint to valgus rotation (1, 2, 10, 13, 14, 16, 19, 22, 23, 26, 34, 35) and a secondary restraint to anterior tibial translation (1, 2, 4, 5, 15, 19, 22, 28, 30, 34). The MCL is involved in approximately 40% of all severe knee injuries (24), while approximately 50% of partial MCL tears and 80% of complete MCL tears occur in conjunction with injury to other knee ligaments (6). In alpine skiing, the most common ligament that is injured in conjunction with the MCL is the ACL (12).

Animal studies have shown that MCL healing is substantially poorer in the case of a combined MCL/ACL injury than for an isolated MCL injury (1, 2, 5, 16, 34, 35). After 12 weeks of healing, MCLs from knees with combined MCL/ACL injuries had a tensile strength of only 10% of control values (35). It has been proposed that the healing MCL in the ACL-deficient knee is subjected to increased strains and forces as a result of ACL deficiency (1). An ACL graft acts as a stabilizer initially, but as it heals, forces are transferred to the MCL that hinder healing and result in a hypertrophy of the MCL with tissue of lower quality. As long as two years after injury, healing MCLs still had "significantly different biological composition, biomechanical properties, and matrix organization" (34).

Although animal studies have shown that the MCL may be at risk for injury in an ACL deficient knee, conclusions in the literature as to the exact contributions of the MCL and ACL to valgus stability vary within and between studies of ligament healing in animal models and joint kinematics in cadaver models. In animal models, the variation in results is confounded by the variation in the type of injury model used. Results from a rabbit healing study showed that valgus rotation does not increase over time in response to healing of the ACL graft after an O'Donoghue triad injury (rupture of the medial collateral ligament with removal of the anterior cruciate ligament and part of the medial meniscus) although anterior translation did significantly increase over the same healing period (5). The conclusions of this animal study that created an O'Donoghue triad injury are in contrast to other animal studies that have shown that there are higher ACL forces and increased valgus laxity in response to a valgus load in a MCL deficient knee (1, 2, 13, 14, 19, 23). Two previous cadaver studies concluded that valgus laxity is relatively

unaffected by ACL deficiency (10, 22) and Mazzocca et al. concluded that, "the ACL can be compromised in isolated grade III MCL injuries" caused by a valgus load (23). The actual insertion site and contact forces in the MCL in response to a valgus torque in the intact and ACL-deficient knee, which arguably are the most relevant data for interpretation of ligament contribution to joint function, are unknown.

The aim of this study was to examine the effects of ACL deficiency on MCL insertion site and contact forces when the knee is subjected to anterior tibial loading and valgus torque. It was hypothesized that ACL deficiency would cause an increase in MCL insertion site and contact forces in response to both loading conditions.

Methods

Overview

This study combined experimental and computational methods to determine the effect of ACL injury on MCL insertion site and contact forces during anterior tibial loading and valgus loading. Computed tomography (CT) images were used to obtain the subject-specific geometry of the femur, tibia and MCL in a series of six cadaveric knees. Each knee was tested with the ACL intact and the ACL completely severed. For each injury state the knee was subjected to anterior-posterior (A-P) translation and varus-valgus (V-V) rotation at two flexion angles (0° and 30°) with tibial rotation constrained and unconstrained while knee kinematics and MCL strains were recorded. Polygonal surfaces were extracted from the CT data and were used to generate subject-specific FE models of each knee. The FE models were analyzed under the experimentally measured kinematics to determine MCL strains, contact forces, and insertion site forces. FE

predicted fiber stretches were compared to experimental values as a means of validation and the effect of injury state, flexion angle, and tibial constraint on MCL insertion site and contact forces was determined.

Specimen Preparation and CT Scan

Six intact human male cadaver knees were used (donor age 60 ± 8.3 years). Preparation for testing followed the same protocol as Gardiner et al. (9), with the exception that additional contrast markers were used to define gauge lengths for measurement of MCL fiber strain. Markers were distributed along the visible fiber direction of the MCL in a 3x7 grid pattern, forming 18 gauge lengths (Fig. 3.1). Each gauge length was approximately 15 mm long. The position of the markers was chosen based on anatomical landmarks. The boundaries of the MCL insertion sites on the femur and tibia were marked with copper wires to aid with identification of their geometry in the volumetric CT images. Nylon kinematic blocks were fastened to the distal femur and proximal tibia (shown in Figure 3.1), while positioning blocks with three beveled cavities (not shown in figure), forming a right angle, were fastened to the proximal femur and distal tibia (18). After dissection, a volumetric CT scan was obtained for each knee at 0º flexion (slice thickness = 1.3 mm with 1.0 mm overlap, 142-168 mm field of view, 512×512 acquisition matrix).

Kinematic Testing

Following the CT scan, each knee was mounted in fixtures on a custom materials testing machine, which allowed both A-P translation and V-V rotation to be applied at

fixed flexion angles with constrained or unconstrained tibial axial rotation and unconstrained medial-lateral translation and joint distraction (Fig. 3.2). During testing, 10 cycles of A-P translation (load limits of ±100 N at 1.5 mm/sec) and 10 cycles of V-V rotation (torque limits of ±10 N-m at 1 degree/sec) were independently applied to the tibia. The A-P load and V-V torque limits were established so that they were large enough to achieve the terminal stiffness of the ligament without inflicting injury to the

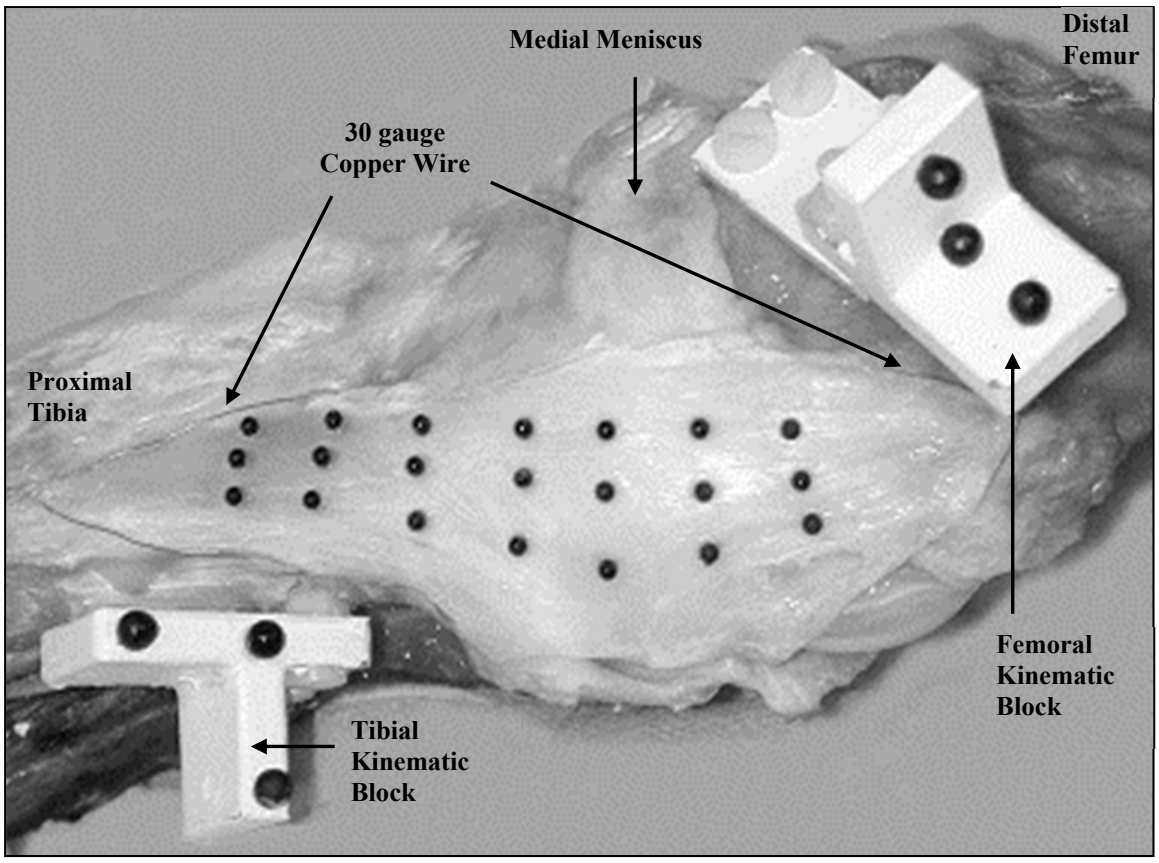

Fig. 3.1. Photograph of test setup for simultaneous measurement of MCL strain and knee joint kinematics. Twenty-one markers (2.38 mm dia.) defined 18 regions for strain measurement. Kinematic blocks were used to measure tibiofemoral kinematics during testing. Femoral and tibial kinematic blocks, each with three contrast markers (4.75 mm dia), were affixed to the cortical bone. The kinematic blocks were used to measure tibiofemoral kinematics and to register the CT data with the configuration of the knee during experimental testing. Insertion sites were marked with 30 gauge copper wire.

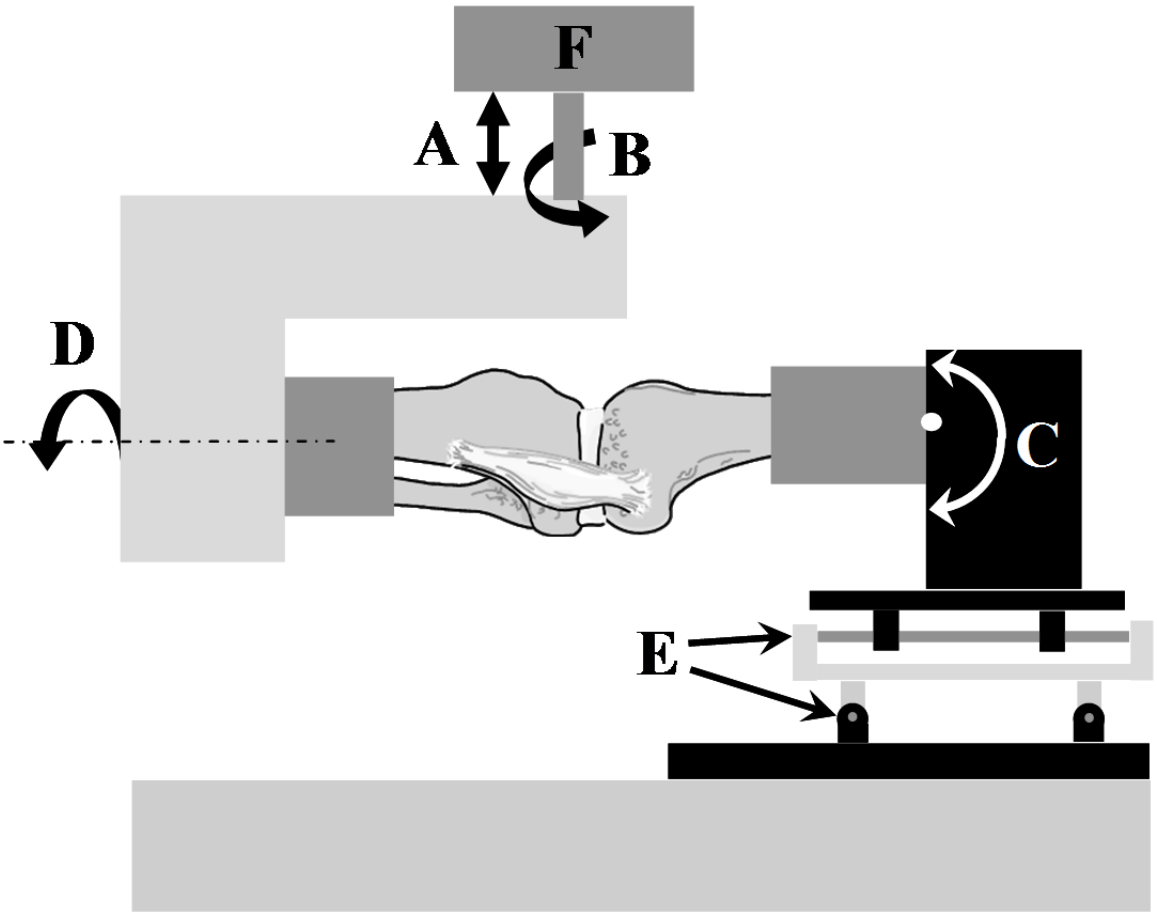

Fig. 3.2. Schematic of the loading apparatus, depicting a medial view of the knee at 0 degrees flexion. A – applied A-P translation. B - applied V-V rotation. C – adjustable flexion angle. D - constrained or unconstrained tibial axial rotation. E - unconstrained medial-lateral translation and joint distraction. F – load/torque cell.

tissue and thereby allowing multiple tests with the same specimen (7). A-P and V-V loading were conducted at 0° and 30° flexion. The tests were repeated with tibial axial rotation constrained and unconstrained at each flexion angle. The load and torque were measured with a multiaxis load cell (Futek T5105, Irvine, CA, accuracy ±2.2 N and ±0.056 N-m). Following the eight ACL intact tests, the ACL was transected through the midsubstance without damage to the PCL or removal of the knee from the fixture and all the tests were repeated. Finally, following ACL transection, the attachment of the medial meniscus to the MCL was transected. This test was performed to verify that the attachment did not influence joint kinematics and MCL strains under A-P and V-V loading; a similar conclusion was reached for the effect of the meniscus attachment on MCL strains in the intact knee in our previous study (9). To minimize hysteresis effects, data from the 10^{th} cycle of loading were analyzed for all tests.

Care was taken to ensure that the relative kinematic positions of the bones were duplicated for a given flexion angle and tibial axial rotation constraint for both injury states. When testing the intact knee, a neutral A-P and V-V position was determined at each flexion angle with tibial axial rotation unconstrained. The neutral A-P and V-V positions were determined by iteratively adjusting the starting position and running A-P and V-V motion cycles until the given load (±100 N) and torque (±10 N-m) limits produced equal anterior and posterior translation and equal varus and valgus rotations, respectively. Once these reference positions were established, actuator translation and rotation positions were logged so the positions could be restored after ACL transection.

The three-dimensional kinematic position of the femur relative to the tibia was verified through the use of a Microscribe digitizer (Immersion Corp, San Jose, CA, accuracy

±0.085 mm) in combination with the positioning blocks. The digitizer and positioning blocks were used to precisely determine the relative three dimensional kinematics of the femur and tibia (11). In this manner, positional repeatability between the different injury states was insured.

Measurement of Joint Kinematics and Ligament Strains

A digital motion analysis system consisting of two high-resolution digital cameras (Pulnix TM-1040, 1024x1024x30 fps, Sunnyvale, CA) and Digital Motion Analysis Software (DMAS, Spica Technology Corporation, Maui, HI) was used to record MCL strain in the 18 measurement regions and joint kinematics simultaneously (strain measurement accuracy: ±0.035 percent; joint kinematic translational accuracy: ±0.025 mm; joint kinematic rotational accuracy: ±0.124 degrees) (18).

In Situ Strain

At the conclusion of testing, the MCL was dissected from the bones and placed in a buffered saline bath for 10 minutes to allow the ligament to achieve a stress-free reference configuration. The 3D coordinates of the fiducial markers on the MCL were determined using the digital motion analysis system. This provided reference (zero-load) lengths for each strain region, l_0 (8, 9, 35). These values were combined with length measurements taken during the kinematic testing to calculate in situ fiber strain between marker pairs. These data were used as input to the subject-specific FE models (9, 32).

CT Scan, Surface Reconstruction and FE Mesh Generation

Using the copper insertion site wires and MCL strain contrast markers as guides, cross-sectional contours of the MCL, femur, and tibia were extracted from the CT dataset (SurfDriver, Kailua, Hawaii). Polygonal surfaces were generated by stacking and lacing together the contours (3) and smoothing was applied (29). The polygons composing the surfaces of the femur and tibia were converted directly to shell elements and used to represent the bones as rigid bodies (21). The MCL surface was imported into FE preprocessing software (TrueGrid, XYZ Scientific, Livermore, CA) and a hexahedral mesh was created.

Constitutive Model

The MCL was represented as transversely isotropic hyperelastic, with the strain energy (W) (9):

$$W = F_1\left(\tilde{I}_1\right) + F_2\left(\tilde{\lambda}\right) + \frac{K}{2}\left(\ln(J)\right)^2. \quad (1)$$

Here, $\tilde{I}_1$ is the first deviatoric invariant, $\tilde{\lambda}$ is the deviatoric part of the stretch ratio along the local fiber direction, and J is the determinant of the deformation gradient, $\boldsymbol{F}$. The matrix strain energy $F_1\left(\tilde{I}_1\right)$ was chosen so that $\partial F_1 / \partial \tilde{I}_1 = C_1$, yielding the neo-Hookean constitutive model.

The derivatives of the fiber strain energy function $F_2\left(\tilde{\lambda}\right)$ were defined as a function of the fiber stretch:

$$\begin{aligned} \tilde{\lambda}\frac{\partial F_2}{\partial \lambda} &= 0, && \tilde{\lambda} \le 1; \\ \tilde{\lambda}\frac{\partial F_2}{\partial \lambda} &= C_3\left[\exp\left(C_4\left(\tilde{\lambda}-1\right)\right)-1\right], && 1 < \tilde{\lambda} < \lambda^*; \\ \tilde{\lambda}\frac{\partial F_2}{\partial \lambda} &= C_5\tilde{\lambda} + C_6, && \tilde{\lambda} \ge \lambda^*. \end{aligned} \tag{2}$$

C_3 scales the exponential stress, C_4 specifies the rate of collagen uncrimping, C_5 is the modulus of straightened collagen fibers, and λ^* is the stretch at which the collagen is straightened. The third term in Eq (1) represents the bulk (volumetric) response, with the bulk modulus K controlling the entire volumetric response of the material. The population-average material coefficients from Gardiner et al. were used (9): $C_1 = 1.44$ MPa, $\lambda^* = 1.062$ (no units), $C_3 = 0.57$ MPa, $C_4 = 48.0$ (no units), $C_5 = 467.1$ MPa. Population average material coefficients were used based on the finding that using average coefficients versus subject specific coefficients yielded no significant difference in the accuracy of FE strain predictions (33). Due to a lack of experimental data describing ligament bulk behavior, the bulk modulus was specified to be two orders of magnitude greater than C_1, yielding nearly incompressible material behavior (9).

Boundary Conditions

The experimentally measured kinematic dataset was used to prescribe the motion of the tibia relative to the femur in the FE analyses (9). The coordinates of the kinematic

blocks in both the CT and kinematic datasets allowed for correlation of the two datasets. The entire FE model was transformed so that the global coordinate system was aligned with the coordinate system of the femur kinematic block. Motion of the tibia was described using incremental translations and rotations referenced to the femur kinematic block (20, 21). The MCL mesh was attached to the bones by defining node sets, based on the area within the copper wires, at the proximal and distal ends of the MCL as the same rigid material as the femur and tibia, respectively. Contact was enforced using the penalty method.

Finite Element Analysis

The implicitly integrated FE code NIKE3D was used for all analyses (20). An automatic time stepping strategy was employed, with iterations based on a quasi-Newton method. Each analysis was performed in three parts. In the first part, the knee was moved from the position in which it was placed at the time of the CT scan to the initial testing position (either 0 or 30 degrees of flexion). During the second part, the experimentally measured in situ strains for a given flexion angle and injury state were applied to the MCL. During the third part the experimental kinematic motion was applied (either anterior translation or valgus rotation). FE results were analyzed with GRIZ (31).

Regional Strains, Insertion Site and Contact Forces

FE predicted fiber stretches for nodes within each measurement region were averaged. Average FE predicted fiber stretches were compared to the experimentally

measured values. The magnitude of ligament forces at the insertion sites and the magnitude of the resultant forces due to MCL-bone contact were obtained from the NIKE3D output.

Statistical Analysis

Regression analyses were used to evaluate the ability of the FE models to predict experimentally measured values of MCL fiber stretch. FE predictions of regional fiber stretch were determined as a function of location along the length of the MCL. The predicted stretches were calculated and tabulated for all six knees according to test case and compared to experimental results. Coefficients of determination (R^2), regression lines, and p-values were determined.

The effect of tibial axial rotation constraint on insertion site and contact forces was assessed with a paired t-test using all the force data (insertion site and contact forces for both injury states at both angles and both loading conditions). The effects of within-subject treatment (injury state and flexion angle) in response to anterior and valgus loading on insertion site and contact forces were assessed using 2-way repeated measures ANOVAs. The results of the paired t-test showed no significant effect of tibial constraint on insertion site and contact forces (see results section below), so only the force data for the tests with constrained tibial axial rotation were used in the 2-way ANOVAs. In cases when significance was found ($p<0.05$), multiple comparisons were performed using the Tukey procedure.

Results

Experimental Kinematics

Before ACL resection, the average anterior displacements at 0º and 30º knee flexion in response to a 100 N anterior tibial load were 6.8 ± 2.6 mm and 6.7 ± 2.2 mm, respectively. ACL transection significantly increased anterior displacement in response to a 100 N anterior tibial load (16.5 ± 6.1 mm and 20.8 ± 4.4 mm at 0º and 30º, respectively) ($p<0.001$ for both flexion angles). Before ACL transection, the average valgus rotation at 0º and 30º knee flexion in response to a 10 N-m valgus torque were 3.6 º ± 1.8 º and 5.1 º ± 2.0 º, respectively. ACL deficiency did not significantly change valgus rotation in response to a 10 N-m valgus torque (4.3 º ± 1.9 º and 5.3 º ± 1.7 º at 0º and 30º, respectively). Subsequent separation of the medial meniscus attachment had no significant effect on knee joint kinematics for both A-P and V-V loading (data not shown). Because there was no change in joint kinematics following separation of the medial meniscus from the MCL in the ACL-deficient knee, these data were not subsequently analyzed via FE analysis.

FE Predictions of Regional Fiber Stretch

The FE values for fiber stretch were excellent predictors of experimental fiber stretch. Regression analysis of FE predicted fiber stretch versus experimentally measured fiber stretch for all regions, knees and test cases of intact and ACL-deficient knees yielded a coefficient of determination of $R^2 = 0.953$ ($p=0.001$) (Fig. 3.3). Fringe plots of the FE fiber strain illustrate the MCL strain patterns and increases in strain caused by ACL-deficiency in response to anterior and valgus loading (Fig. 3.4). In response to both types

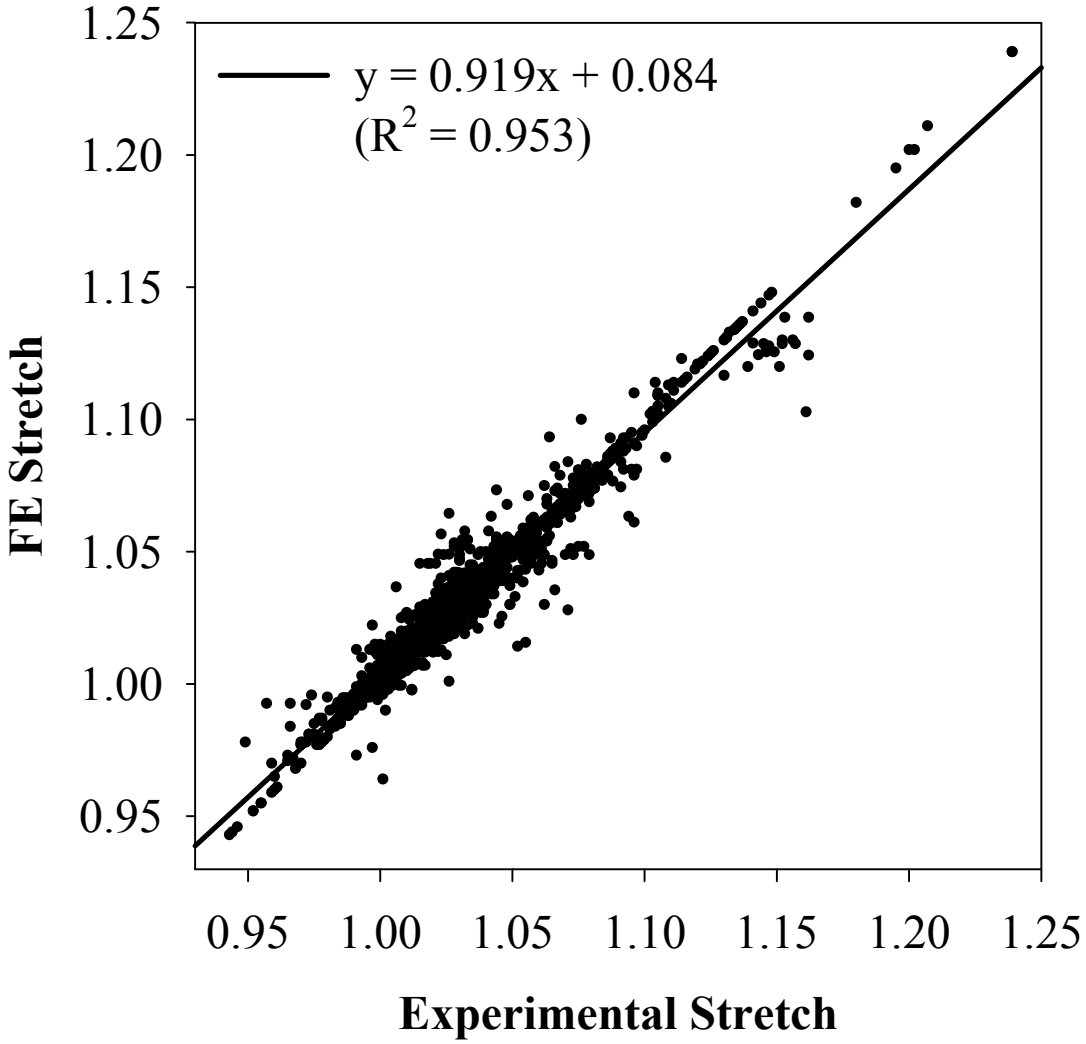

Fig. 3.3. FE predicted vs. experimental fiber stretch for all knees, test conditions, and measurement regions (N=1632).

of load and regardless of injury state, the highest MCL strains were found in the posterior-proximal region (17). MCL strain increased significantly in response to anterior loading when the ACL was injured, but the increase was not significantly different in response to a valgus load. Higher MCL strains tended to be more distributed in response to valgus loading than anterior loading regardless of injury state. A comprehensive set of MCL strain data as well as the kinematic data from this testing can be found in Lujan et al. (17).

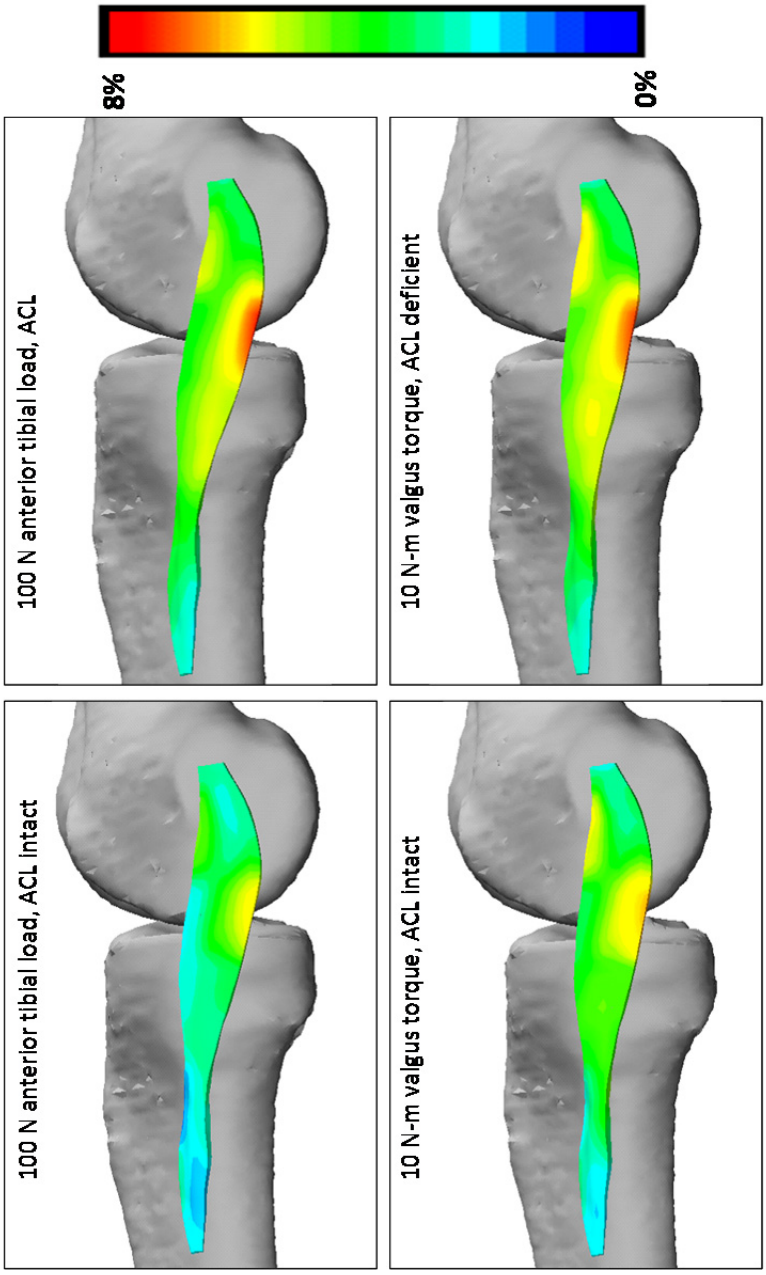

Fig. 3.4. Representative fringe plots of FE predicted fiber strain for a 100 N anterior load (top row) and a 10 N-m valgus load (bottom row) for the uninjured knee and the ACL-deficient knee. MCL strains increased in response to anterior tibial loading when the ACL was injured. MCL strains also increased locally in the ACL-deficient knee in response to a valgus torque, but these local increases did not result in significant changes in insertion site or contact forces.

Tibial Axial Rotation Constraint

A paired t-test using all insertion site and contact forces for both flexion angles and loading conditions showed that there was no effect of tibial axial rotation constraint on the predicted forces ($p = 0.154$).

Insertion Site Force

ACL deficiency caused significant increases in MCL insertion site forces at both the femur and tibia during anterior tibial translation. The forces at both insertion sites were significantly higher at 0º than at 30º in ACL-deficient knees in response to the 100 N anterior tibial load. The MCL femoral insertion site forces corresponding to the in situ strains in the intact knee (before application of the experimental kinematics) at 0º and 30º were 39.7 ± 38.1 N and 6.0 ± 5.4 N, respectively. The MCL tibial insertion site forces due to in situ strain in the intact knee at 0º and 30º were 42.9 ± 43.1 N and 6.0 ± 5.5 N, respectively. Before ACL resection, the MCL femoral insertion site forces during anterior translation at 0º and 30º were 55.9 ± 38.2 N and 8.3 ± 5.4 N, respectively. Before ACL resection, the MCL tibial insertion site force during anterior tibial translation at 0º and 30º were 58.7 ± 42.0 N and 8.3 ± 5.5 N, respectively (Fig. 3.5, left panel). ACL-deficiency significantly increased MCL insertion site forces at the femur (126.6 ± 84.8 N and 74.1 ± 57.8 N at 0º and 30º, respectively) and tibia (133.9 ± 88.5 N and 80.9 ± 62.4 N at 0º and 30º, respectively) during anterior tibial translation ($p<0.05$ for all cases). Insertion site forces were significantly higher at 0° than at 30° during anterior tibial translation ($p=0.012$ for both insertions).

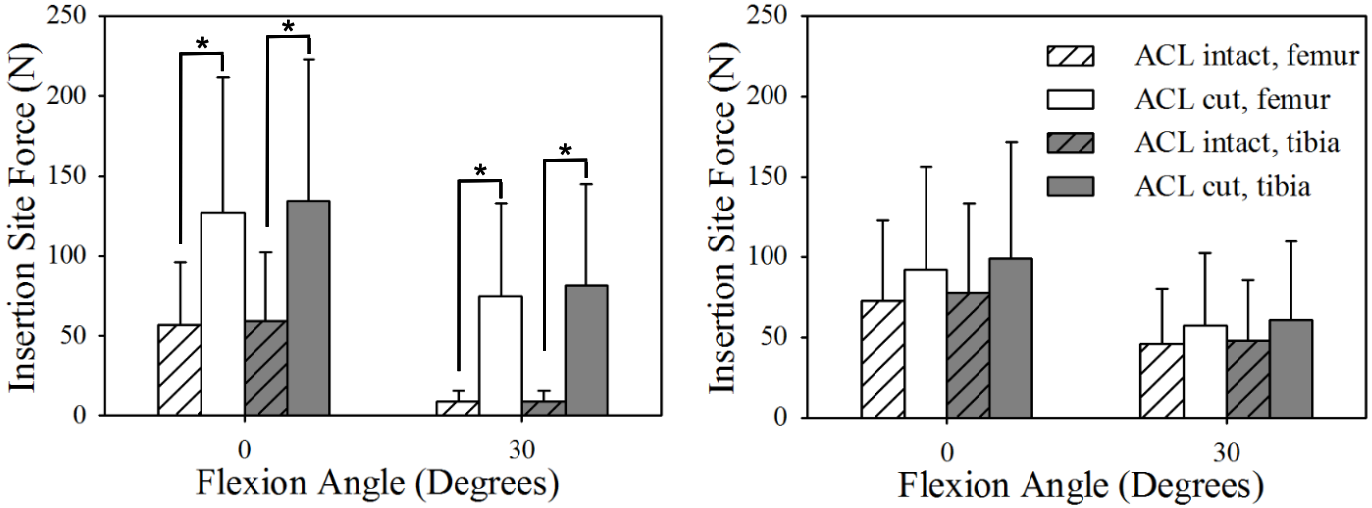

Fig. 3.5. FE predictions of insertion site forces for femoral and tibial insertion sites as a function of flexion angle and ACL state. Left panel - anterior tibial translation. Right panel – valgus rotation. Asterisks indicate statistically significant comparisons. There was a significant increase in MCL insertion site forces at the femur and tibia during anterior tibial translation after ACL injury at both 0º and 30º. In contrast, there was no significant effect of ACL deficiency on MCL insertion site forces in response to valgus loading. Both tibial and femoral insertion site forces were significantly higher at 0º than at 30º in the ACL-deficient knee during anterior tibial translation. (mean ± standard deviation).

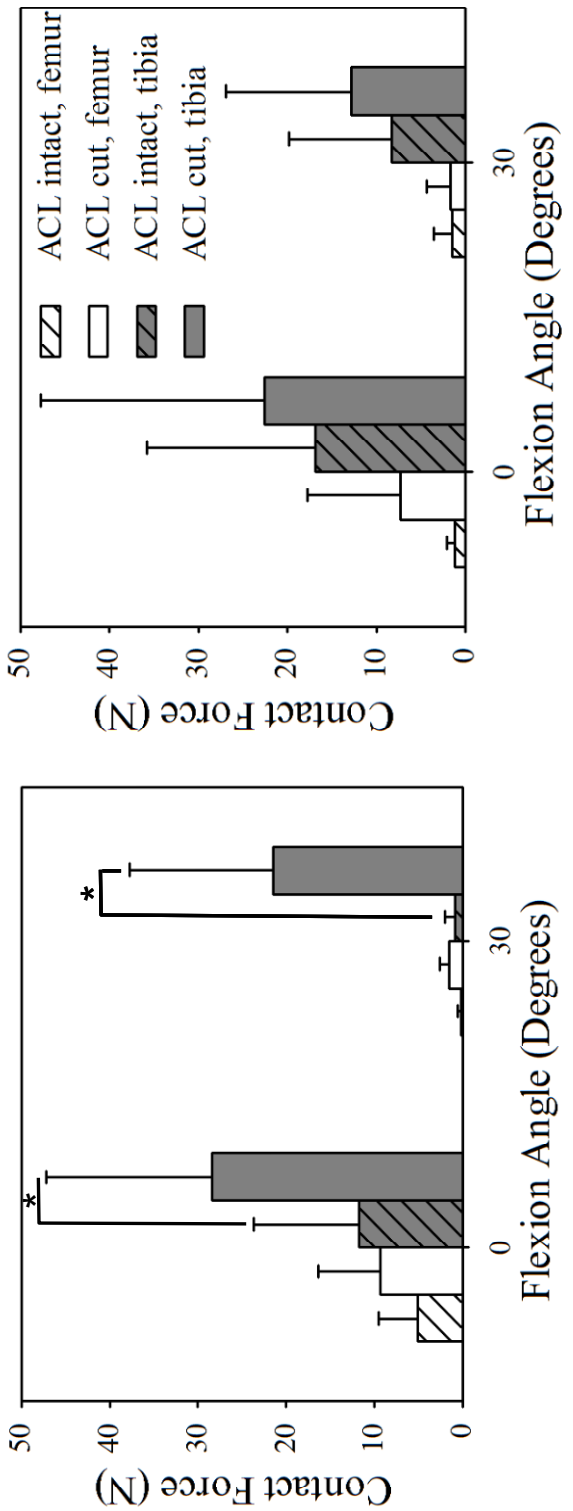

Fig. 3.6. FE predictions of contact forces between the MCL and femur and between the MCL and tibia as a function of flexion angle and ACL injury state. Left - anterior tibial translation. Right – valgus rotation. Asterisks indicate statistically significant comparisons. ACL deficiency significantly increased tibial contact forces at both flexion angles during anterior tibial translation. Further, tibial contact forces in the ACL-deficient knee at 0º were significantly higher than at 30º during anterior loading. In contrast, there was no significant effect of ACL deficiency on MCL contact forces during valgus loading (mean ± standard deviation).

In contrast to the anterior loading results, ACL deficiency did not significantly affect insertion site forces during application of valgus torque (Fig. 3.5, right panel). This was true at both the femoral and tibial insertion sites and for both flexion angles. Although the increases caused by ACL deficiency were not statistically significant in response to a valgus load, the results followed the same trend as the anterior loading results, with higher forces and increases in forces at the tibial insertion and at 0° flexion. Before ACL resection, the MCL femoral insertion site forces during valgus rotation at 0º and 30º were 72.8 ± 49.9 N and 46.0 ± 34.4 N, respectively. Before ACL resection, the MCL tibial insertion site forces during valgus rotation at 0º and 30º were 77.8 ± 55.6 N and 47.9 ± 37.9 N, respectively. After the ACL was transected, the MCL femoral insertion site forces during valgus rotation at 0º and 30º were 92.0 ± 64.0 N and 57.5 ± 45.0 N, respectively. After the ACL was transected, the MCL tibial insertion site forces during valgus rotation at 0º and 30º were 99.0 ± 72.2 N and 60.7 ± 49.3 N, respectively.

Contact Forces

ACL deficiency resulted in significantly increased MCL contact forces on the tibia during anterior tibial translation at both flexion angles, and MCL contact forces on the tibia were significantly higher at 0º than at 30º in the ACL-deficient knee. Before ACL resection, the MCL contact forces on the tibia during anterior translation at 0º and 30º were 11.6 ± 11.9 N and 0.7 ± 0.9 N, respectively (Fig. 3.6, left panel). ACL deficiency significantly increased MCL contact forces on the tibia (28.4 ± 18.9 N and 21.1 ± 15.8 N at 0º and 30º, respectively) during anterior translation ($p=0.001$ at both angles). MCL contact forces on the tibia in the ACL-deficient knee were significantly higher at 0º than

at 30º in response to anterior tibial loading (p=0.044). ACL deficiency did not significantly affect contact forces during application of valgus torque (Fig. 3.6, right panel).

Discussion

The hypothesis of this research was that ACL deficiency would increase MCL insertion site forces at the femur and tibia and increase contact forces between the MCL and the bones in response to both anterior and valgus loading. This hypothesis was partially disproved. In the ACL-deficient knee, the MCL is indeed subjected to higher insertion site and contact forces in response to an anterior load. However, MCL forces due to a valgus torque are not significantly increased in the ACL-deficient knee. It follows that the MCL resists anterior tibial translation in knees with intact ACLs, but the ACL is not a restraint to valgus rotation when a healthy MCL is present.

ACL deficiency caused a significant increase in MCL insertion site and contact forces in response to anterior tibial loading. This result is supported by an FE study that examined MCL insertion site and contact forces in the ACL-deficient knee (25) and by cadaver studies that have utilized a robotic/universal force-moment sensor system to calculate MCL insertion site forces in the ACL-deficient knee (15, 28). Moglo et al. created a single FE model of the knee including the MCL, ACL, posterior cruciate ligament, lateral collateral ligament, menisci, and cartilage (25). A 100 N posterior load was applied to the femur at a range of flexion angles from 0 to 90 degrees to study the forces in the remaining structures after removing the ACL. At full extension, forces in collateral ligaments increased in the ACL-deficient knee. Better support for our findings

can be found in two studies that used a robotic/universal force-moment sensor system to calculate MCL insertion site forces in the intact and ACL-deficient knee (15, 28). In each study, anterior loads were applied to intact and ACL-deficient cadaver knees and the resulting MCL insertion site forces were measured. Both studies found a significant increase in MCL insertion site forces during anterior tibial loading in the ACL-deficient knee.

In vivo studies of MCL healing have demonstrated that MCL healing is inferior when injured in conjunction with the ACL (1, 2, 5, 35). Each of these studies found increased knee laxity and decreased MCL material properties when the MCL is injured in conjunction with the ACL as compared to MCL injury with intact ACL, but only one of these studies measured MCL forces. Using a goat model, the insertion site forces in healing MCLs in response to an anterior tibial load in knees with reconstructed ACLs were measured by Abramowitch et al. using a robotic/universal force-moment sensor system (1). It was their conclusion that "the healing MCL may have been required to take on excessive loads and was unable to heal sufficiently as compared to an isolated MCL injury." Although these conclusions were reached based on healing studies in animal models, application of the results of the present study suggest that differences in MCL healing between knees with intact ACLs and those with transected ACLs could be due to either anterior or valgus loading. The insertion site forces in response to a valgus torque were generally of the same magnitude for a given flexion angle as the insertion site forces in response to an anterior tibial load, although they did not significantly increase with ACL deficiency, and the types and magnitudes of loads that hinder MCL healing are unknown.

The ACL is not a restraint to valgus rotation if the MCL is intact (Figures 3.4 and 3.5, right panels). At first this may seem contradictory to the widely held notion that the ACL is a secondary restraint to valgus rotation (1, 2, 14, 16, 19, 26, 34). However, upon closer examination, these studies reached this conclusion based on the results of MCL transection. Specifically, when the MCL was injured or transected, the ACL experienced increased loading during application of a valgus torque. Although our conclusion has not been reported previously in the literature, the results of other studies support the conclusions indirectly. Engle et al. examined the effect of ACL repair and graft restructuring on MCL healing after an O'Donoghue triad injury (5). At 0, 6, and 12 weeks postoperatively, the anterior translation and valgus rotation of the knees were tested. From time point zero to 12 weeks anterior laxity significantly increased, but valgus laxity did not. Markolf et al. found that valgus knee laxity was relatively unaffected by sectioning of the cruciate ligaments (22). This idea is further supported by a study looking at medial and lateral laxity in intact cadaver knees (10). Using a six degree of freedom linkage attached to six different knees with applied varus-valgus loading, Grood et al. found that the ACL and PCL combined accounted for only 14.8% of the medial restraining moment at 5 degrees knee flexion and only 13.4% of the restraining moment at 25 degrees knee flexion. Thus, when evaluating valgus laxity in the ACL-injured knee, any increase in valgus laxity indicates a compromised MCL.

Applying the in situ strain to the MCL during the second part of the FE analysis creates insertion site forces. These forces represent the contribution of the MCL to knee stability when there is little or no muscle activation or external loading. The insertion site forces caused by the in situ strain were smaller than the insertion site forces present after

anterior or valgus loading in the intact knee, although not always significantly smaller. This result is reflective of the relatively low load limits used in this study. In the ACL-deficient knee, insertion site forces significantly increased in response to an anterior tibial load, but not a valgus load, from the insertion site forces caused by the in situ strain. This followed the trend of the results comparing the insertion site forces in the ACL-deficient knee to the intact knee.

Changes in MCL contact forces followed the trend of MCL insertion site forces in that there was a significant increase in contact forces between the MCL and tibia following ACL transection in response to an anterior tibial load, but not a valgus torque. Contact forces were generated between the MCL and tibia during anterior tibial translation as the MCL slid over the convex surface of the tibia. These forces were relatively small in knees with intact ACL. Contact forces increased when the ACL was transected, and on average anterior tibial translation was more than doubled, forcing the MCL to slide over parts of the bone that have increased curvature. To our knowledge this is the first study to examine ligament contact forces using subject-specific FE modeling.

The attachment of the medial meniscus to the MCL was not represented in the FE analyses. This approach was justified by the results of our previous study, which demonstrated that transection of the attachment had no effect on knee kinematics under valgus loading in the intact knee (9). In the present study, it was confirmed that separation of the attachment of the medial meniscus to the MCL had no significant effect on joint kinematics for both A-P and V-V loading in the ACL-deficient knee. Of course, it is possible that other soft tissue structures that were dissected away from the knees may

contribute to knee stability under A-P and V-V loading, and thus as with any cadaveric study, caution should be taken when extrapolating results to other situations.

Improvements in the experimental methods that were used in the present study resulted in substantially better agreement between FE predictions and experimental measurements of fiber stretch than was obtained in our previous study (9). Improvements included the use of a more accurate digital motion analysis system, placement of wires around the MCL insertion sites to aid in identifying their locations in the CT images, and the placement of additional strain markers along and across the MCL (18). The excellent correlation between experimental and FE predicted fiber strains (R^2 = 0.953) provides confidence in the fidelity of the subject-specific FE model predictions. Data such as insertion site forces and contact forces, which elucidate other injury mechanisms and risks, can be evaluated using subject-specific FE methods. Further, the combination of results available through a combined experimental and computational protocol can be used to determine the likely location of injury and to what extent it may occur.

Several assumptions were made in the constitutive model used for the MCL to decrease both the experimental and computational time it took to conduct the study. Average MCL material coefficients from a previous study (9) were used. In the previous study, results from FE simulations using subject-specific material properties were compared to those using average material properties and no statistical differences were found. The MCL was assumed to have homogenous material properties. This assumption was used in our previous study (9) that yielded good correlations between experimental and FE strain results so the assumption was used again for this study which yielded an even better correlation.

It should be noted that the A-P and V-V mechanical testing performed for this research simulated an ideal clinical exam for knee laxity and no attempt was made to simulate weight bearing or muscle forces. Caution should be used when extrapolating the results reported here to a knee under muscle activation forces and/or ground contact forces. The anterior load and valgus torque limits for this research were specifically chosen to allow multiple tests on a single knee. Future research examining other loading conditions including muscle and body weight forces during regular daily activities is still needed.

In summary, ACL deficiency significantly increases MCL insertion site and contact forces in response to an anterior tibial load, and the largest increases occur at full extension. In contrast, ACL deficiency does not significantly increase MCL insertion site and contact forces in response to a valgus torque. Since it was demonstrated that the ACL is not a restraint to valgus rotation if the MCL is intact, increased valgus laxity in the ACL-deficient knee indicates a compromised MCL.

References

1. Abramowitch SD, Yagi M, Tsuda E, Woo SL: The healing medial collateral ligament following a combined anterior cruciate and medial collateral ligament injury--a biomechanical study in a goat model. *J Orthop Res* 21:1124-30, 2003

2. Anderson DR, Weiss JA, Takai S, Ohland KJ, Woo SL: Healing of the medial collateral ligament following a triad injury: a biomechanical and histological study of the knee in rabbits. *J Orthop Res* 10:485-95, 1992

3. Boissonnat JD: Shape reconstruction from planar cross-sections. *Computer Vision, Graphics and Image Processing* 44:1-29, 1988

4. Butler DL, Noyes FR, Grood ES: Ligamentous restraints to anterior-posterior drawer in the human knee. A biomechanical study. *J Bone Joint Surg Am* 62:259-70, 1980

5. Engle CP, Noguchi M, Ohland KJ, Shelley FJ, Woo SL: Healing of the rabbit medial collateral ligament following an O'Donoghue triad injury: effects of anterior cruciate ligament reconstruction. *J Orthop Res* 12:357-64, 1994

6. Fetto JF, Marshall JL: Medial collateral ligament injuries of the knee: a rationale for treatment. *Clin Orthop*:206-18, 1978

7. Gardiner JC: Computational Modeling of Ligament Mechanics. In: *Department of Bioengineering*. Salt Lake City, University of Utah, 2002

8. Gardiner JC, Weiss JA: Simple shear testing of parallel-fibered planar soft tissues. *J Biomech Eng* 123:170-5, 2001

9. Gardiner JC, Weiss JA: Subject-specific finite element analysis of the human medial collateral ligament during valgus knee loading. *J Orthop Res* 21:1098-106, 2003

10. Grood ES, Noyes FR, Butler DL, Suntay WJ: Ligamentous and capsular restraints preventing straight medial and lateral laxity in intact human cadaver knees. *J Bone Joint Surg Am* 63:1257-69, 1981

11. Grood ES, Suntay, W.J.: A joint coordinate system for the clinical description of the three-dimensional motions: application to the knee. *J Biomech Eng* 105:136-44, 1983

12. Hull ML: Analysis of skiing accidents involving combined injuries to the medial collateral and anterior cruciate ligaments. *Am J Sports Med* 25:35-40, 1997

13. Ichiba A, Nakajima M, Fujita A, Abe M: The effect of medial collateral ligament insufficiency on the reconstructed anterior cruciate ligament: a study in the rabbit. *Acta Orthop Scand* 74:196-200, 2003

14. Inoue M, McGurk-Burleson E, Hollis JM, Woo SL: Treatment of the medial collateral ligament injury. I: The importance of anterior cruciate ligament on the varus-valgus knee laxity. *Am J Sports Med* 15:15-21, 1987

15. Kanamori A, Sakane M, Zeminski J, Rudy TW, Woo SL: In situ force in the medial and lateral structures of intact and ACL-deficient knees. *J Orthop Sci* 5:567-71, 2000

16. Loitz-Ramage BJ, Frank CB, Shrive NG: Injury size affects long-term strength of the rabbit medial collateral ligament. *Clin Orthop*:272-80, 1997

17. Lujan TJ, Dalton MS, Thompson BM, Ellis BJ, Rosenberg TD, Weiss JA: MCL strains and joint kinematics in the ACL-deficient and posteromedial meniscus injured knee. *American Journal of Sports Medicine* In Review, 2005

18. Lujan TJ, Lake SP, Plaizier TA, Ellis BJ, Weiss JA: Simultaneous measurement of three-dimensional joint kinematics and ligament strains with optical methods. *ASME Journal of Biomechanical Engineering* 127:193-197, 2005

19. Ma CB, Papageogiou CD, Debski RE, Woo SL: Interaction between the ACL graft and MCL in a combined ACL+MCL knee injury using a goat model. *Acta Orthop Scand* 71:387-93, 2000

20. Maker BN: NIKE3D: A nonlinear, implicit, three-dimensional finite element code for solid and structural mechanics. *Lawrence Livermore Lab Tech Rept* UCRL-MA-105268, 1995

21. Maker BN: Rigid bodies for metal forming analysis with NIKE3D. *University of California, Lawrence Livermore Lab Rept* UCRL-JC-119862:1-8, 1995

22. Markolf KL, Mensch JS, Amstutz HC: Stiffness and laxity of the knee--the contributions of the supporting structures. A quantitative in vitro study. *J Bone Joint Surg Am* 58:583-94, 1976

23. Mazzocca AD, Nissen CW, Geary M, Adams DJ: Valgus medial collateral ligament rupture causes concomitant loading and damage of the anterior cruciate ligament. *J Knee Surg* 16:148-51, 2003

24. Miyasaka K, et al.: The incidence of knee ligament injuries in the general population. *Am J Knee Surg* 4:3-8, 1991

25. Moglo KE, Shirazi-Adl A: Biomechanics of passive knee joint in drawer: load transmission in intact and ACL-deficient joints. *Knee* 10:265-76, 2003

26. Norwood LA, Cross MJ: Anterior cruciate ligament: functional anatomy of its bundles in rotatory instabilities. *Am J Sports Med* 7:23-6, 1979

27. Robins AJ, Newman AP, Burks RT: Postoperative return of motion in anterior cruciate ligament and medial collateral ligament injuries. The effect of medial collateral ligament rupture location. *Am J Sports Med* 21:20-5, 1993

28. Sakane M, Livesay GA, Fox RJ, Rudy TW, Runco TJ, Woo SL: Relative contribution of the ACL, MCL, and bony contact to the anterior stability of the knee. *Knee Surg Sports Traumatol Arthrosc* 7:93-7, 1999

29. Schroeder WJ, Zarge J, Lorensen WE: Decimation of triangle meshes. *Comp Graph (Proc SIGGRAPH)* 25, 1992

30. Seering WP, Piziali RL, Nagel DA, Schurman DJ: The function of the primary ligaments of the knee in varus-valgus and axial rotation. *J Biomech* 13:785-94, 1980

31. Speck D: GRIZ - Finite Element analysis results visualization for unstructured grids - user manual. *Lawrence Livermore National Laboratory* UCRL-MA-115696 Rev.2, 2001

32. Weiss JA, Gardiner JC, Ellis BJ, Lujan TJ, Phatak NS: Three-dimensional finite element modeling of ligaments: technical aspects. *Medical Engineering and Physics* In Press, 2005

33. Weiss JA, Maker BN: Finite element implementation of incompressible, transversely isotropic hyperelasticity. *Computer Methods in Applied Mechanics and Engineering*:107-128, 1996

34. Woo SL, Jia F, Zou L, Gabriel MT: Functional tissue engineering for ligament healing: potential of antisense gene therapy. *Ann Biomed Eng* 32:342-51, 2004

35. Woo SL, Young EP, Ohland KJ, Marcin JP, Horibe S, Lin HC: The effects of transection of the anterior cruciate ligament on healing of the medial collateral ligament. A biomechanical study of the knee in dogs. *J Bone Joint Surg Am* 72:382-92, 1990

CHAPTER 4

METHODOLOGY AND SENSITIVITY STUDIES FOR FINITE ELEMENT MODELING OF THE INFERIOR GLENOHUMERAL LIGAMENT COMPLEX [1]

Abstract

The objectives of this research were to develop a methodology for three-dimensional finite element (FE) modeling of the IGHL complex as a continuous structure, to determine optimal mesh density for FE simulations, to examine strains and forces in the IGHL complex in clinically relevant joint positions, and to perform sensitivity studies to assess the effects of assumed material properties. A simple translation test in the anterior direction was performed on a cadaveric shoulder, with the humerus oriented at 60º of glenohumeral abduction and 0º of flexion/extension, at 0º, 30º and 60º of humeral external rotation. The geometries of the relevant structures were extracted from volumetric CT data to create a FE model. Experimentally measured kinematics were applied to the FE model to simulate the simple translation test. First principal strains, insertion site forces and contact forces were analyzed. At maximum anterior humeral translation, strains in the IGHL complex were highly inhomogeneous for all external

[1] Reprinted from *Journal of Biomechanics*, Vol. 40, No. 3. Ellis, B.J., Debski, R.E., Moore, S.M., McMahon, P.J., Weiss, J.A., *"Methodology and Sensitivity Studies for Finite Element Modeling of the Inferior Glenohumeral Ligament Complex,"* pp: 603-612, 2007, with permission from ELSEVIER

rotation angles. The motion of the humerus with respect to the glenoid during the simple translation test produced a tangential load at the proximal and distal edges of the IGHL complex. This loading was primarily in the plane of the IGHL complex, producing an in-plane shear loading pattern. There was a significant increase in strain with increasing angle of external rotation. The largest insertion site forces occurred at the axillary pouch insertion to the humerus (36.7 N at 60º of external rotation) and the highest contact forces were between the anterior band of the IGHL complex and the humeral cartilage (7.3 N at 60º of external rotation). Strain predictions were highly sensitive to changes in the ratio of bulk to shear modulus of the IGHL complex, while predictions were moderately sensitive to changes in elastic modulus of the IGHL complex. Changes to the material properties of the humeral cartilage had little effect on predicted strains. The methodologies developed in this research and the results of the mesh convergence and sensitivity studies provide a basis for the subject-specific modeling of the mechanics of the IGHL complex.

Introduction

Nearly 2% of the population in the United States will dislocate their glenohumeral (GH) joint. (Hovelius, 1982; Nelson and Arciero, 2000). Eighty percent of these injuries will occur due to anterior dislocation of the humerus (Cave, 1974). The injuries include detachment of the inferior glenohumeral ligament complex (IGHL complex) from the anterior glenoid and labrum (Bankart, 1923; Bankart, 1938) and humeral avulsion of the glenohumeral ligaments (Bokor et al., 1999; Bui-Mansfield et al., 2002; Chhabra et al., 2004; Richards and Burkhart, 2004; Sailer and Imhof, 2004; Schippinger et al., 2001;

Warner and Beim, 1997). Initial and differential diagnosis of these injuries is often difficult due to the complex function of the GH capsule.

The specific contribution of regions of the IGHL complex to joint function has continued to be a source of controversy. GH capsule function has been examined via cutting studies (Turkel et al., 1981) and by evaluating the strains (Brenneke et al., 2000), elongation (Warner et al., 1993), in situ forces (Debski et al., 1999b), and material properties (Bigliani, 1992; Itoi et al., 1993; McMahon, 1998; Moore et al., 2004a; Ticker et al., 1996) of capsular regions. A recent study of strain in the antero-inferior capsule under subluxation demonstrated that maximum principal strains were highly variable (Malicky et al., 2001). Strain patterns did not correspond to any specific capsular region and instead encompassed several regions. Additionally, bidirectional material properties of the axillary pouch and posterior capsular regions have recently been evaluated (Moore et al., 2003; Moore et al., 2004a) and collagen fiber organization was quantified for several regions (Debski et al., 2003). Debski et al. reported that significant forces were transmitted by the capsular regions, both between scapula and humerus and between capsular regions (Debski et al., 1999b).

These and other studies support the notion that capsular regions experience multi-axial loading when subjected to joint kinematics that are representative of normal and injurious motions, and that the IGHL complex functions as a continuous structure (Debski et al., 2003; Debski et al., 1999b; Malicky et al., 2001; Moore et al., 2003; Moore et al., 2004a). However, previous computational models have represented the capsule as a collection of discrete one-dimensional structures (Debski et al., 1999a; Miller, 1991; Novotny et al., 2000). Similarly, computational models of the musculature

at the GH joint have neglected the capsule due to its complex function (Luo et al., 1998; Novotny et al., 2000; Van der Helm, 1994a; Van der Helm, 1994b). A methodology to evaluate function of the capsule as a continuous structure would provide greater insight into the mechanical contribution of the IGHL to joint function, provide a means to identify joint positions that place the capsule at risk, identify potential improvements to surgical repair techniques, and provide a quantitative means for developing low-risk rehabilitation protocols.

The finite element (FE) method can represent the capsular regions as three-dimensional and continuous, providing predictions of strain, insertion site forces, and contact. However, there are a number of difficulties associated with FE modeling of the IGHL complex as a continuous structure. The geometry of both the bones and the capsule are complex and can vary appreciably between individuals (DePalma et al., 1949; Schwartz et al., 1988; Warner et al., 1993; Warner et al., 1992). IGHL material properties also exhibit variation between donors (Bigliani, 1992; Itoi et al., 1993; McMahon, 1998; Moore et al., 2004a; Ticker et al., 1996). The capsule develops folds and creases during anatomical motion (Malicky et al., 2001), which presents difficulties for analysis with the FE method (Weiss et al., 2005). The establishment of a reference configuration for strain and stress measurement causes additional complications (Malicky et al., 2001). Finally, the appropriate mesh discretization needed to produce accurate predictions of capsular strains and insertion site forces, and the sensitivity of the continuum FE models to variations in model inputs are unknown. Previous efforts to model the IGHL complex have not addressed these issues (Debski et al., 1999a; Miller, 1991; Novotny et al., 2000).

The objective of this research was to develop a combined experimental-computational framework that can be used in the future for subject-specific FE modeling of the IGHL complex. The specific objectives of this study were 1) to develop an approach for FE representation of the IGHL complex as a continuous structure based on subject-specific geometry and discretization with shell elements, 2) to examine the patterns of IGHL strains, insertion site forces and contact forces during a simulated clinical examination, and 3) to test the sensitivity of the FE model to changes in IGHL complex and humeral articular cartilage material properties.

Methods

Experimental Kinematics

An intact shoulder (Male, 46 yrs.) with no signs of arthritis or previous injury was used. After thawing for 12 hours, the shoulder was dissected, leaving the humerus, scapula, rotator cuff tendons and capsule intact. The capsule was vented at the rotator cuff interval to allow insertion of compressed air during the CT scan. Plexiglas blocks and magnetic sensors were adhered to the scapula and humerus to allow definition of local coordinate systems for co-registration of kinematic and CT datasets. A load of 13.4 N was applied to each of the rotator cuff tendons (Debski, 1995). Using a magnetic tracking device (Flock of Birds, Ascension Technologies, Inc.), the Plexiglas blocks were digitized and local coordinate systems were established. Soft tissues were preconditioned to minimize viscoelastic effects by cycling the joint between the neutral position and maximum anterior and posterior translation. A clinician translated the humeral head to its limit in the anterior direction at 0º, 30º, and 60º of external rotation (ER) and 60° of

abduction while joint kinematics were recorded. The reproducibility of this loading method and the accuracy of the measurements have been published previously (Moore et al., 2004b). Accuracy of the magnetic sensors is <0.3% of the distance between the sensors and <1.0º (Moore et al., 2004b; Zeminski, 2001).

Reference Strain State and Volumetric CT Scan

Rubber tubes (1/8" diameter) were used to facilitate visualization of the regions and insertion sites of the IGHL complex in the CT images (Fig. 4.1). Spherical nylon markers (6x6 grid, 1.6 mm diameter) were affixed to the regions of the IGHL complex. To establish a reference strain state, the joint was first positioned at 60° of glenohumeral abduction, 0° of horizontal abduction, and 15° of external rotation.

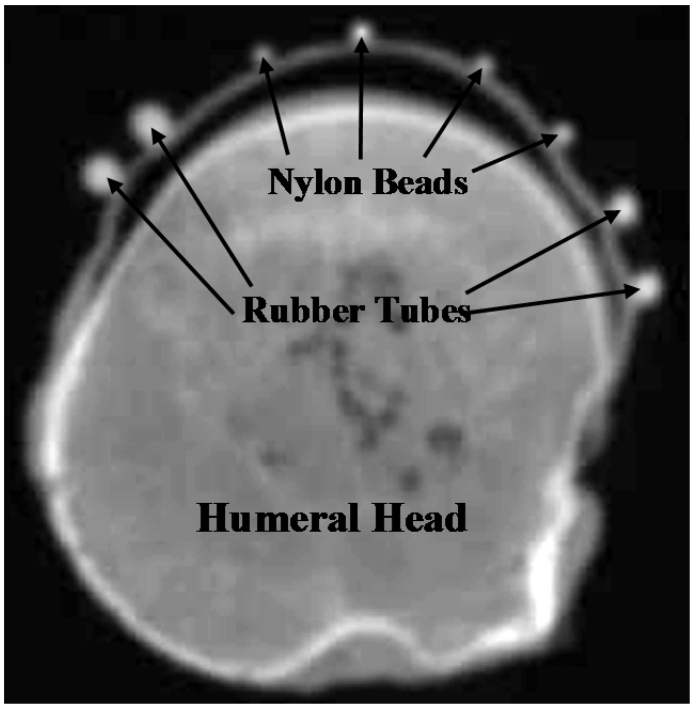

Fig. 4.1. CT image of the humeral head and IGHL complex. Rubber tubes and nylon beads mark the boundaries of the AB-IGHL, PB-IGHL, and axillary pouch.

The humerus was then internally rotated in 5° increments from 15° of external rotation to 15° of internal rotation, yielding seven joint positions. At each joint position, the capsule was inflated with compressed air to 0.7 kPa and 4.8 kPa and photographs were taken at each pressure from two digital cameras. For each joint position, the images obtained from the digital cameras were superimposed. By visual inspection of the superimposed images, the joint position corresponding to the least marker movement between 0.7 kPa and 4.8 kPa was determined (Malicky et al., 2001). With the joint in this position (60° abduction, 0° flexion, 45° external rotation), a volumetric CT scan was acquired (CTI; General Electric, Milwaukee, WI). Thus, the folds and wrinkles of the capsule were minimized and the reference strain state was established. CT slices were collected (191 slices, thickness = 1 mm, FOV = 150 mm, in-plane resolution = 512×512).

Finite Element Mesh Generation

Cross-sectional contours of the scapula, humerus, humeral articular cartilage and IGHL complex were extracted from the CT dataset (SurfDriver, Kailua, Hawaii). Polygonal surfaces were generated (Boissonnat, 1988) and the surfaces were smoothed (Schroeder et al., 1992). Polygons composing the surfaces of the scapula and humerus were converted directly to shell elements, which were used to represent the bones as rigid bodies (Ellis et al., 2006; Maker, 1995b). The IGHL complex and humeral cartilage surfaces were imported into FE preprocessing software (TrueGrid, XYZ Scientific, Livermore, CA). A quadrilateral shell mesh was created for the IGHL, while a hexahedral mesh was created for the humeral cartilage (Debski et al., 2005) (Fig. 4.2).

The initial mesh for the IGHL complex consisted of 5,750 shells, while the cartilage mesh contained 7,200 hexahedrons.

Material Properties

The IGHL complex was represented as isotropic hypoelastic and the baseline modulus and Poisson's ratio (E=10.1 MPa, ν=0.4) were obtained from a previous study (Moore et al., 2004a). Note that hypoelasticity is objective for finite deformations (i.e., large strains and rotations) (Simo and Hughes, 1998). The humeral head articular cartilage was represented as neo-Hookean hyperelastic (Maker et al., 1990) and the shear modulus (C_1=0.3055 MPa) was calculated from the modulus and Poisson's ratio (E=0.66 MPa, ν=0.08) obtained from a previous study (Matsen et al., 1993). The scapula and humerus were modeled as rigid bodies.

Boundary Conditions

The experimentally measured kinematic dataset was used to prescribe motion of the humerus (Ellis et al., 2006; Gardiner and Weiss, 2003). The coordinates of the Plexiglas blocks in both the CT and kinematic datasets allowed for correlation of the two datasets. Motion was described using incremental translations and rotations (Maker, 1995b; Simo and Vu-Quoc, 1988), based on the experimental measurements of the motion of the Plexiglas blocks on the humerus and scapula. Separate node sets were defined for the attachment of each IGHL region to each bone so that insertion site forces could be

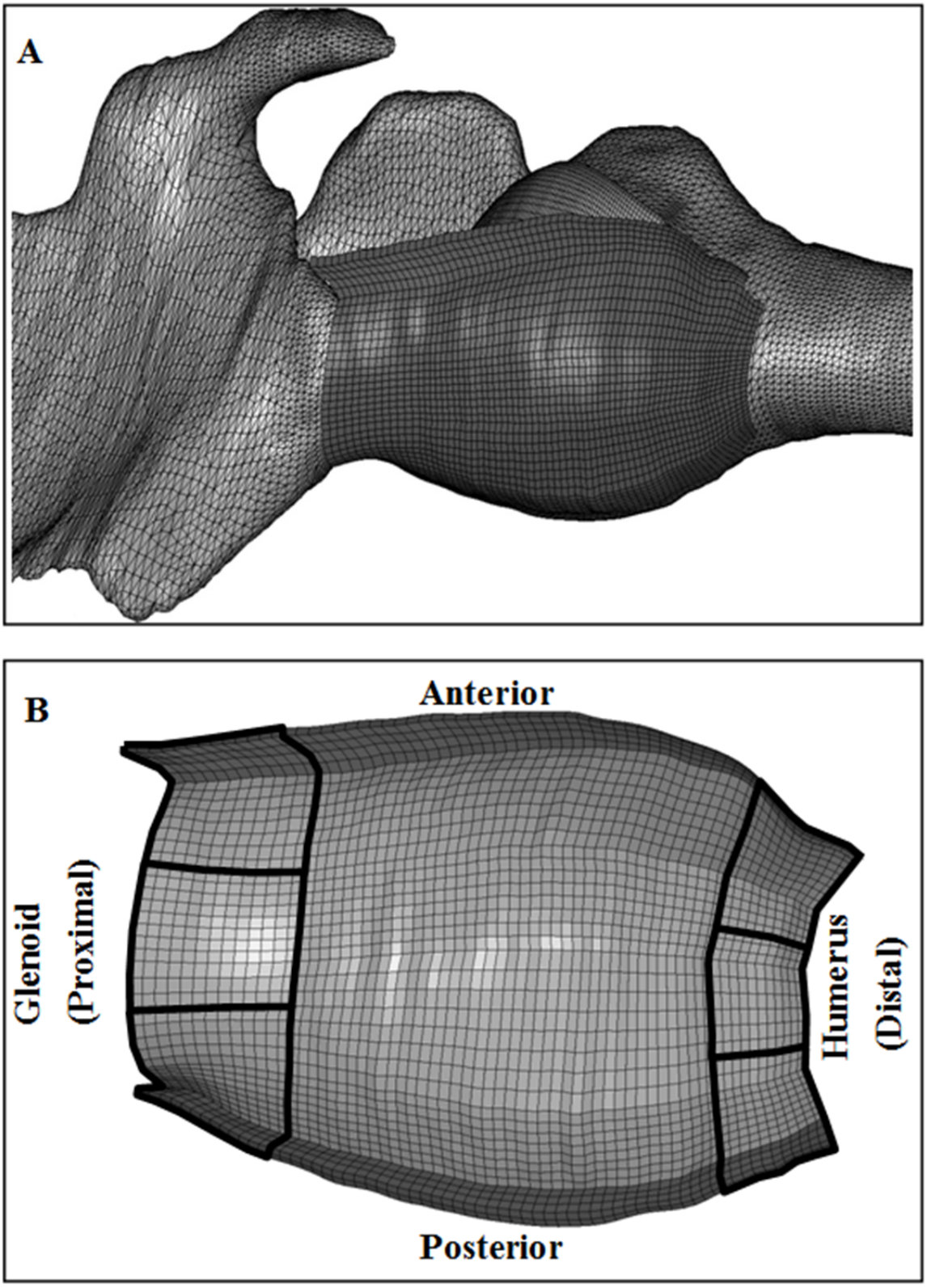

Fig. 4.2. FE meshes and IGHL strain regions. A) FE mesh of the IGHL complex, humerus, humeral cartilage, and scapula. B) IGHL complex marked with the six strain regions (anterior distal, anterior proximal, middle distal, middle proximal, posterior distal, and posterior proximal) used for 1st principal strain analysis.

obtained for each region of the IGHL complex. Contact between capsular regions and the articular cartilage was enforced using the penalty method.

FE Solution Procedure

The nonlinear FE code NIKED was used for all analyses (Maker, 1995a). Nonlinear iterations were based on a quasi-Newton method and convergence was based on the L_2 displacement and energy norms. LSPOST (Livermore Software Technology Corporation, Livermore, CA) was used to visualize and output strains while contact and insertion site forces were obtained directly from NIKED.

Regional Strains, Contact Forces, and Insertion Site Forces

To compare strains in regions of the IGHL complex, six areas were defined to represent the anterior distal, anterior proximal, middle distal, middle proximal, posterior distal, and posterior proximal regions (Fig. 4.2). Average 1st principal Green-Lagrange strains were calculated for each area. Insertion site forces and contact forces were also determined at the glenoid and humerus for the AB-IGHL, PB-IGHL and axillary pouch.

Mesh Convergence Study

To determine the mesh refinement level necessary to predict converged values of IGHL strains and forces, three additional FE models with mesh densities of twice, half, and a quarter the number of elements as the original mesh were analyzed.

Sensitivity Studies

Studies were conducted to determine the sensitivity of FE predictions of IGHL strains and forces to assumed material properties. To assess the influence of elastic modulus on strains in the IGHL complex, the baseline modulus was increased and decreased by both 25% and 50%.

Baseline studies assumed a Poisson's ratio of ν=0.4, yielding a bulk:shear modulus ratio of 4.67. To assess the influence of the IGHL complex bulk:shear modulus ratio, three additional models were analyzed using bulk:shear modulus ratios of 1.0, 10.0, and 100.0 by maintaining the same elastic modulus and varying the Poisson's ratio.

Wrapping of the IGHL complex around the cartilage surface of the humeral head influences its deformation, but it is unclear whether the deformation of the cartilage itself influences the strain predictions for the IGHL complex. To test the effect of the cartilage bulk:shear modulus ratio on predicted IGHL strains and forces, three additional simulations were performed with cartilage bulk:shear modulus ratios of 1.0, 10.0, and 1000.0. Finally, one additional simulation was performed to test the effect of changing the cartilage from a deformable material to a rigid body.

Results

Baseline FE Model

The IGHL complex was primarily subjected to shear in the plane of the IGHL during the simple translation test (Fig. 4.3). High strains developed in the anterior distal and posterior proximal portions of the IGHL complex. The motion of the humerus with respect to the glenoid produced a tangential load at the proximal and distal edges of the

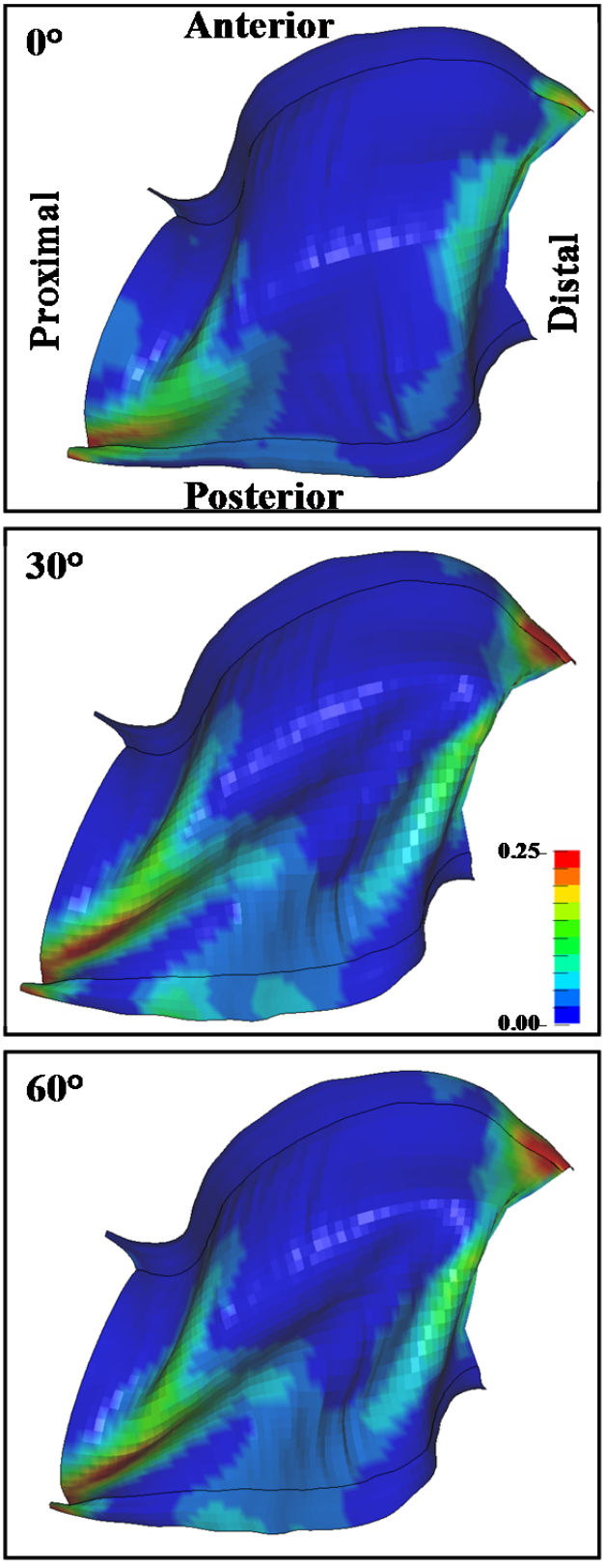

Fig. 4.3. Fringe plots of 1st principal strain at 60° of abduction and full anterior translations at 0º, 30º, and 60º of external rotation. Strains increased from 0º to 30º and from 0º to 60º, but there was little change in strains from 30º to 60º.

IGHL complex. This loading was primarily in plane with the IGHL complex, producing an in-plane shear loading pattern. This pattern was modified and intensified by increased external rotation of the humerus, which increased IGHL wrapping around the humeral head. The IGHL complex experienced folding and creasing at all three external rotation angles. Average wall clock time for each FE simulation was about 2.5 hours, using two processors of an SGI Origin 2000.

IGHL strains were highly non-uniform during FE simulations of simple translation at 0, 30, and 60 degrees of external rotation (Fig. 4.4). Strains in the anterior distal region were 6.3±6.1%, 11.9±12.3%, and 11.5±11.1%, at 0, 30, and 60 degrees, respectively.

The highest insertion site forces occurred at the insertion of the axillary pouch to the humerus (25.8 N, 33.9 N, and 36.7 N, at 0, 30, and 60 degrees, respectively) (Fig. 4.5). There were also relatively high forces at the axillary pouch insertion to the glenoid (16.8 N, 27.4 N, and 25.1 N, at 0, 30, and 60 degrees, respectively). Insertion site forces at the AB-IGHL insertion to the humerus (16.8 N, 21.0 N, and 22.0 N, respectively) and the PB-IGHL insertion to the glenoid (12.1 N, 10.7 N, and 11.1 N, respectively) were higher than the AB-IGHL insertion to the glenoid (6.0 N, 6.2 N, and 5.5 N, respectively) and the PB-IGHL insertion to the humerus (2.5 N, 3.3 N, and 3.6 N, respectively).

The highest contact forces occurred between the AB-IGHL and the humerus (5.2 N, 6.8 N, and 7.3 N, at 0, 30, and 60 degrees, respectively). Contact forces between the axillary pouch and each bone were also relatively large (3.5 N at the humerus and 4.0 N at the glenoid, at 60º).

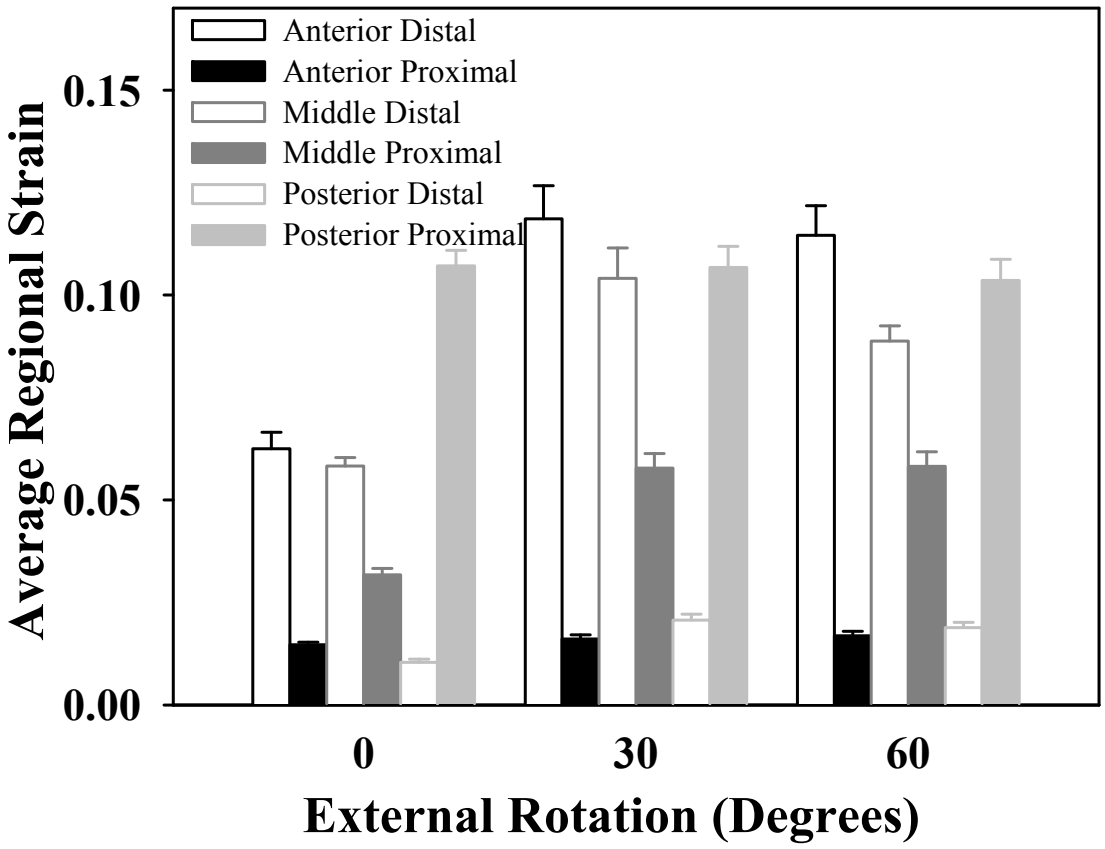

Fig. 4.4. First principal strain at 60° of abduction and full anterior translations at 0º, 30º, and 60º of external rotation. Strains in the anterior distal region and posterior proximal region were larger than strains in the other four regions.

Mesh Convergence Study

Changes in mesh density had a large effect on strains, but little effect on forces. The mesh with twice as many elements as the original mesh produced strains that on average were less than one percent different from the original mesh, but the mesh with a quarter as many elements produced strains that on average were 109% higher than the original mesh (Fig. 4.6). Meshes with twice as many elements and a quarter as many elements as the original mesh produced insertion site forces that on average were one percent less and

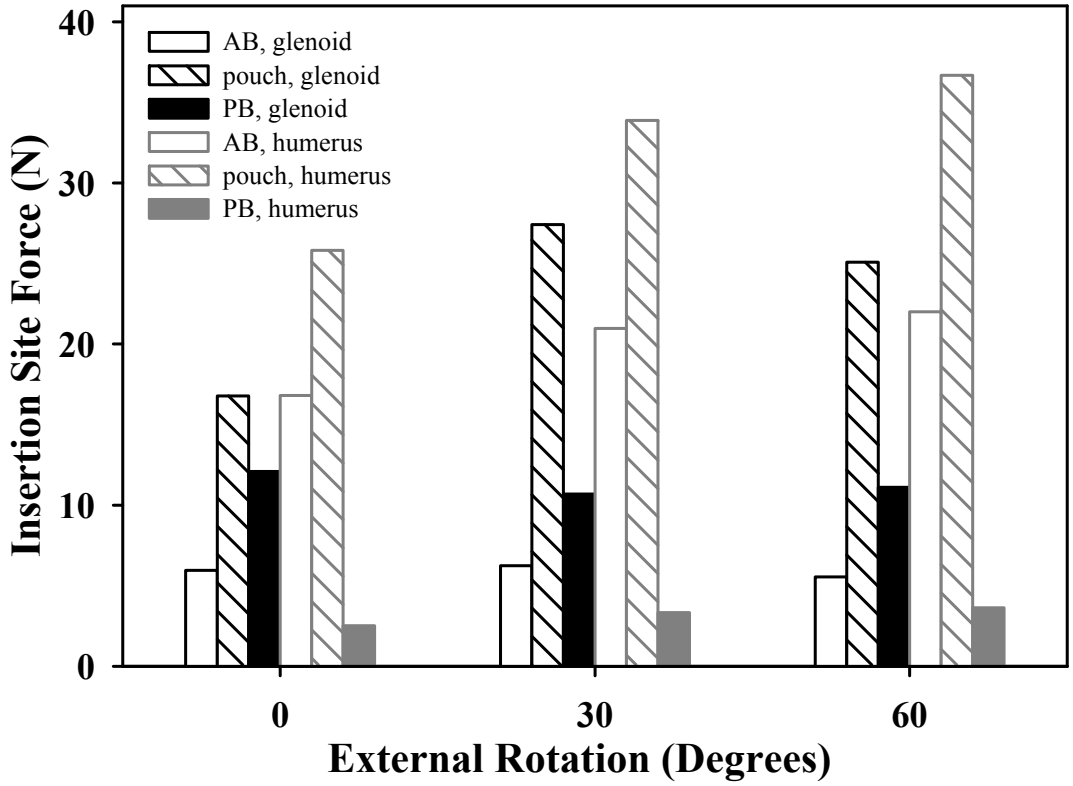

Fig. 4.5. Insertion site forces for the AB-IGHL, PB-IGHL, and axillary pouch at 60º of abduction and full anterior translations at 0º, 30º, and 60º of external rotation. The largest insertion site forces were consistently at the axillary pouch insertion to the humerus.

five percent higher than the original mesh, respectively. Doubling the number of elements increased the average contact force by 2.4 N and the mesh with a quarter as many elements produced contact forces that were on average 0.96 N smaller than the original mesh. It was concluded that the original mesh provided a balance between accuracy and computational expense, and this FE mesh was used for the sensitivity studies.

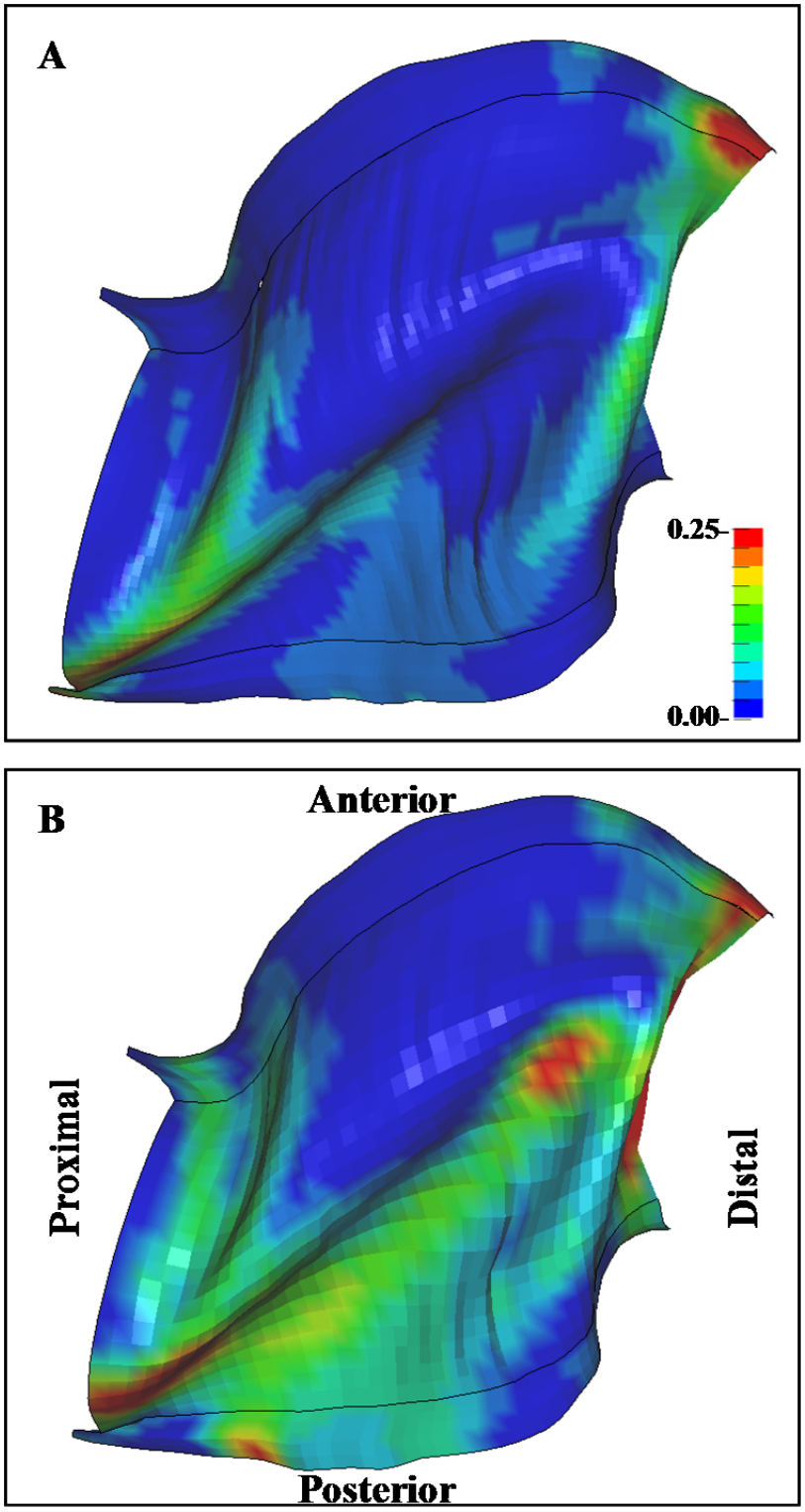

Fig. 4.6. Fringe plots of 1st principal strain at 60° of abduction and full anterior translations at 60º of external rotation for A) the original mesh and B) the mesh with a quarter as many elements as the original mesh. Due to the fact that large elements were bending around relatively tight folds, the mesh with a quarter as many elements produced 1st principal strains that were on average 109% higher than those for the original mesh.

Sensitivity to IGHL Complex Material Properties

In general, there were small changes in strains with changes in elastic modulus of the IGHL complex. Average changes in strain over the six areas were 16%, -7%, -6%, and 14% with changes in the IGHL complex modulus of –50%, -25%, 25%, and 50%, respectively. The effect on the average change of the six insertion site forces with changes in the IGHL complex modulus was nearly linear (Fig. 4.7). The average changes in the insertion site forces were –46%, -26%, 31%, and 54% with changes in the IGHL

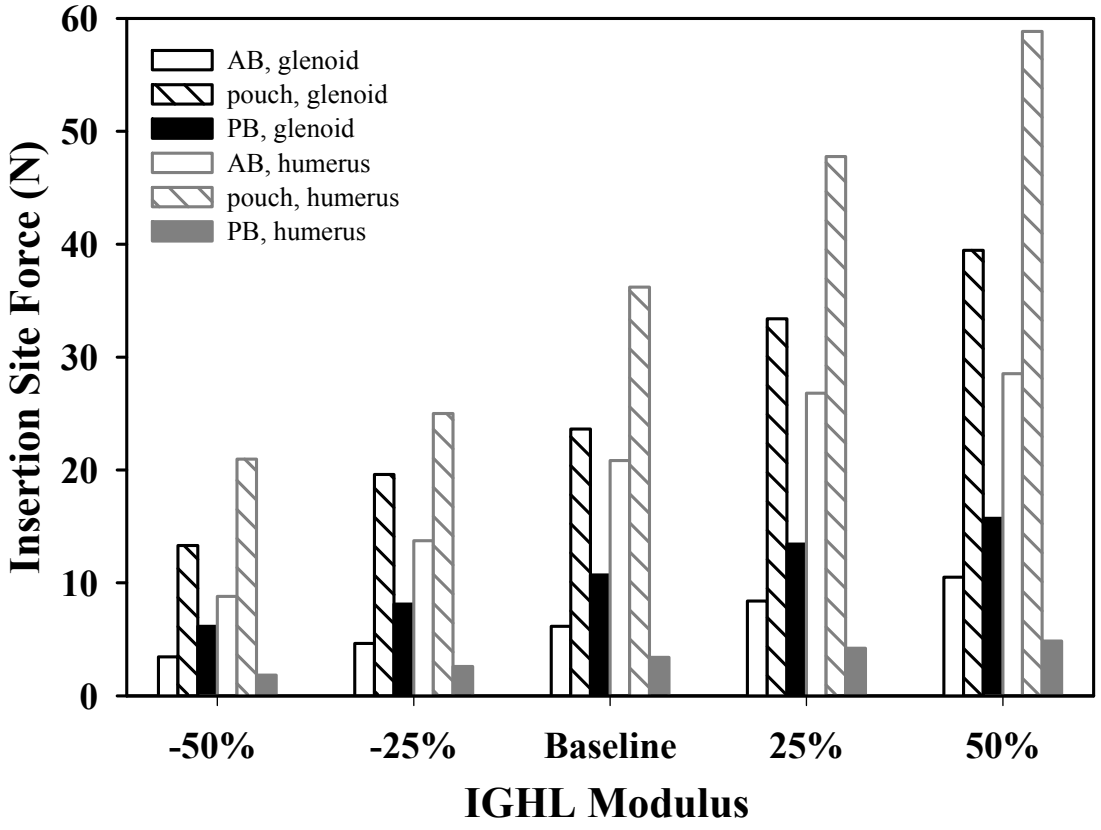

Fig. 4.7. Insertion site forces for the AB-IGHL, PB-IGHL, and axillary pouch at 60° of abduction and full anterior translations at 60º of external rotation for the baseline modulus, ±25% of baseline modulus, and ±50% of baseline modulus. The effect on the average change of the six insertion site forces with changes in the IGHL complex modulus was nearly linear.

complex modulus of –50%, -25%, 25%, and 50%, respectively. On average, there was less than a 2 N change in contact force.

Changes to the bulk:shear modulus ratio of the IGHL complex had a large effect on the strains and forces. Increasing the bulk:shear modulus ratio of the IGHL complex from 1.0 to 10.0 increased the average strains, insertion site and contact forces by 43%, 25%, and 470%, respectively. Increasing the IGHL complex bulk to shear modulus ratio from one to a hundred increased the average strains, insertion site and contact forces by 68%, 31%, and 100%, respectively.

Sensitivity to Cartilage Material Properties

Changes to the elastic modulus and bulk:shear modulus ratio for the articular cartilage had little effect on predictions of strains and forces. There was less than a one percent change in average strains, a one Newton increase in average insertion site force, and less than a one Newton change in average contact force when the ratio of cartilage bulk:shear modulus was increased from 1.0 to 1000.0. Similarly, representing the cartilage as rigid decreased average strains by less than 1 percent, increased average insertion site forces by two Newtons and decreased average contact force by less than one Newton.

Discussion

The FE models of the IGHL complex represented the three adjacent capsular regions as a continuous structure, using shell elements. This is in contrast with previous efforts that discretized the capsular regions with discrete one-dimensional elements (Debski et

al., 1999a; Miller, 1991; Novotny et al., 2000). The ability to predict the three-dimensional strain distribution in the IGHL complex is a major advance of the current research over previous modeling efforts. Furthermore, the current model includes the wrapping of capsular tissue around the humeral head. Capsular wrapping has been previously described in external rotation (O'Brien et al., 1990), where the IGHL complex is the primary static restraint (Turkel et al., 1981). Thus, capsular wrapping may play a role in force transmission from the humerus to the glenoid, providing additional joint stability.

This study used quadrilateral shell elements to represent the IGHL complex (Hughes and Liu, 1981a; Hughes and Liu, 1981b). Our previous studies of ligament mechanics (Ellis et al., 2006; Gardiner and Weiss, 2003) have demonstrated that difficulties can arise when using hexahedral elements to represent ligaments that experience folding and creasing. In our previous study of the anterior band of the IGHL complex (Debski et al., 2005), we were successful in obtaining converged solutions using hexahedral elements. However, when attempting to simulate the entire IGHL complex in the present study, hexahedral elements failed to yield converged solutions due to element inversion at the locations of developing folds. In fact, three different hexahedral element formulations were applied unsuccessfully to the simulations in this study (Puso, 2000; Simo and Armero, 1993; Simo and Taylor, 1991). Modeling the IGHL with shell elements also reduced computational expense. Not only do shell elements have fewer degrees of freedom than trilinear hexahedral elements, but only a single element is required to describe variations in strain through the thickness of the IGHL complex.

Strain predictions were much more sensitive than the forces to changes in mesh density. The sensitivity of the strains to mesh density was caused by folding of the IGHL complex. The use of fewer elements caused the (larger) shell elements to bend around relatively tight folds in the IGHL complex. Thus, models with a quarter and half as many elements produced higher strains than the original mesh and the mesh with twice as many elements (Fig. 4.6). In contrast, because the kinematics of the simple translation test subjected the IGHL complex to primarily in-plane shear loading, the forces were not sensitive to mesh density.

The sensitivity of FE predictions to changes in the IGHL complex material properties has important implications for future modeling efforts. Subject specific material properties may be needed to obtain accurate predictions of strain and force when future studies examine a population of subject-specific models for the IGHL complex. In contrast, the articular cartilage of the humeral head may be represented as rigid, decreasing the computational demand of future analyses. The strong tie between assumed material properties and predicted strains and forces, along with the high variation of IGHL complex material properties seen in experimental studies (Bigliani, 1992; Itoi et al., 1993; McMahon, 1998; Moore et al., 2004a; Ticker et al., 1996), suggests that there will also be a high variation in IGHL complex strains and forces in a population of specimens.

IGHL strains, insertion site and contact forces were all sensitive to changes in the IGHL bulk:shear modulus ratio. This is an important finding because there are little data available in the literature about the bulk (volumetric) behavior of ligaments in general.

An experimental study to characterize the bulk behavior of the IGHL would help to eliminate the uncertainty associated with this parameter.

In contrast to the effects of IGHL complex material properties, IGHL complex strains and forces were insensitive to changes in articular cartilage elastic modulus and bulk:shear modulus ratio. This finding has implications for future IGHL modeling. Experiments will not be needed to characterize the material properties of the humeral articular cartilage in order to produce accurate subject-specific models of the IGHL complex. This will lead to a reduction in the time needed for model construction because a hexahedral mesh will not be needed for the cartilage. Instead, the surface of the humeral articular cartilage can be generated as part of the humerus, converted directly to shell elements, and represented as a composite rigid body. Modeling the humeral articular cartilage as a rigid body saves computational expense in two ways. First, simulations of contact between a deformable body and a rigid body are computationally less expensive than simulations of contact between two deformable bodies. Second, representing cartilage as a rigid body directly saves computational time by removing the thousands of degrees of freedom introduced by a deformable hexahedral mesh.

To provide a framework for FE analysis in the absence of available experimental data, several assumptions regarding material behavior of the IGHL complex were made. First, a hypoelastic constitutive framework was used in the FE analyses. Although hypoelasticity is objective for large strains and rotations (Simo and Hughes, 1998), it neglects the upward-concave material behavior of the IGHL (Moore et al., 2003; Moore et al., 2004a). This assumption was justified based on data on the material behavior of the axillary pouch and anterior band of the IGHL complex (Moore et al., 2005; Moore et

al., 2003; Moore et al., 2004a). Figure 4.8 illustrates the tensile response of the axillary pouch of the IGHL and the FE simulated tensile response, using hypoelasticity and the material coefficients fit to these data. The agreement is reasonable for the purposes of this study. Second, the IGHL complex was represented as isotropic. The average tensile material behavior of the IGHL is mildly anisotropic (Debski et al., 2003; Moore et al., 2005; Moore et al., 2004a). Further, the collagen fiber organization in the IGHL is quite random (Debski et al., 2003). Thus, isotropic material symmetry provided a reasonable starting point for baseline FE simulations of the IGHL complex.

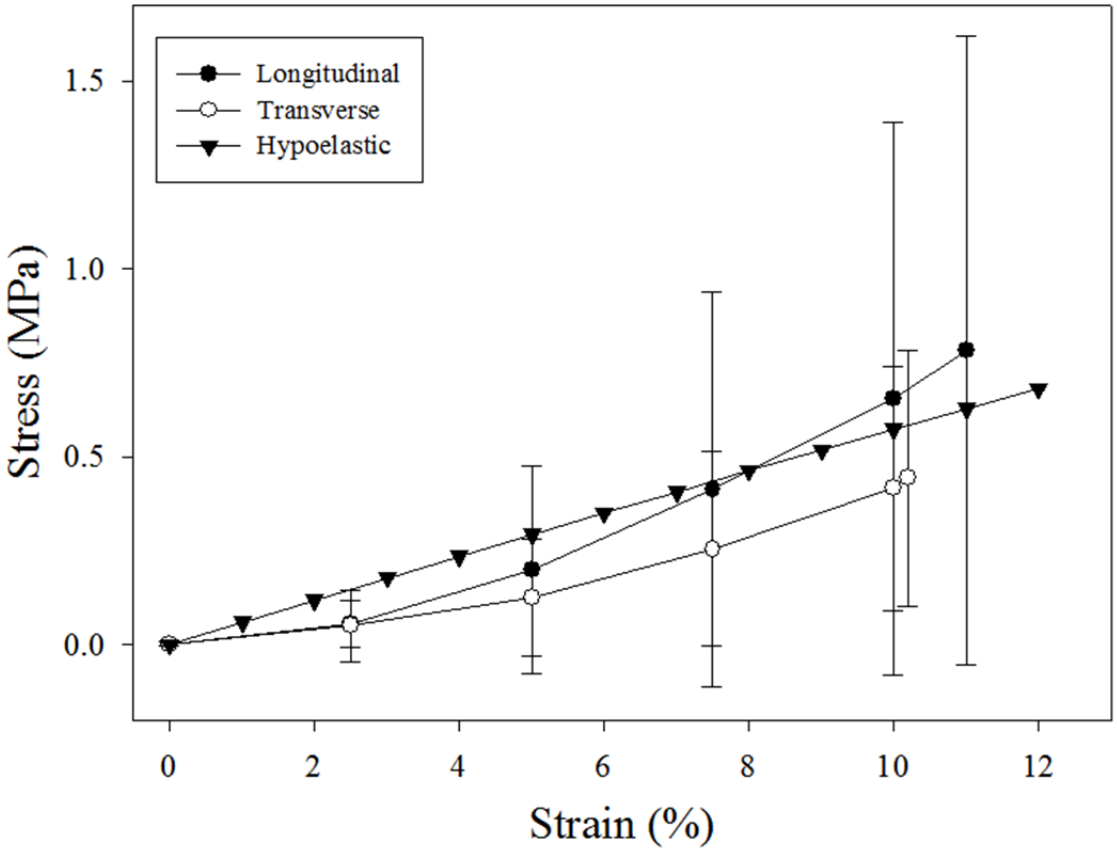

Fig. 4.8. Uniaxial tensile stress-strain response of the axillary pouch of the IGHL complex. Longitudinal – response parallel to the anterior band of the IGHL. Transverse – response transverse to the direction defined by the anterior band of the IGHL. Hypoelastic – material response of the hypoelastic constitutive model with best-fit material coefficients. Error bars are mean ± standard deviation.

Although this FE model was not directly validated with subject-specific experimental strains and/or forces, strain predictions are in reasonable agreement with data of previous studies that measured strain during tensile testing or functional loading experiments (Malicky et al., 2001; McMahon, 1998; Moore et al., 2004a; Stefko, 1997). Malicky and coworkers (Malicky et al., 2001) determined that the mean maximum principal strain in the anterior-inferior capsule was 14% during subluxation in the anterior direction. Additionally, failure strains for the axillary pouch and posterior capsule have reported to be as high as 33% (Moore et al., 2004a) and 23% (Moore et al., 2003), respectively, for the midsubstance of the tissue. However, since specimen-specific validation was not performed, caution should be used in interpretation of the absolute values for predictions of strains, insertion site and contact forces. Further experiments are needed to obtain subject-specific validation of predicted regional strains.

References

Bankart, A.S.B., 1923. Recurrent or habitual dislocation of the shoulder joint. Br Med J 2, 1132-3.

Bankart, A.S.B., 1938. The pathology and treatment of recurrent dislocation of the shoulder joint. Br J Surg 26, 23-9.

Bigliani, L.U., Pollock, R. G., Soslowsky, L. J., Flatow, E. V., Pawluk, R. J., Mow, V. C., 1992. Tensile properties of the inferior glenohumeral ligament. Journal of Orthopaedic Research 10, 187-197.

Boissonnat, J.D., 1988. Shape reconstruction from planar cross-sections. Computer Vision, Graphics and Image Processing 44, 1-29.

Bokor, D.J., Conboy, V.B., Olson, C., 1999. Anterior instability of the glenohumeral joint with humeral avulsion of the glenohumeral ligament. A review of 41 cases. J Bone Joint Surg Br 81, 93-6.

Brenneke, S.L., Reid, J., Ching, R.P., Wheeler, D.L., 2000. Glenohumeral kinematics and capsulo-ligamentous strain resulting from laxity exams. Clin Biomech (Bristol, Avon) 15, 735-42.

Bui-Mansfield, L.T., Taylor, D.C., Uhorchak, J.M., Tenuta, J.J., 2002. Humeral avulsions of the glenohumeral ligament: imaging features and a review of the literature. AJR Am J Roentgenol 179, 649-55.

Cave, E., Burke, J., Boyd, R., 1974. Trauma Management. Chicago, IL: Year Book Medical Publishers. 437 pp..

Chhabra, A., Diduch, D.R., Anderson, M., 2004. Arthroscopic repair of a posterior humeral avulsion of the inferior glenohumeral ligament (HAGL) lesion. Arthroscopy 20 Suppl 2, 73-6.

Debski, R.E., McMahon, P. J., Thompson, W.O., Warner, J.P.P., Woo, SL-Y, Fu, F. U., 1995. A new dynamic testing apparatus to study glenohumeral joint motion. J Biomech 27, 869-874.

Debski, R.E., Moore, S.M., Mercer, J.L., Sacks, M.S., McMahon, P.J., 2003. The collagen fibers of the anteroinferior capsulolabrum have multiaxial orientation to resist shoulder dislocation. J Shoulder Elbow Surg 12, 247-52.

Debski, R.E., Weiss, J.A., Newman, W.J., Moore, S.M., McMahon, P.J., 2005. Stress and strain in the anterior band of the inferior glenohumeral ligament during a simulated clinical examination. J Shoulder Elbow Surg 14, S24-31.

Debski, R.E., Wong, E.K., Woo, S.L.-Y., Fu, F.H., Warner, J.J., 1999a. An analytical approach to determine the in situ forces in the glenohumeral ligaments. J Biomech Eng 121, 311-5.

Debski, R.E., Wong, E.K., Woo, S.L.-Y., Sakane, M., Fu, F.H., Warner, J.J., 1999b. In situ force distribution in the glenohumeral joint capsule during anterior-posterior loading. Journal of Orthopaedic Research 17, 769-76.

DePalma, A.F., Callery, G., Bennett, G.A., 1949. Variational anatomy and degenerative lesions of the shoulder joint. American Academy of Orthopaedic Surgery Instructional Course Lecture Series 6, 225-81.

Ellis, B.J., Lujan, T.J., Dalton, M.S., Weiss, J.A., 2006. MCL insertion site and contact forces in the ACL-deficient knee. Journal of Orthopaedic Research To Appear, December.

Gardiner, J.C., Weiss, J.A., 2003. Subject-specific finite element analysis of the human medial collateral ligament during valgus knee loading. Journal of Orthopaedic Research 21, 1098-106.

Hovelius, L., 1982. Incidence of shoulder dislocation in Sweden. Clin Orthop, 127-31.

Hughes, T.J., Liu, W.K., 1981a. Nonlinear finite element analysis of shells: Part II. three dimensional shells. Computational Methods in Applied Mechanics 27, 331-362.

Hughes, T.J., Liu, W.K., 1981b. Nonliner finite element analysis of shells: Part I. two dimensional shells. Compuational Methods in Applied Mechanics 27, 167-181.

Itoi, E., Grabowski, J.J., Morrey, B.F., An, K.N., 1993. Capsular properties of the shoulder. Tohoku J Exp Med 171, 203-10.

Luo, Z.P., Hsu, H.C., Grabowski, J.J., Morrey, B.F., An, K.-N., 1998. Mechanical environment associated with rotator cuff tears. J Should Elbow Surg 7, 616-20.

Maker, B.N., 1995a. NIKE3D: A nonlinear, implicit, three-dimensional finite element code for solid and structural mechanics. Lawrence Livermore Lab Tech Rept UCRL-MA-105268.

Maker, B.N., 1995b. Rigid bodies for metal forming analysis with NIKE3D. University of California, Lawrence Livermore Lab Rept UCRL-JC-119862, 1-8.

Maker, B.N., Ferencz, R.M., Hallquist, J.O., 1990. NIKE3D: A nonlinear, implicit, three-dimensional finite element code for solid and structural mechanics. Lawrence Livermore National Laboratory Technical Report UCRL-MA-105268.

Malicky, D.M., Soslowsky, L.J., Kuhn, J.E., Bey, M.J., Mouro, C.M., et al, 2001. Total strain fields of the antero-inferior shoulder capsule under subluxation: a stereoradiogrammetric study. J Biomech Eng 123, 425-31..

Matsen, F.A., Fu, F.H., Hawkins, R.J., 1993. The Shoulder: a balance of mobility and stability: workshop, Vail, Colorado, September 1992. Presented at American Academy of Orthopedic Surgeons., Rosemount, IL.

McMahon, P.J., Tibone, J. E., Cawley, P. W., Hamilton, C., Fechter, J. D., ElAttrache, N. S., Lee, T. Q., 1998. The anterior band of the inferior glenohumeral ligament: Biomechanical properties from tensile testing in the position of apprehension. J Should Elbow Surg 7, 467-471.

Miller, M.S., PJ; Bains, PK; Klein, AH; Fu, FH, 1991. A mathematical and experimental model of length change in the inferior glenohumeral ligament in the late cocking phase of pitching. Trans Orthopaedic Research Society 16, 609.

Moore, S.M., McMahon, P.J., Azemi, E., Debski, R.E., 2005. Bi-directional mechanical properties of the posterior region of the glenohumeral capsule. J Biomech 38, 1365-9.

Moore, S.M., McMahon, P.J., Debski, R.E., 2003. Bi-directional mechanical properties of the posterior region of the glenohumeral capsule. Proc 2003 Summer Bioengineering Conference, 107-108.

Moore, S.M., McMahon, P.J., Debski, R.E., 2004a. Bi-directional mechanical properties of the axillary pouch of the glenohumeral capsule: implications for modeling and surgical repair. J Biomech Eng 126, 284-8.

Moore, S.M., Musahl, V., McMahon, P.J., Debski, R.E., 2004b. Multidirectional kinematics of the glenohumeral joint during simulated simple translation tests: impact on clinical diagnoses. Journal of Orthopaedic Research 22, 889-94.

Nelson, B.J., Arciero, R.A., 2000. Arthroscopic management of glenohumeral instability. Am J Sports Med 28, 602-14.

Novotny, J.E., Beynnon, B.D., Nichols, C.E., 2000. Modeling the stability of the human glenohumeral joint during external rotation. J Biomech 33, 345-54.

O'Brien, S.J., Neves, M.C., Arnoczky, S.P., Rozbruck, S.R., Dicarlo, E.F., et al, 1990. The anatomy and histology of the inferior glenohumeral ligament complex of the shoulder. Am J Sports Med 18, 449-56.

Puso, M.A., 2000. A highly efficient enhanced assumed strain physically stabilized hexahedral element. International Journal for Numerical Methods in Engineering 49, 1029-1064.

Richards, D.P., Burkhart, S.S., 2004. Arthroscopic humeral avulsion of the glenohumeral ligaments (HAGL) repair. Arthroscopy 20 Suppl 2, 134-41.

Sailer, J., Imhof, H., 2004. Shoulder instability. Radiologe 44, 578-90.

Schippinger, G., Vasiu, P.S., Fankhauser, F., Clement, H.G., 2001. HAGL lesion occurring after successful arthroscopic Bankart repair. Arthroscopy 17, 206-8.

Schroeder, W.J., Zarge, J., Lorensen, W.E., 1992. Decimation of triangle meshes. Comp Graph (Proc SIGGRAPH) 26, 65-70.

Schwartz, R.E., O'Brien, S.J., Warren, R.F., Torzilli, P.A., 1988. Capsular restraints to anterior-posterior motion of the abducted shoulder. A biomechanical study. Orthopaedic Transactions 12, 727.

Simo, J.C., Armero, F., 1993. Improved versions of enhanced strain tri-linear elements for 3D finite deformation problems. 110, 359-386.

Simo, J.C., Hughes, T.J.R., 1998. Computational Inelasticity. New York.

Simo, J.C., Taylor, R.L., 1991. Quasi-incompressible finite elasticity in principal stretches: Continuum basis and numerical algorithms. Computer Methods in Applied Mechanics and Engineering 85, 273-310.

Simo, J.C., Vu-Quoc, 1988. On the dynamics in space of rods undergoing large deformations - a geometrically exact approach. Comp Meth Appl Mech Eng 66, 125-61.

Stefko, J.M., Tibone, J. E., Cawley, P. W., ElAttrache, N. E., McMahon, P. J., 1997. Strain of the anterior band of the inferior glenohumeral ligament during capsule failure. J Should Elbow Surg 6, 473-479.

Ticker, J.B., Bigliani, L.U., Soslowsky, L.J., Pawluk, R.J., Flatow, E.L., Mow, V.C., 1996. Inferior glenohumeral ligament: geometric and strain-rate dependent properties. J Shoulder Elbow Surg 5, 269-79.

Turkel, S.J., Panio, M.W., Marshall, J.L., Girgis, F.G., 1981. Stabilizing mechanisms preventing anterior dislocation of the glenohumeral joint. J Bone Joint Surg Am 63, 1208-17.

Van der Helm, F.C., 1994a. Analysis of the kinematic and dynamic behavior of the shoulder mechanism. J Biomech 27, 527-50.

Van der Helm, F.C., 1994b. A finite element musculoskeletal model of the shoulder mechanism. J Biomech 27, 551-69.

Warner, J.J., Beim, G.M., 1997. Combined Bankart and HAGL lesion associated with anterior shoulder instability. Arthroscopy 13, 749-52.

Warner, J.J.P., Caborn, D.N., Berger, R., Fu, F.H., Seel, M., 1993. Dynamic capsuloligamentous anatomy of the glenohumeral joint. J Should Elbow Surg 2, 115-33.

Warner, J.J.P., Deng, X.H., Warren, R.F., Torzilli, P.A., 1992. Static capsuloligamentous restraints to superior-inferior translation of the glenohumeral joint. Am J Sports Med 20, 675-85.

Weiss, J.A., Gardiner, J.C., Ellis, B.J., Lujan, T.J., Phatak, N.S., 2005. Three-dimensional finite element modeling of ligaments: Technical aspects. Med Eng Phys 27, 845-61.

Zeminski, J., 2001. Development of a Combined Analytical and Experimental Approach to Reproduce Knee Kinematics for the Evaluation of Anterior Cruciate Ligament Function. Master's Thesis. University of Pittsburgh, Pittsburgh.

CHAPTER 5

FINITE ELEMENT MODELING OF THE GLENOHUMERAL CAPSULE CAN HELP ASSESS THE TESTED REGION DURING A CLINICAL EXAM [1]

Abstract

The objective of this research was to examine the efficacy of evaluating the region of the glenohumeral capsule being tested by clinical exams for shoulder instability using finite element models of the glenohumeral joint. Specifically, the regions of high capsule strain produced by glenohumeral joint positions commonly used during a clinical exam were identified. Kinematics that simulated a simple translation test with an anterior load at three external rotation angles were applied to a validated, subject-specific finite element model of the glenohumeral joint at 60° of abduction. Maximum principal strains on the glenoid side of the IGHL were significantly higher than the maximum principal strains on the humeral side, for all three regions of the IGHL at 30° and 60° of external rotation. These regions of localized strain indicate that these joint positions might be used to test the glenoid side of the IGHL during this clinical exam, but are not useful for assessing the humeral side of the IGHL. The use of finite element models will facilitate

[1] Reprinted from *Comput Methods Biomech Biomed Engin*, Vol. 13, No. 3. Ellis, B.J., Drury, N.J., Moore, S.M., McMahon, P.J., Weiss, J.A., Debski, R.E., *"Finite Element Modeling of the Glenohumeral Capsule Can Help Assess the Tested Region During a Clinical Exam,"* pp: 413-418, 2009, with permission from Taylor & Francis Group

the search for additional joint positions that isolate high strains to other IGHL regions, including the humeral side of the IGHL.

Introduction

Approximately 5.6 million people will dislocate their glenohumeral joint (Hovelius, 1982, Nelson and Arciero, 2000) during their lifetime and 80% of these dislocations will occur in the anterior direction (Cave, 1974). Common injuries resulting from anterior dislocation are detachment of the inferior glenohumeral ligament (IGHL) from the anterior glenoid and labrum (Bankart, 1923, Bankart, 1938) and humeral avulsion of the glenohumeral ligaments (Bokor et al., 1999, Bui-Mansfield et al., 2002, Chhabra et al., 2004, Richards and Burkhart, 2004, Sailer and Imhof, 2004, Schippinger et al., 2001, Warner and Beim, 1997). Physical diagnostic exams are the most crucial step for diagnosis of the location of injury to the capsule (Brenneke et al., 2000, Mallon and Speer, 1995, Matsen, 1991, Pollock and Bigliani, 1993), but the exams are relatively imprecise and the glenohumeral joint positions used for these exams are not standardized between physicians. Treatments for these injuries depend on the region of the capsule that is injured (Gerber and Ganz, 1984), but misdiagnosis of the injured region has been blamed for over 38% of recurring injuries (Cooper and Brems, 1992, Hawkins and Hawkins, 1985, Lusardi et al., 1993).

During these exams, clinicians apply forces to the humerus to translate the humeral head with respect to the glenoid. These forces also produce strains in the glenohumeral capsule (Malicky et al., 2002, Moore, 2008b), which is the primary passive stabilizer of the glenohumeral joint. The magnitudes of the resulting translations are then graded

(Rockwood, 1998). Assessments are based on the application of a manual maximum force so that a firm end point is reached, restricting further translation (Harryman, 1992, Lippitt and Matsen, 1993, Rockwood, 1998). The orientation of the glenohumeral joint has been shown to influence both the magnitude of the translations (Moore et al., 2004) and the clinician's diagnostic reproducibility (Levy et al., 1999, Tzannes et al., 2004). Finally, as the external rotation angle is increased patients often feel a sense of apprehension and/or discomfort caused by the exam (Gerber and Ganz, 1984, Lo et al., 2004, Silliman and Hawkins, 1993). Currently, the patient's indication of apprehension and/or pain is useful for the physician to help diagnose the injury, but this method is purely subjective, depending as much on the patient's pain threshold as on the extent of the injury.

Poor clinical outcomes, inconsistent clinical exams and complex glenohumeral capsule anatomy have motivated researchers to investigate the function of the specific regions of the glenohumeral capsule by evaluating their strain distributions (Turkel et al., 1981, Moore, 2008c, Bigliani et al., 1992, Brenneke et al., 2000, Malicky et al., 2001a). Subject-specific finite element modeling of the glenohumeral joint is a useful tool for predicting capsule strains (Debski et al., 2005, Ellis et al., 2007) (Moore, 2008a) and this method is able to predict experimentally measured strains (Ellis et al., 2006, Moore, 2008a).

Using strain to identify positions in which connective soft tissues stabilize a diarthrodial joint has been used extensively for the anterior cruciate ligament (ACL) of the knee (Butler, 1989, Henning et al., 1985, Howe et al., 1990, Renstrom et al., 1986, Woo et al., 1987). These studies led to the development of clinical exams (Katz and

Fingeroth, 1986) to diagnose knee instability and injury to the ACL. It is generally accepted that an anterior load should be applied to the tibia while the knee is at 30° of flexion to test for ACL injury. In this position, the injured knee will usually have increased translation compared to the contralateral, uninjured knee. Although, clinical exams for the ACL are standardized and commonly used, extensive research was needed for their development. The starting point was to improve the understanding of knee positions that strained the ACL. Due to the complexity of the strains in the glenohumeral capsule during joint motion (Malicky et al., 2002, Malicky et al., 2001b, Moore, 2008b), a method to correlate glenohumeral joint positions and the capsule strains produced by these positions is needed. As with the ACL, identifying the positions in which the glenohumeral capsule is strained and where those strains occur in the capsule is the first step to developing clinical exams.

The objective of this research is to conduct a feasibility study to examine the efficacy of developing clinical exams using finite element models of the glenohumeral joint by locating the regions of highly strained capsule tissue at multiple joint positions. The long-term research goal is to find joint positions for clinical exams that isolate the region of the capsule being tested, so that accurate diagnoses can be made, without subjective patient input and causing discomfort to the patient. Based on a qualitative analysis of previously reported experimental strains in the glenohumeral capsule (Moore, 2008b), it was hypothesized that the simple translation test with an anterior load would strain the glenoid side of the IGHL in the finite element model more than the humeral side at 30° and 60° of external rotation. Data addressing this hypothesis could suggest that these

joint positions would be ideal for diagnosing injuries to this frequently injured region of the tissue.

Methods

The details of the construction of the subject-specific finite element model of the glenohumeral joint used in this study and its validation with experimental strain data were reported previously (Moore, 2008a); a brief description follows. The geometry of the humerus, scapula, and capsule were obtained from a computed tomography (CT) data set of a shoulder cadaver specimen (male, 45 years old, left) while the humerus and scapula were in the reference position and the capsule was in its reference configuration. For the finite element model, bones and humeral cartilage were represented with rigid bodies and the glenohumeral capsule was modeled with shell elements. Based on material testing of the capsular tissue from this shoulder, an isotropic hypoelastic constitutive model with regionally varying subject-specific elastic modulii and Poisson's ratios of 0.495 were used to represent the three regions of the IGHL (anterior band (AB-IGHL), axillary pouch, and posterior band (PB-IGHL)) and the anterior-superior and posterior capsule regions. Model validation was performed by comparing predicted strains from the finite element model to experimentally measured strains during kinematics that simulated the simple translation test. Eight of the eleven sampling regions were found to be within two times the repeatability of the experimental strain measurements (±7%).

For this study, the kinematics applied to the finite element model simulated the simple translation test with an anterior load performed at three external rotation angles

that are commonly used by physicians to examine anterior stability. To experimentally simulate the clinical exam, a cadaveric shoulder specimen (same as that used for the validated finite element model) was mounted in a robotic/universal force-moment sensor testing system that has been extensively used previously (Debski et al., 2005, Ellis et al., 2007, Moore, 2008a, Moore, 2008b). The humerus was secured within a thick-walled aluminum cylinder and fixed in a custom clamp mounted to the base of the system. The scapula was rigidly attached to the end-effector of the manipulator through another specially designed clamp and the universal force-moment sensor. The coordinate system of the robotic/universal force-moment sensor testing system was then defined as the anatomic coordinate system of the glenohumeral joint as previously described (Burkart and Debski, 2002, Debski et al., 1999).

The initial joint orientation in the testing system was 60° of glenohumeral abduction, 0° of horizontal abduction, and 0° of external rotation. The horizontal abduction angle was held constant throughout the entire experimental protocol. Force control was then used to apply a 22 Newton (N) compressive load (medially directed) to the humerus while the forces in the two orthogonal directions were minimized (~0 N). This centered the humeral head within the glenoid cavity and determined the joint position at 60° of glenohumeral abduction and 0° of external rotation. At this joint position, a 25 N anterior load was applied to the humerus, while maintaining the 22 N compressive force, and the resulting kinematics were recorded by recording the locations of registration blocks attached to the humerus and scapula with an external digitizer (Microscribe 3DX, Immersion Corporation, San Jose, CA). Preliminary testing indicated that, with the skin and musculature removed, an anterior load of 25N, while maintaining a compressive load

of 22 N, would translate the humeral head to the edge of the glenoid without resulting in dislocation or subluxation.

To simulate the clinical exam at 30° and 60° external rotation, an increasing moment with a maximum of 3 Newton-meters (Nm) was applied to the humerus about its longitudinal axis while maintaining the 22 N joint compressive force until the joint positions corresponding to 30° and ~60° external rotation, respectively, were reached. At these joint positions, the 25 N anterior load was applied to the humerus, while maintaining the 22 N compressive force, and the resulting kinematics were recorded.

The kinematics at each external rotation angle, recorded by the external digitizer during testing, were input into the finite element code as previously described (Debski et al., 2005, Ellis et al., 2007, Moore, 2008a). The coordinates of the registration blocks in both the CT and kinematic datasets allowed for correlation of the two datasets. Motion was described during the finite element simulations using incremental translations and rotations (Maker, 1995) from the reference position to the positions during the simple translation test, based on the experimental measurements of the locations of the registration blocks on the humerus and scapula in each position. The nonlinear finite element code NIKE3D was used for all analyses (Maker, 1995). LSPOST (Livermore Software Technology Corporation, Livermore, CA, USA) was used to visualize and process the predicted strains.

To compare strains within regions of the IGHL, the AB-IGHL, axillary pouch, and PB-IGHL were divided midway between their glenoid and humeral insertion sites, yielding a total of six IGHL subregions for analysis (Fig. 5.1). The nodal maximum principal strains in each subregion were averaged for each external rotation angle. An

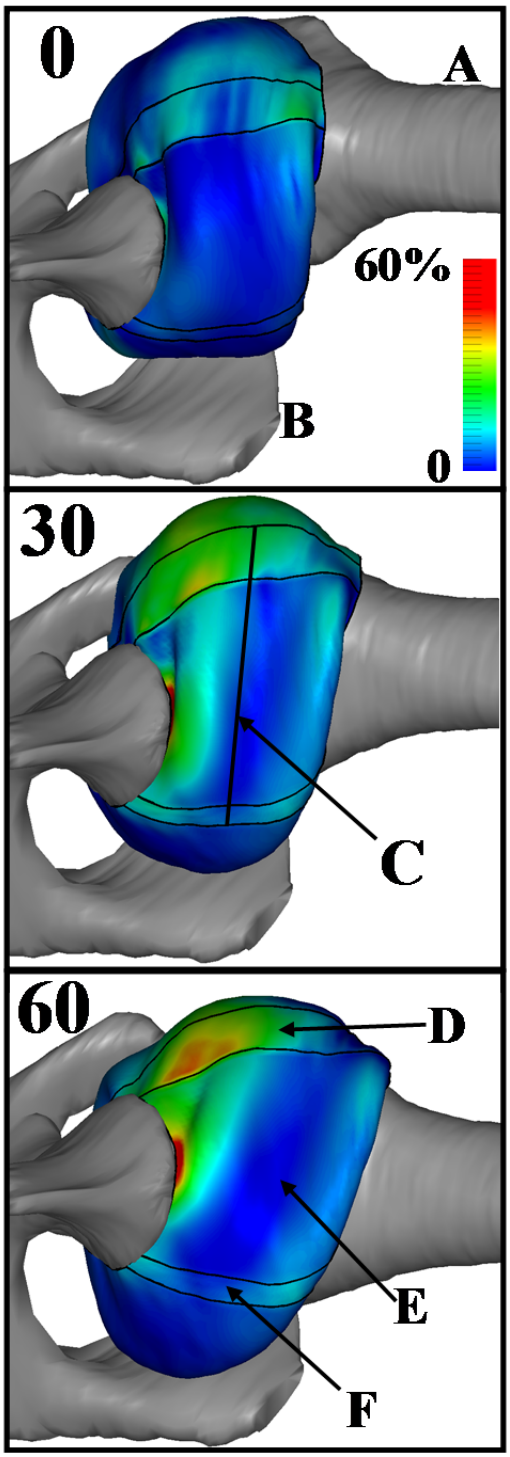

Fig. 5.1. Inferior view (left shoulder) of fringe plots of IGHL 1st principal strains at 60° degrees abduction and full anterior translation at 0°, 30°, and 60° of external rotation. (A) Humerus. (B) Glenoid. (C) IGHL Mid-line. (D) AB-IGHL. (E) Axillary Pouch. (F) PB-IGHL. The glenoid side of the IGHL is consistently loaded more than the humerus side at 30° and 60° of external rotation.

unbalanced GLM 2-way ANOVA procedure in SPSS (SPSS Inc., Chicago, IL) was used to compare regional strains at each rotation angle. Post-hoc comparisons were performed using the Tukey test. Statistical comparisons were only considered to be significant if the differences were statistically significant ($p<0.05$) and the average strain difference was greater than the repeatability of the experimental strain measurements (±3.5%).

Results

While IGHL strains were relatively small and more evenly dispersed between the glenoid and humeral sides of the IGHL during finite element simulations of the simple translation test at 0° of external rotation, more tissue was strained with much higher peak strains on the glenoid side of the IGHL when the simple translation test was simulated at 30° and 60° of external rotation (Fig. 5.1). The end result of these loading conditions was highly strained tissue on the glenoid side of the IGHL, especially the AB-IGHL, with slack, essentially nonstrained tissue on the humeral side of the IGHL, especially the PB-IGHL.

Quantitative comparisons between the glenoid and humeral sides of the IGHL support the qualitative evaluations. Maximum principal strains on the glenoid side of the IGHL were significantly higher than the maximum principal strains on the humeral side when the simple translation test was simulated at 30° and 60° of external rotation ($p<0.05$ for all three regions at both rotation angles), but not at 0° of external rotation (Fig. 5.2). Maximum principal strains on the glenoid side of the AB-IGHL were more than 1.5 times higher and nearly four times higher than on the humeral side at 30° and 60° of external rotation, respectively. The maximum principal strains in the axillary pouch on the

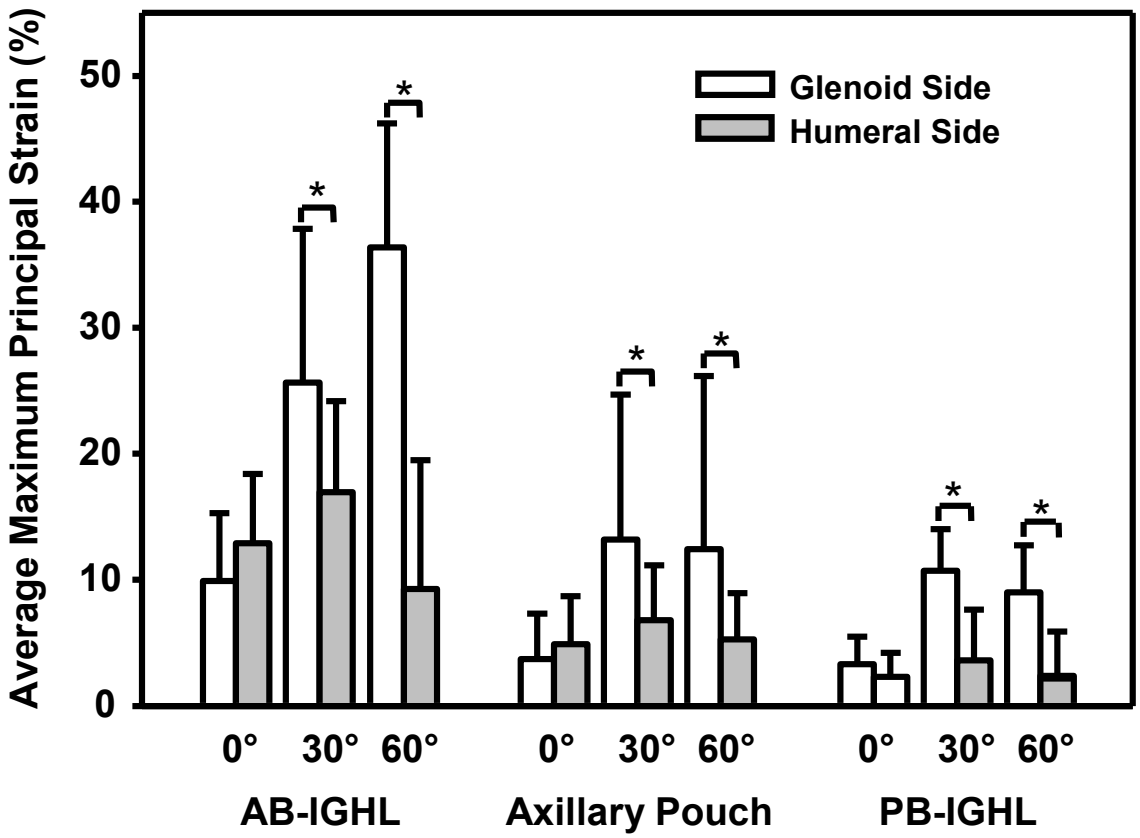

Fig. 5.2. Maximum principal strains at 0°, 30°, and 60° of external rotation on the glenoid and humeral sides of each IGHL region. Maximum principal strains were significantly higher on the glenoid side for each IGHL region at 30° and 60° of external rotation, but not at 0°. (* $p<0.05$) (mean±SD).

glenoid side were more than two times higher than the humeral side at both 30° and 60° of external rotation. Maximum principal strains on the glenoid side of the PB-IGHL were over three times higher than on the humeral side at 30° and over four times higher at 60° of external rotation. There were no significant differences in the maximum principal strains between the humeral and glenoid sides of all three subregions of the IGHL when the simple translation test was conducted at 0° of external rotation. Finally, the strains in the AB-IGHL were significantly higher than the other regions on both the glenoid and humeral sides of the IGHL ($p<0.05$ for all comparisons) with the glenoid side of the AB-

IGHL consistently having the highest strains compared to all the other regions at every external rotation angle ($p<0.05$ for all comparisons).

Discussion

In this study the maximum principal strain throughout the IGHL was determined during a simple translation test at three external rotation angles using a validated subject-specific finite element model of the glenohumeral joint. The strains on the glenoid side of each IGHL region were significantly higher than on the humeral side at 30° and 60° of external rotation, but not at 0°, which supported the hypothesis of this study. Further, the strain predictions from the subject-specific finite element model compared well with experimental data from a sample of five shoulders subjected to the simple translation test that was reported previously (Moore, 2008b). Both studies indicate that the simple translation test with an anterior load performed at 30° and 60° of external rotation localizes tissue strains to the glenoid side of the IGHL. This agreement further validates the results in the previous finite element study (Moore, 2008a).

The similar strain magnitudes between 30° and 60° of external rotation for most subregions of the IGHL imply that clinicians are testing the glenoid side of the IGHL when this exam is performed anywhere from 30° to 60° of external rotation. The data also suggest that different regions of the IGHL, particularly the AB-IGHL, may be strained significantly more than other areas of the IGHL during the simple translation test, potentially allowing clinicians to further isolate the area being tested.

The glenoid side of the AB-IGHL also had the greatest amount of strain at all external rotation angles, supporting the general concept that the AB-IGHL is frequently injured at

its glenoid insertion (Bankart, 1923, Bankart, 1938). In the context of the simple translation test with an anterior load, it appears that when this test is administered at 60° of external rotation, the area around the glenoid side of the AB-IGHL is isolated. It can also be inferred that the apprehension test, a clinical exam that determines the patient's apprehension to external rotation is probably isolating the same area, with some bias to the glenoid side of the IGHL.

Both this study and the previous experimental study (Moore, 2008b) clearly show that the humeral side of the IGHL is not loaded when the simple translation test is administered at external rotation angles equal to or exceeding 30°. Further, when the results of these studies are taken together, it appears that the strains on the humeral side are fairly inconsistent between specimens when the simple translation test with an anterior load is performed at 0° of external rotation. For these reasons, the simple translation test with an anterior load may not be appropriate for testing the humeral side of the IGHL. Injuries such as humeral avulsion of the glenohumeral capsule (Bokor et al., 1999, Bui-Mansfield et al., 2002, Chhabra et al., 2004, Richards and Burkhart, 2004, Sailer and Imhof, 2004, Schippinger et al., 2001, Warner and Beim, 1997) would probably be missed using this simple translation test.

This computational analysis had three primary weaknesses: sample size (n=1); the exclusion of the labrum; and the use of a hypoelastic constitutive equation in the finite element model. Previous studies have shown that there are variations in the strain patterns between specimens (Moore, 2008a), but this study used only a single validated FE model based on a single specimen (Moore, 2008b). In the future, a population of finite element models will be constructed and validated to predict the variation in the

population on a subject-specific basis and assess the current trends predicted in the current study. Furthermore, the finite element model used for this study does not include the labrum. The lack of a labrum will increase strains at the glenoid insertion (where the labrum would be), but will slightly decrease strains in the midsubstance tissue adjacent to the glenoid for every region of the IGHL (Drury, 2009). In this study, strains were averaged over large areas to compare the strain distribution between regions and joint position. Therefore, the IGHL subregion (i.e., glenoid side of the AB-IGHL) that is tested by this clinical exam can be distinguished, but the location of the peak strain values might not be correct (i.e., midtissue vs. labrum vs. labrum-capsule interface). Finally, a hypoelastic material model was used to represent the glenohumeral capsule material. Hypoelasticity is objective for finite deformations (i.e., large strains and rotations) (Simo and Hughes, 1998) and the limitations of using this material model for the IGHL have previously been discussed (Ellis et al., 2007). In the context of the current study, use of a hypoelastic material might change the magnitudes of the strains, but will have very little effect on their distribution. Even though a few weaknesses exist, our results are strongly supported by previous experimental data that examined five cadaveric shoulders (Moore, 2008a).

This study established a methodology to assess the capsule regions tested (strained) by clinical exams using a computational model. Once the region tested is identified, the next step, as was done for the ACL, is to look for side-to-side differences in translation between injured and uninjured shoulders in these joint positions using a repeatable methodology. Many of the discrepancies and complications with clinical exams for shoulder injuries (Levy et al., 1999, Tzannes et al., 2004) may be due to a lack of a

systematic approach while developing the exams. In the future, diagnostic methods that are based on quantitative results from standardized clinical exams that do not cause discomfort to the patient or require their subjective responses would be advantageous. Our research group is currently in the process of constructing subject-specific finite element models of the glenohumeral capsule that include the labrum (Drury, 2009) and the proper constitutive model representing the capsule with a fiber-reinforced, hyperelastic material model. We hope to determine effective joint positions for clinical exams using a population of subject-specific finite element models of the glenohumeral joint.

References

Bankart, A. S. B. (1923) Recurrent or habitual dislocation of the shoulder joint. *Br Med J,* 2**,** 1132-3.

Bankart, A. S. B. (1938) The pathology and treatment of recurrent dislocation of the shoulder joint. *Br J Surg,* 26**,** 23-9.

Bigliani, L. U., Pollock, R. G., Soslowsky, L. J., Flatow, E. L., Pawluk, R. J. & Mow, V. C. (1992) Tensile properties of the inferior glenohumeral ligament. *J Orthop Res,* 10**,** 187-97.

Bokor, D. J., Conboy, V. B. & Olson, C. (1999) Anterior instability of the glenohumeral joint with humeral avulsion of the glenohumeral ligament. A review of 41 cases. *J Bone Joint Surg Br,* 81**,** 93-6.

Brenneke, S. L., Reid, J., Ching, R. P. & Wheeler, D. L. (2000) Glenohumeral kinematics and capsulo-ligamentous strain resulting from laxity exams. *Clin Biomech (Bristol, Avon),* 15**,** 735-42.

Bui-Mansfield, L. T., Taylor, D. C., Uhorchak, J. M. & Tenuta, J. J. (2002) Humeral avulsions of the glenohumeral ligament: imaging features and a review of the literature. *AJR Am J Roentgenol,* 179**,** 649-55.

Burkart, A. C. & Debski, R. E. (2002) Anatomy and function of the glenohumeral ligaments in anterior shoulder instability. *Clin Orthop Relat Res***,** 32-9.

Butler, D. L. (1989) Kappa Delta Award paper. Anterior cruciate ligament: its normal response and replacement. *J Orthop Res,* 7**,** 910-21.

Cave, E., Burke, J., Boyd, R. (1974) *Trauma Management,* Chicago, IL, Year Book Medical Publishers.

Chhabra, A., Diduch, D. R. & Anderson, M. (2004) Arthroscopic repair of a posterior humeral avulsion of the inferior glenohumeral ligament (HAGL) lesion. *Arthroscopy,* 20 Suppl 2**,** 73-6.

Cooper, R. A. & Brems, J. J. (1992) The inferior capsular-shift procedure for multidirectional instability of the shoulder. *J Bone Joint Surg Am,* 74**,** 1516-21.

Debski, R. E., Weiss, J. A., Newman, W. J., Moore, S. M. & Mcmahon, P. J. (2005) Stress and strain in the anterior band of the inferior glenohumeral ligament during a simulated clinical examination. *J Shoulder Elbow Surg,* 14**,** S24-31.

Debski, R. E., Wong, E. K., Woo, S. L.-Y., Sakane, M., Fu, F. H. & Warner, J. J. (1999) In situ force distribution in the glenohumeral joint capsule during anterior-posterior loading. *J Orthop Res,* 17**,** 769-76.

Drury, N. J., Ellis, B. J., Weiss, J. A., Mcmahon, P.J., Debski, R. E. (2009) The Impact of Glenoid Labrum Thickness and Modulus on Labrum and Glenohumeral Capsule Pathology. Submitted to *J Shoulder Elbow Surg.*

Ellis, B. J., Debski, R. E., Moore, S. M., Mcmahon, P. J. & Weiss, J. A. (2007) Methodology and sensitivity studies for finite element modeling of the inferior glenohumeral ligament complex. *J Biomech,* 40**,** 603-12.

Ellis, B. J., Lujan, T. J., Dalton, M. S. & Weiss, J. A. (2006) Medial collateral ligament insertion site and contact forces in the ACL-deficient knee. *J Orthop Res,* 24**,** 800-10.

Gerber, C. & Ganz, R. (1984) Clinical assessment of instability of the shoulder. With special reference to anterior and posterior drawer tests. *J Bone Joint Surg Br,* 66**,** 551-6.

Harryman, D. T., 2nd, Sidles, J.A., Matsen, F.A., 3rd (1992) Laxity of the normal glenohumeral joint: A quantitative in vivo assessment. *J Should Elbow Surg,* 1**,** 66-76.

Hawkins, R. H. & Hawkins, R. J. (1985) Failed anterior reconstruction for shoulder instability. *J Bone Joint Surg Br,* 67**,** 709-14.

Henning, C. E., Lynch, M. A. & Glick, K. R., Jr. (1985) An in vivo strain gage study of elongation of the anterior cruciate ligament. *Am J Sports Med,* 13**,** 22-6.

Hovelius, L. (1982) Incidence of shoulder dislocation in Sweden. *Clin Orthop***,** 127-31.

Howe, J. G., Wertheimer, C., Johnson, R. J., Nichols, C. E., Pope, M. H. & Beynnon, B. (1990) Arthroscopic strain gauge measurement of the normal anterior cruciate ligament. *Arthroscopy,* 6**,** 198-204.

Katz, J. W. & Fingeroth, R. J. (1986) The diagnostic accuracy of ruptures of the anterior cruciate ligament comparing the Lachman test, the anterior drawer sign, and the pivot shift test in acute and chronic knee injuries. *Am J Sports Med,* 14**,** 88-91.

Levy, A. S., Lintner, S., Kenter, K. & Speer, K. P. (1999) Intra- and interobserver reproducibility of the shoulder laxity examination. *Am J Sports Med,* 27**,** 460-3.

Lippitt, S. & Matsen, F. (1993) Mechanisms of glenohumeral joint stability. *Clin Orthop Relat Res***,** 20-8.

Lo, I. K., Nonweiler, B., Woolfrey, M., Litchfield, R. & Kirkley, A. (2004) An evaluation of the apprehension, relocation, and surprise tests for anterior shoulder instability. *Am J Sports Med,* 32**,** 301-7.

Lusardi, D. A., Wirth, M. A., Wurtz, D. & Rockwood, C. A., Jr. (1993) Loss of external rotation following anterior capsulorrhaphy of the shoulder. *J Bone Joint Surg Am,* 75**,** 1185-92.

Maker, B. N. (1995) NIKE3D: A nonlinear, implicit, three-dimensional finite element code for solid and structural mechanics. *Lawrence Livermore Lab Tech Rept,* UCRL-MA-105268.

Malicky, D. M., Kuhn, J. E., Frisancho, J. C., Lindholm, S. R., Raz, J. A. & Soslowsky, L. J. (2002) Neer Award 2001: nonrecoverable strain fields of the anteroinferior glenohumeral capsule under subluxation. *J Shoulder Elbow Surg,* 11**,** 529-40.

Malicky, D. M., Soslowsky, L. J., Kuhn, J. E., Bey, M. J., Mouro, C. M., Raz, J. A. & Liu, C. A. (2001a) Total strain fields of the antero-inferior shoulder capsule under subluxation: a stereoradiogrammetric study. *J Biomech Eng,* 123**,** 425-31.

Malicky, D. M., Soslowsky, L. J., Kuhn, J. E., Bey, M. J., Mouro, C. M., Raz, J. A. & Liu, C. A. (2001b) Total strain fields of the antero-inferior shoulder capsule under subluxation: a stereoradiogrammetric study. *J Biomech Eng,* 123**,** 425-31.

Mallon, W. J. & Speer, K. P. (1995) Multidirectional instability: current concepts. *J Shoulder Elbow Surg,* 4**,** 54-64.

Matsen, F. A., 3rd (1991) Capsulorrhaphy with a staple for recurrent posterior subluxation of the shoulder. *J Bone Joint Surg Am,* 73**,** 950.

Moore, S. M., Ellis, B.J., Weiss, J.A., Mcmahon, P.J., Debski, R.E. (2008a) The glenohumeral capsule should be evaluated as a sheet of fibrous tissue: validation of a subject-specific finite element model. *Annals of Biomedical Engineering,,* In Review.

Moore, S. M., Musahl, V., Mcmahon, P. J. & Debski, R. E. (2004) Multidirectional kinematics of the glenohumeral joint during simulated simple translation tests: impact on clinical diagnoses. *J Orthop Res,* 22**,** 889-94.

Moore, S. M., Stehle, J.H., Rainis, E.J, Mcmahon, P.J, Debski, R.E. (2008b) The current anatomical description of the inferior glenohumeral ligament does not correlate with its functional role in positions of external rotation. *J Orthop Res, In Press.*

Nelson, B. J. & Arciero, R. A. (2000) Arthroscopic management of glenohumeral instability. *Am J Sports Med,* 28**,** 602-14.

Pollock, R. G. & Bigliani, L. U. (1993) Glenohumeral instability: evaluation and treatment. *J Am Acad Orthop Surg,* 1**,** 24-32.

Renstrom, P., Arms, S. W., Stanwyck, T. S., Johnson, R. J. & Pope, M. H. (1986) Strain within the anterior cruciate ligament during hamstring and quadriceps activity. *Am J Sports Med,* 14**,** 83-7.

Richards, D. P. & Burkhart, S. S. (2004) Arthroscopic humeral avulsion of the glenohumeral ligaments (HAGL) repair. *Arthroscopy,* 20 Suppl 2**,** 134-41.

Rockwood, C. A., F.A. Matsen, 3rd, M.A. Wirth, and D.T.Harryman, 2nd, (1998) *The Shoulder*. *2nd ed. 1998, Philadelphia, PA: W. B. Saunders Co.*

Sailer, J. & Imhof, H. (2004) Shoulder instability. *Radiologe,* 44**,** 578-90.

Schippinger, G., Vasiu, P. S., Fankhauser, F. & Clement, H. G. (2001) HAGL lesion occurring after successful arthroscopic Bankart repair. *Arthroscopy,* 17**,** 206-8.

Silliman, J. F. & Hawkins, R. J. (1993) Classification and physical diagnosis of instability of the shoulder. *Clin Orthop Relat Res***,** 7-19.

Simo, J. C. & Hughes, T. J. R. (1998) *Computational Inelasticity,* New York.

Turkel, S. J., Panio, M. W., Marshall, J. L. & Girgis, F. G. (1981) Stabilizing mechanisms preventing anterior dislocation of the glenohumeral joint. *J Bone Joint Surg Am,* 63**,** 1208-17.

Tzannes, A., Paxinos, A., Callanan, M. & Murrell, G. A. (2004) An assessment of the interexaminer reliability of tests for shoulder instability. *J Shoulder Elbow Surg,* 13**,** 18-23.

Warner, J. J. & Beim, G. M. (1997) Combined Bankart and HAGL lesion associated with anterior shoulder instability. *Arthroscopy,* 13**,** 749-52.

Woo, S. L., Hollis, J. M., Roux, R. D., Gomez, M. A., Inoue, M., Kleiner, J. B. & Akeson, W. H. (1987) Effects of knee flexion on the structural properties of the rabbit femur-anterior cruciate ligament-tibia complex (FATC). *J Biomech,* 20**,** 557-63.

CHAPTER 6

DISCUSSION

Summary

The research described in this dissertation investigated the mechanics of three commonly injured diarthrodial joint ligaments. Specifically, MCL mechanics in the intact and ACL-deficient knee due to anterior and valgus loading was investigated, as well as IGHL mechanics due to loading that simulated a common clinical exam for anterior shoulder stability was studied. Although the focus of this research was finite element modeling, both experimental and computational methods were developed and utilized for this research. Further, one of the major strengths of this research is the combined experimental and computational approach that was used, providing the model verification, validation and sensitivity studies necessary to allow the results of the models to be trusted. This body of work also highlights FE model development at two distinctly different stages. In Chapter 3, the methods used were honed from previous studies [1-5] allowing for clinically relevant conclusions to be made. In contrast, Chapter 4 highlights FE model development in its early stages, where it must be decided what methods should be used and the accuracy necessary for model inputs to allow for proper model verification and validation in future studies. This model development then came full

circle in Chapter 5, after an additional study [6], allowing us to use the glenohumeral capsule model to develop clinically relevant methods for assessing shoulder clinical exams. Finally, the methods and concepts put forth by this dissertation research have already lead to other studies [7-9], of which two produced award winning papers [7, 9]. Finally, parts of this dissertation research have been highlighted in two review articles [10, 11].

Medial Collateral Ligament Mechanics in the Anterior Cruciate Ligament Deficient Knee

In Chapter 3 it was hypothesized that ACL deficiency would increase MCL insertion site forces at the femur and tibia and increase contact forces between the MCL and bones in response to both anterior and valgus loading. This hypothesis was partially disproved. In the ACL-deficient knee, the MCL is indeed subjected to higher insertion site and contact forces in response to an anterior load. However, MCL forces due to a valgus torque are not significantly increased in the ACL-deficient knee. It follows that the MCL resists anterior tibial translation in knees with intact ACLs, but the ACL is not a restraint to valgus rotation when a healthy MCL is present.

The conclusion that the ACL is not a restraint to valgus rotation if the MCL is intact may seem contradictory to the widely held notion that the ACL is a secondary restraint to valgus rotation [12-18]. However, upon closer examination, these studies reached this conclusion based on the results of MCL transection. Specifically, when the MCL was injured or transected, the ACL experienced increased loading during application of a valgus torque. Although the conclusion of this dissertation research has not been

reported previously in the literature, it was highlighted that the results of other studies support the conclusions indirectly.

Improvements in the experimental methods that were used in Chapter 3 resulted in substantially better agreement between FE predictions and experimental measurements of fiber stretch than was obtained in a previous study from our lab [1]. Improvements included the use of a more accurate digital motion analysis system, placement of wires around the MCL insertion sites to aid in identifying their locations in the CT images, and the placement of additional strain markers along and across the MCL [19]. The excellent correlation between experimental and FE predicted fiber strains (R^2 = 0.953) provides confidence in the fidelity of subject-specific FE modeling. Data such as insertion site forces and contact forces, which elucidate other injury mechanisms and risks, can be evaluated using subject-specific FE methods.

The results available through a combined experimental and computational protocol can also be used to determine the likely location of injury and to what extent it may occur. This dissertation research confirmed that MCL strains are highly heterogeneous and this appears to be caused by the difference in contact forces that the MCL experiences at each bone. From the graph of MCL contact forces during anterior tibial translation (Fig. 3.6, left), it can be seen that MCL contact forces at the tibia are twice those at the femur when the knee is intact and 3 to 5 times higher with an ACL injury. From the fringe plots of MCL strain in the ACL-deficient knee during anterior tibial loading (Fig. 3.4, top right) it can be seen that the area of highest MCL strains occurs between the tibial plateau and the femoral insertion site. This is an area of low contact force between an area of high contact force and the femoral insertion.

In summary, in Chapter 3 it was shown that ACL deficiency significantly increases MCL insertion site and contact forces in response to an anterior tibial load, and the largest increases occur at full extension. In contrast, ACL deficiency does not significantly increase MCL insertion site and contact forces in response to a valgus torque. Since it was demonstrated that the ACL is not a restraint to valgus rotation if the MCL is intact, increased valgus laxity in the ACL-deficient knee indicates a compromised MCL.

Inferior Glenohumeral Ligament Modeling and Clinical Exams

The objectives of the 4th and 5th chapters of this dissertation were to develop methods for FE modeling of the IGHL portion of the glenohumeral capsule for elucidating the IGHL's role in anterior shoulder stability and for assessing the region of the IGHL being tested during clinical exams. This dissertation research is part of a larger shoulder project that has accomplished four objectives. First, methods were developed for subject-specific finite element modeling of the IGHL and second, it was shown that this structure needs to be modeled with the rest of the shoulder capsule (Chapter 4). Third, we have created the most complex finite element model of the shoulder capsule with the most stringent validation criteria to date for this structure [6]. Finally, from this model we have been able to gain insight into the role of the IGHL in anterior shoulder stability and have developed a method for locating the region of the capsule being tested by clinical exams (Chapter 5).

One of the objectives of this project was to create a validated model of the IGHL region of the shoulder capsule, but before validation procedures could begin it was first necessary to verify that the structure was discretized properly. Some of the earlier

research on this project, before this dissertation research, modeled just the AB-IGHL using hexehedral elements [20]. This modeling approach was similar to the MCL project, but worked for the AB-IGHL model only because the discrete structure and applied kinematics did not produce the folds and wrinkles that occurred when the entire IGHL was modeled. As we modeled more of the capsule structure, it was necessary to move from hexahedral elements to shell elements and to investigate different shell element formulations. For Chapter 4 we used Hughes-Liu quadrilateral shell elements to discretize the IGHL [21, 22] and for all subsequent research we have used YASE quadrilateral shell elements [23]. As the structure complexity increased and the element formulations changed we conducted mesh convergence studies to verify proper discretization so that we did not get mesh induced hot spots (Fig. 4.6, B). Modeling the IGHL with shell elements also reduced computational expense.

Another important modeling consideration that was answered in Chapter 4 was the complexity necessary for the representation of the articular cartilage of the humeral head. The IGHL makes contact with the humeral head cartilage during most shoulder clinical exams. From this research it was concluded that the humeral head cartilage may be represented as rigid. This decision came from the fact that IGHL strains and forces were insensitive to changes in articular cartilage elastic modulus and bulk:shear modulus ratio. This finding had implications for all of our future IGHL modeling. Experiments were not needed to characterize the material properties of the humeral articular cartilage in order to produce accurate subject-specific models of the IGHL. Further, modeling the humeral articular cartilage as a rigid body saved computational expense in two ways. First, simulations of contact between a deformable body and a rigid body are computationally

less expensive than simulations of contact between two deformable bodies. Second, representing cartilage as a rigid body directly saved computational time by removing the thousands of degrees of freedom introduced by a deformable hexahedral mesh.

Along with the methods for developing IGHL models, we developed new methods for analyzing the results from those models. This dissertation research constitutes the first time that IGHL strains, insertion-site and contact forces were collected from an IGHL model, so a methodology for collecting and presenting these results also needed to be developed. New methods for acquiring the insertion-site and contact forces for the individual structures as well as the identification of strain regions for these structures were all part of the research that went into Chapter 4 of this dissertation.

The methods presented in Chapter 4 were used to create the first validated model of the IGHL as part of the entire glenohumeral capsule [6]. For that research, FE predicted strains were compared to experimental strains for 11 strain regions around the AB-IGHL. The repeatability of the experimental strain measurements was +/- 3.5%. The strain predictions from the FE model nearly matched the experimental measurements in the mid-substance regions, but there was more disagreement in the data near the insertion sites. On the glenoid side, this was most likely due to the labrum not being included, even though the representative from Dr. Jeffrey Weiss' lab repeatedly suggested that it should be included. The representative from Dr. Jeffrey Weiss' lab did add the labrum to this model for a later, award winning paper that is also not included directly in this dissertation [7].

Still, with the validated model we were able to examine the functions of the IGHL regions during the clinical exam known as the simple translation test. At 60°ER, the

relative difference in strain between the glenoid and humeral side of the IGHL regions was significant for all IGHL regions. The magnitude of the difference between glenoid side and humeral side strains was highest for the AB-IGHL. The average strain results for the 30° case also showed that the glenoid side strains were significantly greater, but there were no differences between the glenoid and humeral side strains when the test was performed at 0° external rotation. Further, it was shown that at each external rotation angle used for the simple translation test, the glenoid side strains in the AB-IGHL were higher than the glenoid side strains of the axillary pouch and the PB-IGHL. The average strain in all 3 regions significantly increased from 0° to 30° external rotation, but only the AB-IGHL strains increased from 30° to 60° degrees.

In conclusion, from this dissertation research we know the level of complexity necessary to model the midsubstance of the IGHL and can make some implications as to the functional roles of its regions and what regions are being tested during the clinical exam known as the simple translation test. Finally, with this research we have developed a methodology for assessing the regions of the glenohumeral capsule being tested by other clinical exams.

Limitations and Future Work

Limitations

As with all research, the work presented in this dissertation has limitations and there was one limitation that was applicable to this entire body of work. The boundary and loading conditions used for this research simulate clinical exams and are not indicative of the boundary and loading conditions caused by muscle activation forces, ground contact

forces, or those that cause ligament injury. This research specifically used boundary and loading conditions that isolated the ligaments and load limits that allowed multiple tests to be used on a single specimen during the experimental portion. Great caution should be used when extrapolating the results reported here to knees and shoulders under different boundary and loading conditions.

The limitations of the boundary and loading conditions are arguably the only limitations of the knee research in this dissertation worth addressing here. Other more minor considerations are discussed in Chapter 3. In contrast, the shoulder research in this dissertation and presented in Moore et al. [6] does have several other limitations that should be discussed. Foremost is the small number of specimens (n=1) that were tested and modeled for each of the studies presented in Chapters 4 and 5, and Moore et al. In defense, these were all essentially methods development studies for a very difficult structure to model. Further, we improved upon and showed the repeatability of the modeling and validation methods for two specimens in Drury et al. [8].

These studies also did not include the glenoid labrum, which will increase strains at the glenoid insertion (where the labrum would be), but will slightly decrease strains in the midsubstance tissue adjacent to the glenoid for every region of the IGHL [7]. Essentially, the results presented in Chapter 5 and Moore et al. are only valid for the mid-substance of the IGHL. Again, this discrepancy was alleviated in Drury et al. where the labrum was included in both models [8].

Finally, the studies presented in Chapters 4 and 5 and Moore et al. used a hypoelastic constitutive equation to represent the glenohumeral capsule material. Hypoelasticity is objective for finite deformations (i.e., large strains and rotations) [24] and the limitations

of using this material model for the IGHL are well discussed in Chapters 4 and 5. The logistical reasons this material representation was used, not discussed previously, was due to the IGHL material properties not being available while this research was being conducted and the limited material constitutive models available in the FE solver that was used for these studies [25]. The IGHL material characterization was being conducted in conjunction with this dissertation research and was reported in Rainis et al. [26]. Further, this entire modelling project was ported from NIKE3D [25] to FEBio [27, 28] where a hyperelastic constitutive equation was available to more accurately represent the IGHL material for our most recent publication [8].

In conclusion, the boundary and loading conditions used in this dissertation research limit the applicability of its findings to the ligament mechanics associated with and similar to clinical exams. While this is the only limitation of the knee research worth addressing here, the shoulder research had other limitations. But, these discrepancies were all alleviated in our most recent publication [8].

Future Work

As discussed in Chapter 2, ligaments are only one of the structures that stabilize joint motion. Muscles and bone articulating surfaces, as well as the meniscus in the knee and the labrum in the shoulder all contribute to the joints stability. In the knee, during regular activities of daily living and during many activities that cause knee injuries there is a complex combination of muscle, ligament and body weight forces, as well as ground, bone articulating surface and meniscus contact forces all contributing to knee stability or the lack of knee stability. During synonymous shoulder activities, muscle, bone

articulating surfaces and the labrum play a much larger role in shoulder stability than the capsule. Finally, there is one shoulder clinical exam known as the apprehension test during which the humerus external rotation angle is increased until patients feel a sense of apprehension and/or discomfort caused by the exam [29-31]. It is arguable that the apprehension and/or discomfort caused by this exam will cause a reaction leading to muscle forces, so muscle forces should be included to properly asses this exam. To conclude, future research examining other loading conditions that simulate regular daily activities and those that cause injury, as well as clinical exams were muscle forces are a contributor is still needed. The FE models used for this research will need to include all the passive and active stabilizers to diarthrodial joint motion.

As mentioned at the beginning of this chapter the methods and concepts developed in this dissertation research have already lead to other studies [7-9, 32, 33]. Two of these studies produced award winning papers [7, 9]. Further, this dissertation research has been highlighted in two review articles [10, 11]. Finally, this research is also the basis for a developing research project investigating the extensor hood of the index finger [32, 33]. This aponeurosis is fundamental to the study of the effects of stroke on finger extension, which is the motor function most impaired by stroke [34]. It is hoped that this research project as well as other future studies developed using the methods and concepts from this dissertation research will be successful at answering questions that could not be addressed otherwise.

References

[1] Gardiner, J.C. and Weiss, J.A., 2003, "Subject-specific finite element analysis of the human medial collateral ligament during valgus knee loading," J Orthop Res, 21(6), pp. 1098-106.

[2] Gardiner, J.C., Weiss, J.A., and Rosenberg, T.D., 2001, "Strain in the human medial collateral ligament during valgus loading of the knee," Clin Orthop, (391), pp. 266-74.

[3] Quapp, K.M. and Weiss, J.A., 1998, "Material characterization of human medial collateral ligament," J Biomech Eng, 120(6), pp. 757-63.

[4] Weiss, J.A., Gardiner, J.C., and Bonifasi-Lista, C., 2002, "Ligament material behavior is nonlinear, viscoelastic and rate-independent under shear loading," J Biomech, 35(7), pp. 943-50.

[5] Weiss, J.A. and Maker, B.N., 1996, "Finite element implementation of incompressible, transversely isotropic hyperelasticity," Computer Methods in Applied Mechanics and Engineering, (135), pp. 107-128.

[6] Moore, S.M., Ellis, B., Weiss, J.A., McMahon, P.J., and Debski, R.E., 2010, "The glenohumeral capsule should be evaluated as a sheet of fibrous tissue: a validated finite element model," Annals of Biomedical Engineering, 38(1), pp. 66-76.

[7] Drury, N.J., Ellis, B. J., Weiss, J. A., McMahon, P.J., Debski, R. E. , 2009, "The Impact of Glenoid Labrum Thickness and Modulus on Labrum and Glenohumeral Capsule Pathology," Submitted.

[8] Drury, N.J., Ellis, B.J., Weiss, J.A., McMahon, P.J., and Debski, R.E., 2011, "Finding consistent strain distributions in the glenohumeral capsule between two subjects: implications for development of physical examinations," Journal of biomechanics, 44(4), pp. 607-13.

[9] Elkins, J.M., Stroud, N.J., Rudert, M.J., Tochigi, Y., Pedersen, D.R., Ellis, B.J., Callaghan, J.J., Weiss, J.A., and Brown, T.D., 2011, "The capsule's contribution to total hip construct stability - A finite element analysis," Journal of Orthopaedic Research: Official Publication of the Orthopaedic Research Society.

[10] Anderson, A.E., Ellis, B.J., and Weiss, J.A., 2007, "Verification, validation and sensitivity studies in computational biomechanics," Computer Methods in Biomechanics and Biomedical Engineering, 10(3), pp. 171-84.

[11] Weiss, J.A., Gardiner, J.C., Ellis, B.J., Lujan, T.J., and Phatak, N.S., 2005, "Three-dimensional finite element modeling of ligaments: technical aspects," Med Eng Phys, 27(10), pp. 845-61.

[12] Abramowitch, S.D., Yagi, M., Tsuda, E., and Woo, S.L., 2003, "The healing medial collateral ligament following a combined anterior cruciate and medial collateral ligament injury--a biomechanical study in a goat model," J Orthop Res, 21(6), pp. 1124-30.

[13] Anderson, D.R., Weiss, J.A., Takai, S., Ohland, K.J., and Woo, S.L., 1992, "Healing of the medial collateral ligament following a triad injury: a biomechanical and histological study of the knee in rabbits," J Orthop Res, 10(4), pp. 485-95.

[14] Inoue, M., McGurk-Burleson, E., Hollis, J.M., and Woo, S.L., 1987, "Treatment of the medial collateral ligament injury. I: The importance of anterior cruciate ligament on the varus-valgus knee laxity," Am J Sports Med, 15(1), pp. 15-21.

[15] Loitz-Ramage, B.J., Frank, C.B., and Shrive, N.G., 1997, "Injury size affects long-term strength of the rabbit medial collateral ligament," Clin Orthop, (337), pp. 272-80.

[16] Ma, C.B., Papageogiou, C.D., Debski, R.E., and Woo, S.L., 2000, "Interaction between the ACL graft and MCL in a combined ACL+MCL knee injury using a goat model," Acta Orthop Scand, 71(4), pp. 387-93.

[17] Norwood, L.A. and Cross, M.J., 1979, "Anterior cruciate ligament: functional anatomy of its bundles in rotatory instabilities," Am J Sports Med, 7(1), pp. 23-6.

[18] Woo, S.L., Jia, F., Zou, L., and Gabriel, M.T., 2004, "Functional tissue engineering for ligament healing: potential of antisense gene therapy," Ann Biomed Eng, 32(3), pp. 342-51.

[19] Lujan, T.J., Lake, S.P., Plaizier, T.A., Ellis, B.J., and Weiss, J.A., 2005, "Simultaneous measurement of three-dimensional joint kinematics and ligament strains with optical methods," ASME Journal of Biomechanical Engineering, 127, pp. 193-197.

[20] Debski, R.E., Weiss, J.A., Newman, W.J., Moore, S.M., and McMahon, P.J., 2005, "Stress and strain in the anterior band of the inferior glenohumeral ligament during a simulated clinical examination," J Shoulder Elbow Surg, 14(1 Suppl), pp. S24-31.

[21] Hughes, T.J. and Liu, W.K., 1981, "Nonliner finite element analysis of shells: Part I. two dimensional shells," Computational Methods in Applied Mechanics, 27, pp. 167-181.

[22] Hughes, T.J. and Liu, W.K., 1981, "Nonlinear finite element analysis of shells: Part II. three dimensional shells," Computational Methods in Applied Mechanics, 27, pp. 331-362.

[23] Engelmann, B.E., Whirley, R.G., Goudreau, G.L., A simple shell element formulation for large-scale elastoplastic analysis, in Analytical and Computational Models of Shells 1989, The American Society of Mechanical Engineers: New York.

[24] Simo, J.C. and Hughes, T.J.R., *Computational Inelasticity* 1998, New York.

[25] Maker, B.N., 1995, "NIKE3D: A nonlinear, implicit, three-dimensional finite element code for solid and structural mechanics," Lawrence Livermore Lab Tech Rept, UCRL-MA-105268.

[26] Rainis, E.J., Maas, S.A., Henninger, H.B., McMahon, P.J., Weiss, J.A., and Debski, R.E., 2009, "Material properties of the axillary pouch of the glenohumeral capsule: is isotropic material symmetry appropriate?," Journal of Biomechanical Engineering, 131(3), pp. 031007.

[27] Maas, S., Rawlins, D., Weiss, J.A., and Ateshian, G.A. *FEBio Online Documentation*. 2010. **http://help.mrl.sci.utah.edu/help/index.jsp**.

[28] Maas, S., Rawlins, D., Weiss, J.A., and Ateshian, G.A. *FEBio Source Code Online Documentation*. 2010. **http://mrl.sci.utah.edu/source/doxygen/**.

[29] Gerber, C. and Ganz, R., 1984, "Clinical assessment of instability of the shoulder. With special reference to anterior and posterior drawer tests," J Bone Joint Surg Br, 66(4), pp. 551-6.

[30] Lo, I.K., Nonweiler, B., Woolfrey, M., Litchfield, R., and Kirkley, A., 2004, "An evaluation of the apprehension, relocation, and surprise tests for anterior shoulder instability," Am J Sports Med, 32(2), pp. 301-7.

[31] Silliman, J.F. and Hawkins, R.J., 1993, "Classification and physical diagnosis of instability of the shoulder," Clin Orthop Relat Res, (291), pp. 7-19.

[32] Ellis, B.J., Lee, S.W., Traylor, K., Weiss, J.A., Kamper, D.G. *Impact of anatomical adhesions on stress distribution within the extensor hood of the index finger*. in *American Society of Biomechanics Conference*. 2011.

[33] Kamper, D.G., Lee, S.W., Ellis, B.J., Weiss, J.A. *Force Transmission through the Extensor Hood*. in *6th World Congress of Biomechanics*. 2010.

[34] Trombly, C.A., ed. *Stroke*. Occupational Therapy for Physical Dysfunction, ed. C.A. Trombly1989, Williams and Wilkins: Baltimore. 454-471.